

## **Distribution Agreement**

In presenting this thesis or dissertation as a partial fulfillment of the requirements for an advanced degree from Emory University, I hereby grant to Emory University and its agents the non-exclusive license to archive, make accessible, and display my thesis or dissertation in whole or in part in all forms of media, now or hereafter known, including display on the world wide web. I understand that I may select some access restrictions as part of the online submission of this thesis or dissertation. I retain all ownership rights to the copyright of the thesis or dissertation. I also retain the right to use in future works (such as articles or books) all or part of this thesis or dissertation.

Signature:

---

Nicole Lynn Umberger

---

Date

The role of cilia transport in oligodendrocyte development and regulation of PP2A  
activity

By Nicole L Umberger  
Doctor of Philosophy

Graduate Division of Biological and Biomedical Sciences  
Genetics and Molecular Biology

---

Tamara Caspary, Ph.D  
Advisor

---

Ping Chen, Ph.D  
Committee Member

---

Andrew Escayg, Ph.D  
Committee Member

---

Yue Feng, Ph.D  
Committee Member

---

Xiao-Jiang Li, Ph.D  
Committee Member

Accepted:

---

Lisa A. Tedesco, Ph.D  
Dean of the James T. Laney School of Graduate Studies

---

Date

The role of cilia transport in oligodendrocyte development and regulation of PP2A  
activity  
By Nicole L Umberger

B. Sc, University of Georgia, 2007

Advisor: Tamara Caspary, PhD

An abstract of

A dissertation submitted to the Faculty of the  
James T. Laney School of Graduate Studies of Emory University

in partial fulfillment of the requirements for the degree of

Doctor of Philosophy

in Graduate Division of Biological and Biomedical Science

Genetics and Molecular Biology

2014

## Abstract

The role of cilia transport in oligodendrocyte development and regulation of PP2A activity

By Nicole L Umberger

Platelet derived growth factor AA/ $\alpha\alpha$  (PDGF-AA/ $\alpha\alpha$ ) signaling is essential for development of oligodendrocyte progenitors (OLPs) into mature oligodendrocytes (OLs), the cells which produce myelin to insulate axons of neurons in the central nervous system. OLPs are derived from the precursor motor neuron (pMN) domain in the neural tube (which later becomes the spinal cord), and specification of the pMN domain requires cilia. Cilia are microtubule based organelles, and are required for regulation of sonic hedgehog (Shh) signaling activity, which specifies the pMN domain. *Arl13b<sup>hemmin</sup>* (*Arl13b<sup>hmn</sup>*) mouse embryos have short cilia, disrupted Shh activity, and, despite an expanded pMN domain, do not specify OLPs before embryos die during midgestation. Based upon this observation and previous connections of PDGF-AA/ $\alpha\alpha$  signaling to cilia, I asked if Arl13b and cilia are required for OLP development.

In this dissertation, I examine the role of Arl13b and of the cilia transport protein Ift88 in OLP development *in vivo*, and present data which indicate that Arl13b is not required for OLP specification or development, and that Ift88 is not required for postnatal OL development. To further dissect the role of Arl13b and cilia in PDGF-AA/ $\alpha\alpha$  signaling, I used an *in vitro* system and analyzed response to PDGF-AA stimulation in several cilia mutant cell lines. These experiments demonstrate that inhibited response to PDGF-AA stimulation in cilia mutant MEFs is due to up-regulation of mTORC1

signaling, and identify a novel role for PP2A in cilia signaling in vertebrates. Combined, my *in vivo* and *in vitro* results provide a more comprehensive understanding of the role of cilia in PDGF-AA/ $\alpha\alpha$  signaling.

The role of cilia transport in oligodendrocyte development and regulation of  
PP2A activity

By Nicole L Umberger

B. Sc, University of Georgia, 2007

Advisor: Tamara Caspary, PhD

A dissertation submitted to the Faculty of the  
James T. Laney School of Graduate Studies of Emory University  
in partial fulfillment of the requirements for the degree of  
Doctor of Philosophy  
in Graduate Division of Biological and Biomedical Science  
Genetics and Molecular Biology

2014

## TABLE OF CONTENTS

CHAPTER 1: Cilia, signaling, and oligodendrocyte development	1
1.1 Introduction	2
1.2 Cilia	2
Structure	3
Intraflagellar transport	4
1.3 IFT and cilia transport mutants	5
IFT172	5
IFT122	6
DYNC2H1	7
ARL13B	7
1.4 Sonic hedgehog	8
Signaling	8
Sonic hedgehog and cilia	10
Neural tube patterning	11
IFT, Shh, and neural tube patterning	12
1.5 Neural stem cell debate	14
Neural stem cell debate	14
1.6 PDGF-AA/ $\alpha\alpha$ signaling through PI3K/AKT and mTORC1	16
PDGFs and PDGFRs	16
Phosphatidylinositols and Phosphoinositide 3-kinase	17
AKT	18
mTORC1	19

PDGFAA/ $\alpha\alpha$ , and mTORC1 signaling in the context of cilia	21
PDGFAA/ $\alpha\alpha$	21
mTORC1	21
1.7 Oligodendrocytes	23
Oligodendrocyte progenitor specification	23
Oligodendrocyte progenitor maturation	24
PDGF-AA/ $\alpha\alpha$ signaling in OLPs	25
Myelination	26
PDGF-AA/ $\alpha\alpha$ , cilia, and oligodendrocytes	26
1.8 Introduction to PP2A	27
Structure and regulation of PP2A	27
PI3K/AKT/mTOR signaling	28
Hh/Shh signaling	29
PP2A and cilia	30
1.9 Outstanding questions and preview	30
CHAPTER 2: MATERIALS AND METHODS	32
Brain tissue lysis	33
MEF lysis	33
Protein quantification	34
SDS PAGE and Western blotting analysis	35
Embryo dissections	36
Perfusion	37
Sectioning	37

Immunofluorescence	38
Mouse strains and genotyping	38
MEF preparation	41
PDGF-AA, LY294002, rapamycin, okadaic acid, and FTY720 treatments	42
PP2A activity assay	43
CHAPTER 3: THE ROLE OF ARL13B AND IFT88 IN OLIGODENDROCYTE	
DEVELOPMENT <i>IN VIVO</i>	46
3.1 Summary	47
3.2 Introduction	47
3.3 Results	49
3.3.1 Generation of <i>Arl13b</i> <sup><math>\Delta</math>Olig1-Cre</sup> mice, birth incidence, and post-natal weight	49
3.3.2 Deletion of <i>Arl13b</i> in <i>Arl13b</i> <sup><math>\Delta</math>Olig1-Cre</sup> embryos	50
3.3.3 <i>Arl13b</i> <sup><math>\Delta</math>Olig1-Cre</sup> embryos and pups fail to display phenotypes indicative of disrupted OL development	51
3.3.4 Repopulation of the pMN domain with <i>Arl13b</i> expressing Olig2+ progenitors (in <i>Arl13b</i> <sup><math>\Delta</math>Olig1-Cre</sup> embryos at e12.5)	52
3.3.5 Generation and characterization of <i>Ift88</i> <sup><math>\Delta</math>Olig1-Cre</sup> mice	52
3.3.6 Rationale for <i>Nestin-Cre</i>	54
3.3.7 Generation of <i>Arl13b</i> <sup><math>\Delta</math>Nestin1-Cre</sup> mice and turnover of <i>Arl13b</i> in the neural tube	54
3.3.8 <i>Arl13b</i> <sup><math>\Delta</math>Nestin1-Cre</sup> mice do not display defects in prenatal OL development or early postnatal myelination	55

3.3.9	<i>Arl13b</i> <sup><math>\Delta</math>Nestin1-Cre</sup> mice do not display defects in postnatal myelination and develop cystic kidneys	56
3.3.10	Generation and characterization of <i>Ift88</i> <sup><math>\Delta</math>Nestin1-Cre</sup> mice	56
3.4	Discussion	57
3.4.1	Benefits and disadvantages of <i>Olig1-Cre</i> and <i>Nestin-Cre</i>	58
	Table 3.1	58
3.4.2	<i>Arl13b</i> and <i>Ift88</i> are not essential for OL development <i>in vivo</i>	59
3.4.3	Support for a sequential progenitor model from <i>Arl13b</i> <sup><math>\Delta</math>Olig1-Cre</sup> embryos	60
CHAPTER 4: CILIA TRANSPORT REGULATES PDGF-AA/ $\alpha$ $\alpha$ SIGNALING VIA ELEVATED mTOR SIGNALING AND DIMINISHED PP2A ACTIVITY		62
4.1	Introduction	63
4.2	Results	65
4.2.1	PP2Ac localizes to the basal body of MEFs	65
4.2.2	P-Akt <sup>T308</sup> is Increased in Cilia Transport Mutant MEFs	66
4.2.3	PP2A Function is Disrupted in Cilia Transport Mutant MEFs	67
4.2.4	Total PP2A Activity is Similar in WT and Cilia Transport Mutant MEFs	69
4.2.5	mTORC1 Pathway Activity is Increased in Cilia Transport Mutant MEFs	69
4.2.6	Abnormal Response to PDGF Signaling in Cilia Transport Mutant MEFs	70
4.2.7	Rapamycin Treatment Restores PDGFR $\alpha$ Levels and Response to PDGF-AA Stimulation	71
4.3	Discussion	73
CHAPTER 5: PERSPECTIVES		77
5.1	<i>Arl13b</i> and <i>Ift88</i> in oligodendrocyte development	78

5.2	PP2A and cilia trafficking	79
5.3	PDGF-AA/ $\alpha\alpha$ , Akt, and mTORC1	82
5.4	Final summary	84
FIGURES AND TABLES		
Figure 1.2.1	Ciliary structure	85
Figure 1.2.2	IFT	86
Figure 1.4	Neural tube patterning	87
Figure 1.5	Mixed progenitor and sequential models of pMN domain specification	89
Figure 1.6	PDGF ligands and receptors	91
Figure 1.7.1	Stages of oligodendrocyte development	93
Figure 1.7.2	Myelination	95
Figure 1.8	PP2A	96
Figure 3.1	<i>Arll3b</i> <sup><math>\Delta</math>Olig1-Cre</sup> observed vs expected, survival, postnatal weight	97
Figure 3.2	e10.5 neural tube of <i>Arll3b</i> <sup><math>\Delta</math>Olig1-Cre</sup> embryos	100
Figure 3.3	MBP expression from p11 optic nerve of <i>Arll3b</i> <sup><math>\Delta</math>Olig1-Cre</sup> pups	101
Figure 3.4	e16.5 neural tube of <i>Arll3b</i> <sup><math>\Delta</math>Olig1-Cre</sup> embryos	102
Figure 3.5	e15.5 neural tube of <i>Arll3b</i> <sup><math>\Delta</math>Olig1-Cre</sup> embryos	103
Figure 3.6	<i>Ift88</i> <sup><math>\Delta</math>Olig1-Cre</sup> observed vs expected	104
Figure 3.7	e12.5 neural tube of <i>Ift88</i> <sup><math>\Delta</math>Olig1-Cre</sup> embryos	106
Figure 3.8	Observed vs expected for <i>Arll3b</i> <sup><math>\Delta</math>Nestin-Cre</sup> and <i>Ift88</i> <sup><math>\Delta</math>Nestin-Cre</sup>	107
Figure 3.9	e12.5 neural tube of <i>Arll3b</i> <sup><math>\Delta</math>Nestin-Cre</sup> embryos	108
Figure 3.10	e14.5 neural tube of <i>Arll3b</i> <sup><math>\Delta</math>Nestin-Cre</sup> embryos	109

Figure 3.11	e14.5 whole mount of <i>Arl13b</i> <sup><math>\Delta</math>Nestin-Cre</sup> embryos	110
Figure 3.12	PDGFR $\alpha$ and Olig2 expression from p7 optic nerves of <i>Arl13b</i> <sup><math>\Delta</math>Nestin-Cre</sup> pups	111
Figure 3.13	e18.5 neural tube and Olig2, PDGFR $\alpha$ , and CNP expression from optic nerves of <i>Ift88</i> <sup><math>\Delta</math>Nestin-Cre</sup> pups	112
Figure 4.1	PP2Ac localization and P-Akt <sup>T308</sup> levels in WT and cilia transport mutant MEFs	113
Figure 4.2	PP2A activity assay and un-methylated and methylated PP2Ac	115
Figure 4.3	mTORC1 signaling in WT and cilia transport mutant MEFs	116
Figure 4.4	Response to PDGF-AA stimulation with and without rapamycin	117
Figure S1	P-Akt <sup>T308</sup> localization in WT and cilia transport mutant MEFs	119
Figure S2	P-Akt <sup>T308</sup> levels of <i>Dync2h1</i> <sup>lln</sup> MEFs grown in 0.5% serum	120
Figure S3	<i>Ift172</i> <sup>wim</sup> MEFs do not form cilia during rapamycin treatment	122
Figure 5.3	PDGF-AA/ $\alpha\alpha$ , Akt, mTORC1, and PP2A interactions	123
REFERENCES		125

## **Chapter 1: Cilia, signaling, and oligodendrocyte development**

## 1.1 Introduction

Cilia are microtubule-based organelles with essential roles in human development and disease. Primary cilia, specialized cilia that act like antennae, are on nearly every mammalian cell at least once during a cell's life cycle, and are critical for signaling and other functions. A number of syndromes, collectively termed ciliopathies, are caused by mutations in genes that affect cilia structure or ciliary cargo trafficking. Symptoms within this class of disorders may include cystic kidneys, retinal degeneration, left-right patterning defects, and polydactyly (Goetz and Anderson, 2010). Research *in vivo* and *in vitro* demonstrate that disruption of cilia affects multiple signaling pathways, including Sonic hedgehog (Shh), mammalian target of rapamycin (mTOR), and platelet derived growth factor AA/ $\alpha$  (PDGF-AA/ $\alpha$ ) signaling (Boehlke et al., 2010; Huangfu et al., 2003; Schneider et al., 2005, 2010).

This thesis presents the results from *in vitro* and *in vivo* models used to investigate the link between primary cilia and PDGF-AA/ $\alpha$  signaling. In this introduction, I review cilia structure, provide an overview of Shh, mTOR, PDGF-AA/ $\alpha$ , and PI3K/AKT signaling, and discuss a phosphatase called protein phosphatase 2A (PP2A). In chapter 3, I provide evidence to suggest that cilia are not essential for oligodendrocyte (OL) development *in vivo*. Next, in chapter 4, I present a novel link between cilia trafficking and PP2A, and demonstrate that inhibition of mTORC1 in cilia mutants restores response to PDGF-AA/ $\alpha$  signaling *in vitro*. Finally, I discuss the implications of PP2A as a shared component which links Shh, mTOR, PDGF-AA/ $\alpha$ , and PI3K/AKT signaling to cilia in vertebrates.

## 1.2 Cilia

*This section begins with an overview of the microtubule-based structure that forms the core of the cilium, and then describes the structural differences between two classes of cilia. The later half of this section describes the components of intraflagellar transport (IFT) and their roles in ciliary trafficking and structure. It will also cover the roles of non-IFT components in trafficking, structure, and response to ciliary signaling pathways. Section 1.3 will go into detail over specific cilia transport mutants.*

### Structure

The core structure of the cilium is the axoneme, an outer ring of nine microtubule doublets. Each microtubule doublet in the outer ring is composed of a 13 protofilament microtubule (termed the A tubule) connected to an 11 protofilament microtubule (termed the B tubule) (**Figure 1.2.1 A**). Cilia with a central pair of complete microtubules are classified as motile, while those without a central pair are classified as primary (Hopkins, 1970) (**Figure 1.2.1 B, C**). Motile cilia also contain radial spokes and axonemal dyneins which regulate ciliary beating and generate force for ciliary bending (Heuser et al., 2009; Warner, 1976) (**Figure 1.2.1 B**). Microtubules of the axoneme nucleate from the basal body, located at the base of the cilium. The basal body derives from the mother centriole of the centrosome, and is composed of nine microtubule triplets (SOROKIN, 1962; Vorobjev and Chentsov YuS, 1982).

In the transition zone (TZ), the microtubule triplets of the basal body become the doublets of the axoneme (Gilula and Satir, 1972). Transition fibers within this region anchor the basal body to the plasma membrane and may act as a “gate”

which regulates entry of ciliary cargoes (Anderson, 1972; Deane et al., 2001). The ciliary necklace is a region of plasma membrane that surrounds the TZ and may regulate diffusion of membrane associated proteins (Gilula and Satir, 1972).

Beneath the ciliary necklace, and distal to the transition fibers, are Y-shaped fibers of unknown composition which appear to connect the microtubule doublets to the ciliary necklace (Gilula and Satir, 1972; Heller and Gordon, 1986; Reiter et al., 2012).

A septin barrier, localized at the base of the cilium within the TZ, also appears to regulate diffusion of proteins from the plasma membrane to the ciliary membrane (Hu et al., 2010; Kim et al., 2010).

### Intraflagellar transport

IFT is the dynamic process of cargo transport along the outer doublets of cilia, and is essential for ciliary assembly and maintenance (Cole et al., 1998; Kozminski et al., 1993; Pazour et al., 1998, 1999; Piperno and Mead, 1997).

Trafficking of cargo via IFT occurs along the outer doublet microtubules, and is controlled by kinesins and cytoplasmic dyneins (**Figure 1.2.2**). The kinesin motor complex kinesin super family complex 3 (KIF3) controls anterograde trafficking, and cytoplasmic dyneins regulate retrograde trafficking. Cargo is carried in and out of primary cilia by two IFT complexes: IFTA and IFTB. The IFTB complex interacts with kinesin motors for anterograde transport of cargo, and the IFTA complex regulates retrograde transport of cargo with dynein motors.

Kinesin motors bring cytoplasmic dynein, IFTA and IFTB complexes, and IFT cargos from the base of the cilium to the tip (Ou et al., 2005; Pedersen et al., 2005; Williamson et al., 2012). IFT cargo loading and unloading occurs at the tip, and

cytoplasmic dyneins are activated for anterograde transport of IFTA-bound cargos, IFTB, and kinesins (Pazour et al., 1998; Porter et al., 1999). The cargoes carried by IFT include structural components of the axoneme (Cole et al., 1998). Thus, loss or disruption of IFT alters the structure of cilia; in the absence of anterograde transport cilia do not form, and in the absence of retrograde transport cilia become bulged and swollen (Blacque et al., 2006; Hou et al., 2004; Huang et al., 1977; Pazour et al., 1998, 2000; Porter et al., 1999). IFT also regulates ciliary trafficking of proteins and membrane receptors that belong to multiple cilia-linked signaling pathways (Liem et al., 2012; Ocbina and Anderson, 2008). When IFT is disrupted, these proteins and membrane receptors can fail to localize or exit the cilium, which leads to disruptions in cilia dependent signaling pathways (May et al., 2005).

### **1.3 IFT and cilia transport mutants**

*This section introduces several proteins with roles in IFT or ciliary trafficking.*

*The mutant alleles described below are used experimentally in chapter four.*

Much of what is known about IFT comes from work in *Chlamydomonas reinhardtii*, a unicellular algae that uses its two flagella (or cilia) for mobility. In *C. reinhardtii*, defects in IFT disrupt flagellar structure and motility (Huang et al., 1977). Cilia and IFT were first connected to vertebrate signaling in the early 2000's with the publication of two essential papers that revealed links between cilia and signaling in vertebrates. The first paper linked loss of cilia, caused by a hypomorphic mutation in an IFTB component, to the development of cystic kidneys in a mouse model of polycystic kidney disease (PKD) (Pazour et al., 2002). The second paper showed that IFTB components and kinesin regulate cell fate specification of the

developing spinal cord in mouse (Huangfu et al., 2003). Subsequent research in a variety of IFT mutants in mouse further defined the role of cilia in signaling and in human disease.

### IFT172

IFT172 is a 172kDa peripheral component of the IFTB complex that localizes to the basal body and along the axoneme of cilia. While it is not required for assembly of the IFTB core, IFT172 is required for anterograde trafficking of a core IFTA component, and also regulates the switch from anterograde to retrograde IFT at the tip of the cilium (Lucker et al., 2005; Williamson et al., 2012). The IFT172 mutant, *Ift172<sup>wimple</sup>* (*Ift172<sup>wim</sup>*), is a protein null allele of *Ift172*. *Ift172<sup>wim</sup>* embryos die between e10.5-e11.5 and lack cilia (Huangfu et al., 2003). *Ift172<sup>atrioventricular canal 1</sup>* (*Ift172<sup>ave</sup>*) is a hypomorphic allele of *Ift172*; *Ift172<sup>ave</sup>* mutants produce both WT and mis-spliced *Ift172* transcript and protein (Friedland-Little et al., 2011). Unlike *Ift172<sup>wim</sup>* mutants, *Ift172<sup>ave</sup>* mutants survive to birth, and have truncated cilia. Human patients with hypomorphic mutations in *Ift172* have longer cilia and disrupted trafficking (Halbritter et al., 2013).

### IFT122

IFT122 is one of six IFTA components, and is part of the heterotrimeric core with IFT140 and IFT144 that regulates retrograde transport of the IFTB complex and its associated cargo (Behal et al., 2012; Lucker et al., 2005). In the absence of IFT122, retrograde trafficking is reduced, tips of cilia become swollen with accumulated IFTB components, and stability of the IFT140/144 subcomplex is reduced (Behal et al., 2012; Qin et al., 2011; Tsao and Gorovsky, 2008; Walczak-

Sztulpa et al., 2010). *Ift122*<sup>sister of open brain</sup> (*Ift122*<sup>sopb</sup>) mouse mutants, which are protein null for *Ift122*, have short, swollen cilia, similar to cilia of human fibroblasts isolated from patients with mutations in IFT122 (Qin et al., 2011; Walczak-Sztulpa et al., 2010). *Ift122*<sup>sopb</sup> embryos die around e13.5, and display phenotypes similar to other IFT mutants, including polydactyly and exencephaly (Qin et al., 2011).

### DYNC2H1

The cytoplasmic dynein motor complex is composed of dynein cytoplasmic 2 heavy chain 1 (DYNC2H1) and cytoplasmic dynein 2 light intermediate chain 1 (DYNC2LI1) and is required for the retrograde transport of IFA, IFTB, and their associated cargos. In the absence of functional DYNC2H1, IFTA and IFTB complexes accumulate at the tips of cilia (Merrill et al., 2009; Schmidts et al., 2013). The cilia of *Dync2h1*<sup>ling-ling</sup> (*Dync2h1*<sup>ln</sup>) mutants, protein null for *Dync2h1*, are of similar length to WT cilia, but are bulged all along the length due to accumulation of IFTA and IFTB complexes and cargos (Ocbina et al., 2011).

### ARL13B

ADP ribosylation factor (Arf) like 13b (ARL13B) is a small GTPase that localizes to primary and motile cilia in mammalian cells. ARL13B belongs to the Arf family of GTPases and contains a C-terminal tail not found in other Arf family members. *Arl13b* has roles in cilia structure and in localization of Shh signaling components. The *Arl13b*<sup>hennin</sup> (*Arl13b*<sup>hnn</sup>) allele is caused by a T to G transversion in a splice acceptor site of exon 2, and is protein null for *Arl13b* (Caspary et al., 2007). *Arl13b*<sup>hnn</sup> cilia are short and stubby, and the B tubule of the outer doublet fails to connect to the A tubule. *Arl13b*<sup>hnn</sup> embryos do not survive past midgestation (e13.5),

at which point they display exencephaly, spina bifida, polydactyly (extra digits), and abnormal placement of the visceral organs (heterotaxia). ARL13B mutations are found in patients with the ciliopathy Joubert syndrome (Cantagrel et al., 2008).

#### **1.4 Sonic hedgehog**

*In vertebrates, cilia trafficking proteins regulate multiple aspects of Shh signaling. This segment begins with a review of the components of Shh signaling, and then discusses the role of Shh in neural tube patterning. Next, I detail specification of the precursor motor neuron (pMN) domain and the neural-glia switch. I then briefly introduce oligodendrocytes, which are specified from the pMN domain. Finally, I go over the roles of specific IFTs and cilia trafficking components in Shh signaling.*

##### Signaling

The Hedgehog (Hh) family is an evolutionarily conserved signaling pathway with critical roles in multiple aspects of vertebrate and invertebrate development. Vertebrates have three Hh signaling subgroups: Desert Hedgehog (Dhh), Indian Hedgehog (Ihh), and Shh (Echelard et al., 1993). The subgroups share the same components and steps in signal transduction, but differ in temporal and tissue expression. This segment will discuss Hh signaling in the context of Shh.

Shh signaling culminates in the expression or repression of Hh target genes by the Glioma (Gli) transcription factors. In the absence of Hh ligand, full length Gli proteins (Gli<sup>FL</sup>) are processed into cleaved repressors (Gli<sup>R</sup>) and inhibit Hh target gene expression, while presence of Hh ligand promotes Gli<sup>FL</sup> processing into activators (Gli<sup>A</sup>) that stimulate Hh target gene expression (Pan et al., 2006; Wang et al., 2000a). Gli proteins form a complex with Suppressor of Fused (Sufu), which

inhibits the transcriptional activity of both Gli<sup>A</sup> and Gli<sup>R</sup>, and stabilizes Gli's by inhibiting their degradation (Ding et al., 1999; Kogerman et al., 1999; Méthot and Basler, 2000; Pearse et al., 1999; Stone et al., 1999; Wang et al., 2000b; Zhang et al., 2013). In mammals, there are three Gli genes: Gli1, Gli2, and Gli3 (Hui et al., 1994; Ruiz i Altaba, 1998). Gli1 is an activator, while Gli2 and Gli3 can act as either activators (Gli2<sup>A</sup>, Gli3<sup>A</sup>) or repressors (Gli2<sup>R</sup>, Gli3<sup>R</sup>) (Sasaki et al., 1999). Gli2 primarily functions as an activator, while Gli3 is primarily a repressor (Ruiz i Altaba, 1998; Sasaki et al., 1999).

Processing of Gli<sup>FL</sup> into Gli<sup>R</sup> or Gli<sup>A</sup> is influenced by transmembrane receptors Patched-1 (Ptch1) and Smoothed (Smo). In the absence of Shh ligand, Ptch1 inhibits plasma membrane localization and activation of Smo, and Gli<sup>FL</sup> proteins are phosphorylated and undergo proteolytic processing into Gli<sup>R</sup> (Chen et al., 2009; Tukachinsky et al., 2010; Wang et al., 2000a, 2010). Three kinases, protein kinase A (PKA), glycogen synthase kinase 3 $\beta$  (GSK3 $\beta$ ), and casein kinase 1 (CK1), sequentially phosphorylate Gli<sup>FL</sup> proteins at multiple residues, which leads to cleavage of phosphorylated Gli<sup>FL</sup> into Gli<sup>R</sup> (Pan et al., 2006; Tempé et al., 2006; Wang and Li, 2006; Wang et al., 2000a). Cleaved Gli<sup>R</sup> translocates to the nucleus, and inhibits Shh target gene transcription (Haycraft et al., 2005; Krauss et al., 2008, 2009; Wen et al., 2010).

Shh ligand binding to Ptch1 permits the plasma membrane localization and activation of Smo, which facilitates Gli<sup>A</sup> production and transcription of Shh target genes (Denef et al., 2000; Marigo and Tabin, 1996; Marigo et al., 1996; Taipale et al., 2002). Smo then promotes dissociation of the Sufu-Gli complex, which is required

for Gli<sup>FL</sup> processing into Gli<sup>A</sup> (Haycraft et al., 2005; Liu et al., 2012; Tukachinsky et al., 2010).

### Sonic hedgehog and cilia

Vertebrate and invertebrate Hh signaling share many of the same components, and one of several differences is that vertebrate Hh signaling requires primary cilia. Components of Shh signaling localize to primary cilia in vertebrates, and their localization is influenced by Shh ligand, IFT, and other cilia trafficking proteins (Larkins et al., 2011; Liem et al., 2012; Ocbina et al., 2011; Qin et al., 2011; Stottmann et al., 2009). In the absence of Shh ligand, Ptch1 localizes along the length of cilia, small amounts of Gli proteins are present at the tip, and both Smo and Sufu are largely absent (Corbit et al., 2005; Larkins et al., 2011; Rohatgi et al., 2007). Presence of Shh leads to decreased Ptch1 localization in the cilium, increased Smo localization along the axoneme, and accumulation of unphosphorylated Gli proteins and Sufu at the tip (Corbit et al., 2005).

Gli<sup>FL</sup> processing into Gli<sup>A</sup> and Gli<sup>R</sup> requires trafficking to and from the cilium, while the actions of Smo, Sufu, and PKA fine tune Gli processing (Chen et al., 2009; Haycraft et al., 2005; Wen et al., 2010). Sufu shuttles Gli<sup>FL</sup> to and from the cilium, and in the presence of Shh ligand both Sufu and Gli<sup>FL</sup> are enriched at the ciliary tip (Chen et al., 2011; Wen et al., 2010). Activated, ciliary Smo mediates dissociation of the Sufu-Gli complex to permit processing of Gli<sup>FL</sup> and subsequent translocation of processed Gli's to the nucleus (Humke et al., 2010). PKA localizes to the base of the cilium and acts to inhibit ciliary entry and activation of Gli2 (Tuson et al., 2011). PKA also phosphorylates Sufu, which promotes Sufu localization to the cilium;

dephosphorylation of Sufu facilitates its ciliary exit and subsequent degradation (Chen et al., 2011).

### Neural tube patterning

Shh signaling is required for cell fate specification in the neural tube. Patterning of cell fates in the neural tube serves as a readout of Shh activity, and changes in patterning are indicative of changes in Shh activity *in vivo*.

The ventral neural tube is divided into five cell fate domains: going from most ventral to dorsal, they are the floor plate, p3, pMN, p2, p1, and p0 (**Figure 1.4 A**) (Dessaud et al., 2008). Each cell fate domain has distinct gene expression patterns that are specified by an opposing gradient of Gli<sup>A</sup> and Gli<sup>R</sup>, established by diffusion of Shh ligand from the notochord and floor plate (Stamatakis et al., 2005; Yamada et al., 1993) (**Figure 1.4 B**). Gli<sup>R</sup> is greatest in the most dorsal regions of the neural tube, while Gli1 and Gli2<sup>A</sup> are highly expressed in the ventral regions (**Figure 1.4 C**) (Stamatakis et al., 2005).

Gli2 is required for specification of the floorplate and p3 domain, which requires high levels of Shh activity, and Gli3 is required for specification of the p1, p0, and dorsal progenitor domains, which require low levels of Shh activity (Ding et al., 1998; Matise et al., 1998; Persson et al., 2002; Ruiz i Altaba, 1998; Wijgerde et al., 2002). Loss of either Gli2 or Gli3 shifts the Shh activity gradient, and thus disrupts neural tube patterning. In the absence of Gli2, the primary Gli activator, Shh activity is reduced (Ding et al., 1998; Matise et al., 1998; Qi, Yingchuan, Tan, Min, Hui, Chi-Chung, Qui, 2003). As a result, the floorplate and p3 domains are not specified, and the pMN domain, which requires intermediate levels of Shh activity, expands

ventrally. Loss of Gli3, the primary Gli repressor in the neural tube, in the neural tube leads to an increase in Shh activity and a dorsal-ventral progenitor switch in the p1, p0, and most ventral of the dorsal domains (Meyer and Roelink, 2003; Persson et al., 2002; Sasaki et al., 1999). Markers of these domains, which are normally exclusive of one another, are co-expressed in cells that expand dorsally at the expense of the most ventral of the dorsal cell fate domains (Persson et al., 2002).

#### IFT, Shh, and neural tube patterning

Trafficking of Shh components is regulated in part by IFT and ciliary trafficking. As such, perturbations of IFT and cilia trafficking alter Shh component trafficking, Shh activity, and neural tube cell fate specification in distinct ways.

Gli processing into Gli<sup>A</sup> and Gli<sup>R</sup> requires trafficking to and from the cilium, and is facilitated by IFT (Tukachinsky et al., 2010). In the absence of IFTB or kinesin motor function, cilia are lost and no Gli trafficking occurs (Huangfu and Anderson, 2005; Huangfu et al., 2003; Liu et al., 2005). In the absence of IFTA or dynein motor function, Gli proteins can enter the cilium, but anterograde trafficking is blocked and Gli proteins accumulate in the cilium (May et al., 2005; Ocbina et al., 2011). In both cases, Gli processing is disrupted, and neither Gli<sup>A</sup> nor Gli<sup>R</sup> are produced (Friedland-Little et al., 2011; Liem et al., 2012; Liu et al., 2005; Ocbina and Anderson, 2008; Ocbina et al., 2011; Qin et al., 2011).

Smo, and Sufu shuttle in and out the cilium during Shh signaling, and this trafficking is important for regulation of response to Shh ligand. Although IFTA mutants and dynein mutants both disrupt anterograde IFT and accumulate Gli proteins, they differ in trafficking of Smo and Sufu. *Dync2h1<sup>ln</sup>* mutants have

abnormal, constitutive localization of Smo and Sufu, while Smo and Sufu trafficking is unperturbed in *Ift122<sup>sopb</sup>* mutants (Ocbina et al., 2011). The accumulation of Smo and Sufu in *Dync2h1<sup>ln</sup>* mutants seems to be caused by disruptions in cilia structure that interferes with normal trafficking and interactions of Shh components, due to accumulation of IFTBs and other ciliary cargos (Ocbina et al., 2011).

The differences in Shh component trafficking in IFTB, IFTA, kinesin, and dynein mutants contribute to the differences in Shh activity observed between them, and suggests that the dynamics of Shh component trafficking into and out of cilia is important for proper pathway regulation. The neural tube serves as an ideal readout for how changes in IFT alter Shh activity, as various IFT mutants affect neural tube cell fate specification in different ways. Mutants that lack IFTB, kinesin motor function, or dynein motor function show decreased Shh activity, while IFTA mutants show increased Shh activity. In the neural tube of IFTB, kinesin, and dynein mutants, cell fates requiring the highest levels of Shh activity, including the floor plate and p3 domain, are not specified (Huangfu et al., 2003; May et al., 2005). The absence of Gli<sup>R</sup> in these mutants permits specification of cell fates that require lower levels of Shh activity, although their expression is shifted ventrally (Huangfu et al., 2003; May et al., 2005). Conversely, in the neural tubes of certain IFTA mutants, the ventral fates expand dorsally, and the dorsal fates do not expand ventrally (Liem et al., 2012; Qin et al., 2011).

The small GTPase Arl13b has a unique role in trafficking of Shh components and in Gli processing. In the neural tube of *Arl13b<sup>hnn</sup>* mutants, there is an expansion of an intermediate level of Shh activity, and Gli<sup>A</sup>, but not Gli<sup>R</sup>, processing is inhibited

(Caspary et al., 2007). Correspondingly, cell fates which require the highest levels of Shh activity are not specified, while cell fates which require intermediate levels of Shh activity expand ventrally and dorsally (Caspary et al., 2007). At the molecular level, Smo is constitutively localized to cilia, Sufu and Gli proteins fail to enrich at the tips in response to Shh stimulation, and levels of Ptch1 do not change upon Shh stimulation (Larkins et al., 2011). In WT MEFs, Smo is evenly distributed along the length of the cilium, while in *Arl13b<sup>hnn</sup>* MEFs, Smo is found in punctae in one or more regions along the cilium. Thus, Arl13b regulates both the ciliary entry and distribution of Shh components.

### **1.5 Neural stem cell debate**

*Although the molecular markers that identify MNs and OLPs are known, the mechanism of how pMN cells switch from specifying MNs and then OLPs is not. In this section I briefly discuss the mixed and sequential models of MN and OLP specification from the pMN domain.*

#### Neural stem cell debate

The pMN domain is specified at intermediate levels of Shh activity starting at e8.5 in the neural tube, and is recognized by expression of the basic helix-loop-helix (bHLH) Oligodendrocyte Lineage Transcription Factors 1 and 2 (OLIG1 and OLIG2) (Lu et al., 2002; Sun et al., 2001; Zhou and Anderson, 2002; Zhou et al., 2000, 2001). The pMN domain specifies both motor neurons (MNs) at e9.5, and then oligodendrocyte precursors (OLPs) at e12.5. The switch from specification of MNs to specification of OLPs is called the neuron-glia switch, and is controlled by the combination of multiple factors. Olig2 is required for specification of both MNs and

OLPs, while *Olig1* regulates the development of OLPs into mature OLs, but is not sufficient for MN or OLP specification (Lu et al., 2002; Zhou and Anderson, 2002).

The different roles of *Olig1* and *Olig2* in MN and OLP specification led to the mixed model, which proposes that the pMN domain contains two populations: one population gives rise to MNs, and the other to OLPs (Lu et al., 2002) (**Figure 1.5 A**). Another model, the sequential model, proposes that MNs and OLPs are sequentially specified from different waves of *Olig1/2+* progenitors in the pMN domain (Wu et al., 2006) (**Figure 1.5 B**). In this model, an *Olig1/2-* population of NSC gives rise to waves of *Olig1/2+* progenitors at different times. From e9.5 to e12.5, the *Olig1/2+* progenitors specify MNs. At e12.5, a new set of *Olig1/2+* progenitors gives rise to OLPs.

The sequential model is supported by data from *Olig1-DTA* embryos, where expression of the diphtheria toxin fragment A (DTA) gene was placed under the control of *Olig1-Cre*, such that any *Olig1+* cells in were killed due to presence of DTA (Wu et al., 2006). Expression of *Olig1* and DTA at e8.5 led to massive death and depletion of *Olig1+* cells from e9.0-e11.5. However, *Olig2+* cells remained present from e8.5-e16.5. Given that *Olig1* and *Olig2* completely overlap in expression at e10.5, during which there was massive cell death, *Olig2+* cells should also die and be depleted from the neural tube. The presence of *Olig2+* cells was interpreted to mean that an *Olig1/2-* population of NSCs repopulates the pMN domain with *Olig1/2+* cells, and that the *Olig2+* cells are recently specified from NSCs in the pMN domain. The repopulation of the pMN domain would then lead to a continual “generation and killing” *Olig1/2+* pMN cells, and can account for the presence of *Olig2* in *Olig1-DTA*

embryos (Wu et al., 2006). Alternatively, the Olig2+ cells are not constantly specified from NSCs, and instead represent a population of Olig2+ that have yet to express Olig1.

### **1.6 PDGF-AA/ $\alpha$ signaling through PI3K/AKT and mTORC1**

*In this segment, I review PDGFAA/ $\alpha$ , PI3K/AKT, and mTORC1 signaling, all of which are linked to primary cilia (Boehlke et al., 2010; Schneider et al., 2005, 2010). Compared to Shh signaling, very little is known about how these pathways use primary cilia, and how different kinds of IFT and cilia transport mutants. Here, the focus is primarily on the non-ciliary mechanisms of each pathway, and ends with a segment that reviews the current knowledge of their roles in the context of primary cilia.*

#### PDGFs and PDGFRs

The PDGF signaling family consists of four ligands (PDGF-A, B, C, and D) and two receptors (PDGFR $\alpha$  and  $\beta$ ) (**FIGURE 1.6**) (Claesson-Welsh et al., 1989; Haniu et al., 1994; Heldin et al., 1981; Raines and Ross, 1982; Ross et al., 1974). PDGF ligands form homodimers and heterodimers via disulfide linkages, and bind the extracellular domains of PDGF receptors  $\alpha$  and  $\beta$  homodimers and heterodimers. PDGF-AA binds PDGFR $\alpha$ , PDGF-AB and CC bind PDGFR $\alpha$  and  $\alpha\beta$ , PDGF-DD binds PDGFR $\beta\beta$  and  $\alpha\beta$ , and PDGF-BB binds PDGFR $\alpha$ ,  $\alpha\beta$ , and  $\beta\beta$  (**Figure 1.6 A, B**) (Fredriksson et al., 2004).

PDGFRs are transmembrane proteins, and contain two intracellular tyrosine kinase domains. Binding of dimerized PDGF ligand to the immunoglobulin-like (IgG) extracellular domain induces dimerization of PDGFRs and activation of the intracellular tyrosine kinase domains, which autophosphorylate specific tyrosine

residues within the kinase domains in trans (Ek and Heldin, 1984; Kelly et al., 1991). Phosphorylated residues then serve as docking sites for downstream signaling components and facilitate the transfer of phosphate groups from ATP to tyrosine residues on docked protein (Hoch and Soriano, 2003). In the context of PDGF-AA/ $\alpha$  signaling, these include SRC family kinases, growth factor receptor-bound protein 2 (GRB2), phosphatidylinositol-3 kinase (PI3K), PLC $\gamma$ , and CRK proteins (Bazenet et al., 1996; Eriksson et al., 1995; Hooshmand-Rad et al., 1998; Ikuno et al., 2002; Rupp et al., 1994; Yokote et al., 1998). This section will focus on PI3K signaling.

### Phosphatidylinositols and Phosphoinositide 3-kinase

Phosphatidylinositols (PtdIns) are a group of acidic phospholipids composed of a phosphatidic acid backbone linked to an inositol ring by a phosphate group, and regulate a large range of signaling pathways (Falkenburger et al., 2010). The inositol ring contains five free hydroxyl groups, three of which may be phosphorylated, resulting in seven varieties of PtdIns (Cote and Crain, 1993; Stephens et al., 1991). PI3Ks catalyze the conversion of different PtdIns and are divided into groups based upon structure and substrate specificity (Falasca and Maffucci, 2012; Wymann and Pirola, 1998). PDGFR $\alpha$ , phosphorylated on tyrosines 731 and 742 (P-PDGFR $\alpha^{Y731/742}$ ), recruits class IA PI3Ks. Binding of PI3K to P-PDGFR $\alpha^{Y731/742}$  leads to phosphorylation of the regulatory subunit of PI3K, which induces a conformational change that reveals the PI3K kinase domain. This permits PtdIns(4,5)P<sub>2</sub> substrate entry and the subsequent transfer of a phosphate from ATP on to PtdIns(4,5)P<sub>2</sub>, generating PtdIns(3,4,5)P<sub>3</sub>. (Cuevas et al., 2001; Miller et al.,

2010; Zhang et al., 2011). PtdIns(3,4,5)P<sub>3</sub> can then recruit specific substrates to the plasma membrane, such as AKT and its activators.

### AKT

AKT is a serine/threonine protein kinase activated by numerous signaling pathways, including PDGFAA/ $\alpha$  (Andjelković et al., 1996; Bellacosa et al., 1991, 1993; Burgering and Coffey, 1995; Coffey and Woodgett, 1991; Jones et al., 1991; Kohn et al., 1995). In turn, AKT activates a number of pathways involved in cell cycle regulation, apoptosis, glucose metabolism, and synaptic signaling (Calnan and Brunet, 2008; Eijkelenboom and Burgering, 2013; Mayo and Donner, 2001; Okumura et al., 2002; Welburn et al., 2007). The three isoforms of AKT have different signaling functions, as nulls of each isoform have distinct phenotypes, likely due to differences in isoform tissue expression, kinase activity, and sub-cellular localization (Heron-Milhavet et al., 2011; Hers et al., 2011; Lee et al., 2011; Stambolic and Woodgett, 2006; Walker et al., 1998).

All AKT isoforms contain a pleckstrin homology (PH) domain that binds PtdIns(3,4,5)P<sub>3</sub>. Generation of PtdIns(3,4,5)P<sub>3</sub> by PDGF-AA/ $\alpha$  signaling through PI3K recruits AKT and its activators 3-phosphoinositide-dependent kinase 1 (PDK1) and mTORC2 to the plasma membrane (Bellacosa et al., 1991, 1993; Hers et al., 2011; Thomas et al., 2002). AKT binding to PtdIns(3,4,5)P<sub>3</sub> induces a conformational change that facilitates phosphorylation by PDK1 at threonine 308 (P-AKT<sup>T308</sup>) and by mTORC2 at serine 473 (P-AKT<sup>S473</sup>) (Alessi et al., 1997a, 1997b; Gan et al., 2011; Hers et al., 2011; Sarbassov et al., 2004, 2005; Yang et al., 2006). P-AKT<sup>S473</sup> regulates the specificity of AKT towards its substrates, while P-AKT<sup>T308</sup>

regulates the kinase activity of AKT (Alessi et al., 1996; Moore et al., 2011). AKT is inactivated through dephosphorylation of P-AKT<sup>T308</sup> by PP2A and of P-AKT<sup>S473</sup> by PH domain leucine-rich repeat-containing protein phosphatase 1 (PHLPP1).

Activated AKT promotes signaling through mTORC1, which both inhibits AKT, through downregulation of RTKs that promote activation of AKT, and maintains P-AKT<sup>T308</sup> through inhibiting PP2A activity. These roles of mTORC1 are described in more detail below.

### mTORC1

mTORC1 is a multi-complex, rapamycin sensitive, serine-threonine kinase which incorporates signals from growth factors, hormones, and nutrient levels to promote cell growth, survival, and proliferation (Brown et al., 1994; Chiu et al., 1994; Dowling et al., 2010; Hara et al., 2002; Moore et al., 1996; Sabers et al., 1995; Sarbassov et al., 2004, 2006). mTOR is the kinase of the mTORC1, Regulatory Associated Protein of mTORC1 (RAPTOR) recruits substrates for phosphorylation, and mTOR Associated Protein LST8 Homolog (mLST8) promotes complex integrity (Guertin et al., 2006; Hara et al., 2002).

Growth factors signal through PI3K/AKT to activate the kinase activity of mTORC1. Ras homolog enriched in brain (RHEB) is activated by PI3K/AKT signaling and promotes activation of mTORC1. RHEB is maintained in a GDP-bound, inactivate state through the actions of the tuberous sclerosis complex 1/2 (TSC1/2), a GTPase activating protein (GAP) (Cai et al., 2006; Inoki et al., 2002; Potter et al., 2002). AKT promotes the dissociation of TSC1/2, relieving inhibition on RHEB and promoting

its GTP-bound state. GTP-bound RHEB then promotes activation of mTOR kinase activity, and thus mTORC1 signaling (Sancak et al., 2007).

Activation of mTORC1 signaling is assayed by phosphorylation of its targets, although the phosphorylation may be inhibitory or activating, depending on the substrate. For example, phosphorylation of ribosomal serine/threonine-protein kinases (S6Ks) is activating, while phosphorylation of eukaryotic translation initiation factor 4E binding proteins (4E BPs) is inhibitory (Burnett et al., 1998; Isotani et al., 1999). Activation of S6Ks, such as p70 S6K, and inhibition of 4E BP1s, promotes translation, and thus increases protein synthesis and cell growth (Burnett et al., 1998).

mTORC1 has opposing roles that simultaneously maintain its activation and lead to its downregulation. Maintenance of mTORC1 signaling occurs in part through mTORC1 inhibition of PP2A. This inhibits dephosphorylation of P-AKT<sup>T308</sup>, allowing for continued inhibition of TSC1/2 and activation of mTOR activity through RHEB. Inhibition of PP2A also inhibits the dephosphorylation of p70 S6K on threonine 389 (P-p70 S6K<sup>T389</sup>), further promoting translation (Hahn et al., 2010).

Negative feedback through mTORC1 downregulates transcription of RTK's, including PDGFR $\alpha$  (Zhang et al., 2003, 2007). Decreased protein expression of PDGFR $\alpha$ , and of other RTKs, leads to decreased activation of AKT, and eventually decreased activation of mTORC1 signaling. Signaling through AKT is further dampened by relief of mTORC1 inhibition on PP2A, which permits dephosphorylation of P-AKT<sup>T308</sup>.

Because mTORC1 is involved in negative and positive feedback loops, long term inhibition of mTORC1 ultimately leads to the establishment of a new steady state level of AKT signaling, through loss of feedback inhibition of RTKs (Rodrik-Outmezguine et al., 2011). Though inhibition on PP2A is also relieved by inhibition of mTORC1, the initial increase in PP2A dephosphorylation of AKT<sup>T308</sup> is transient due to increased RTKs signaling through PI3K to phosphorylated AKT.

### PDGFAA/ $\alpha$ , and mTORC1 signaling in the context of cilia

#### *PDGFAA/ $\alpha$*

PDGFR $\alpha$  is one of several RTKs found localized to primary cilia *in vitro* and *in vivo*, and AKT, which is activated through PDGF-AA/ $\alpha$  signaling, is found at the basal body (Danilov et al., 2009; Schneider et al., 2005, 2010). Primary cilia seem to be required for PDGF-AA/ $\alpha$  signaling, as cells which lack primary cilia, through a hypomorphic mutation in *Ift88* (*Ift88<sup>orpk</sup>*), have decreased PDGFR $\alpha$  expression and fail to respond to PDGF-AA ligand stimulation (Schneider et al., 2005, 2010). WT cells, when stimulated with PDGF-AA, show increased phosphorylation of PDGF-AA/ $\alpha$  targets, such as AKT (Burgering and Coffey, 1995; Franke et al., 1995). Unlike WT MEFs, *Ift88<sup>orpk</sup>* MEFs do not increase P-AKT<sup>S473</sup> upon PDGF-AA stimulation, nor do they migrate towards a gradient of PDGF-AA ligand (Schneider et al., 2005, 2010). Together, this data was interpreted to mean that PDGF-AA/ $\alpha$  signaling is regulated through primary cilia in fibroblasts.

#### *mTORC1*

Polycystic kidney disease (PKD) is a symptom of several ciliopathies, and is characterized by the formation of fluid filled cysts that prevent normal kidney

functions (Boehlke et al., 2010; Fogelgren et al., 2011; Hildebrandt et al., 2011; Ibraghimov-Beskrovnaya and Natoli, 2011; Kotsis et al., 2013; Tobin and Beales, 2009). In a healthy kidney, the primary cilia of renal epithelial cells bend to detect urine flow, which inhibits abnormal cell growth through downregulation of mTORC1 signaling (Rydholm et al., 2010; Shiba et al., 2005). Defects in cilia are associated with increased mTORC1, and increased activation of the mTOR pathway is seen in patients with PKD and in mouse models of PKD where anterograde IFT is compromised (Boehlke et al., 2010; Brook-Carter et al., 1994; Canaud et al., 2010; Distefano et al., 2009; Pazour et al., 2000; Shillingford et al., 2006).

The first evidence linking PKD to cilia came from work in mice with a hypomorphic allele of *Ift88*, called *Ift88<sup>Oak Ridge Polycystic Kidney</sup>* (*Ift88<sup>orpk</sup>*) (Moyer et al., 1994; Pazour et al., 2000). These mice develop cystic kidneys at a young age, and have short cilia in their kidneys (Pazour et al., 2000, 2002). This provided the first evidence that defects in cilia contributed to PKD *in vivo*. Separate work later demonstrated that knock-down of *Ift88* increased activation of mTORC1 targets and lead to increased cell size *in vitro* (Boehlke et al., 2010).

Components of mTORC1 signaling localize to and around cilia. Liver kinase B1 (*Lkb1*) and AMP-activated protein kinase (*Ampk*), negative regulators of mTORC1, are found at the basal body and along the cilium, respectively (Boehlke et al., 2010). *Lkb1* phosphorylates *Ampk*, and phosphorylated *Ampk* (P-*Ampk*) accumulates at the basal body. P-*Ampk* suppresses mTORC1 activity, thus inhibiting cell growth. Cilia appear necessary for *Lkb1* mediated inhibition of mTOR *in vitro*. In

the absence of cilia, Lkb1 can not phosphorylate Ampk, and as a result both mTORC1 activity and cell size are increased (Boehlke et al., 2010).

### **1.7 Oligodendrocytes**

*Oligodendrocytes are the myelinating glia of the vertebrate central nervous system, and are absolutely indispensable for proper neuronal function and signaling. This segment reviews the specification and maturation of OLPs, discusses the vital role of PDGF-AA/ $\alpha$  signaling in OLP development, and touches on myelination, which is the ultimate purpose of OLs.*

#### Oligodendrocyte progenitor specification

OLPs are specified in several regions of the neural tube and of the brain at different time points. Regardless of the timing or location of their specification, all OLPs express PDGFR $\alpha$  and undergo the same developmental steps in becoming mature, post-mitotic, myelinating OLs (Kessaris et al., 2006) (**Figure 1.7.1**). In the mouse neural tube, the first wave of OLPs are specified from the pMN domain around e12.5 (Wu et al., 2006). Shh signaling, and likewise cilia, are essential for the establishment of the pMN domain, and aside from remyelination, later stages of OLP/OL development are Shh independent (Ellison and de Vellis, 1994; Lu et al., 2002). OLPs are also generated from Olig2+ cells in dorsal domains at e15.5 and from progenitors in the ventricular zone shortly after birth (Pringle and Richardson, 1993; Vallstedt, Anna, Klos, Joanna M., Ericson, 2005). Loss of PDGFR $\alpha$  does not prevent the establishment of OLPs, but it does impair their ability to migrate and proliferate (McKinnon et al., 2005; Soriano, 1997). After specification, PDGFR $\alpha$ + OLPs proliferate and migrate laterally and dorsally through the neural tube in

response to PDGF-AA and other signaling cues (Frost et al., 2009; Noll and Miller, 1993; Vora et al., 2011).

### Oligodendrocyte progenitor maturation

The stages of OLP development into mature OLs are characterized by expression of different markers and by cell morphology (**Figure 1.7.1**). OLPs become pre-OLs, then immature OLs, pre-myelinating OLs, and finally mature/myelinating OLs. Pre-OLs retain the ability to proliferate, but have decreased migration and begin to form thin plasma membrane extensions that will later become the myelin sheath. Pre-OLs also express sulfatides and glycolipids that are expressed through the remainder of OL development, and are recognized by the O4 antibody (Bansal et al., 1989; Gard and Pfeiffer, 1990). Loss of response to PDGF-AA in pre-OLs occurs through inhibition of signaling downstream of PDGFR $\alpha$ , not through decreased PDGFR $\alpha$  expression (Hart et al., 1989).

Immature OLs are marked by expression of galactosylceramides (GalC) and RIP (Berger and Frotscher, 1994; Friedman et al., 1989; Gard and Pfeiffer, 1990; Raff et al., 1979; Sommer and Schachner, 1981; Zalc et al., 1981). At this stage, migration ceases, proliferation diminishes, and 2',3'-cyclic nucleotide-3'-phosphohydrolase (CNP), the earliest marker of myelination, is expressed (Bansal and Pfeiffer, 1992; Sprinkle, 1989; Vogel and Thompson, 1988). Expression of other myelin proteins, proteolipid protein (PLP), myelin-associated glycoprotein (MAG), and myelin basic protein (MBP) characterize mature, pre-myelinating OLs (Ikenaka et al., 1992; Peyron et al., 1997). Expression of myelin/oligodendrocyte glycoprotein (MOG) is unique to myelinating OLs, which wrap extensions of the plasma membrane around

axons from multiple neurons (Solly et al., 1996). The details of myelination are discussed in a separate section of this segment.

#### PDGF-AA/ $\alpha$ signaling in OLPs

PDGF-AA, secreted by neurons and astrocytes, is essential for the proliferation, migration, and early survival of OLPs (Barres et al., 1992; Fruttiger et al., 1999, 2000; Gard and Pfeiffer, 1993; Milner et al., 1997; Richardson et al., 1988; Robinson et al., 1998; Rogister et al., 1999; Yeh et al., 1991). Mice null for PDGF-A have severe defects in OL development and subsequently in myelination (Fruttiger et al., 1999). During embryogenesis, there are significantly fewer immature and mature OLs populating the spinal cord. Most PDGF-A null mice die shortly after birth, but those that survive present with a severe dsymyelinating phenotype in the form of tremor and decreased white matter tracts (Fruttiger et al., 1999).

Knock-in mice with mutations that prevent PDGF-AA/ $\alpha$  signaling to PI3K, *PDGFR $\alpha$ <sup>PI3K</sup>*, or to V-Src Avian Sarcoma (Schmidt-Ruppin A-2) Viral Oncogene Homolog (Src), *PDGFR $\alpha$ <sup>Src</sup>*, have impaired migration and proliferation of OPCs in the spinal cord (Decker and ffrench-Constant, 2004; Klinghoffer et al., 2002a). Both *PDGFR $\alpha$ <sup>PI3K</sup>* and *PDGFR $\alpha$ <sup>Src</sup>* mutants mimic the hypomyelination pattern of the brain seen in PDGF-A knock-outs, demonstrating the importance of PI3K and Src signaling for PDGF-AA/ $\alpha$  induced migration and proliferation of OLs.

In OLPs, PDGF-AA signals primarily through PI3K to promote proliferation and migration, while PDGFAA/ $\alpha$  signaling through PLC $\gamma$  promotes proliferation, but not migration (McKinnon et al., 2005). Response to PDGF-AA is dose dependent, and excess PDGF-AA promotes over-proliferation of OLPs (Calver et al., 1998).

However, excessive OLPs die during differentiation because contact between axons and mature OLs is required to ensure OL survival; in the absence of that contact, mature OLs undergo apoptosis (Calver et al., 1998; Trapp et al., 1997).

### Myelination

The final stage of OL development is myelination, which is indispensable for proper central nervous system function (Taveggia et al., 2010). Mature OLs myelinate axons by wrapping a multilayered sheath of myelin around axon segments (**Figure 1.7.2**). In humans, myelination begins midway through the first trimester and continues on through adolescence (Gao et al., 2009; Taveggia et al., 2010). Mice follow a similar progression of myelination. During midgestation, OLs begin to express myelin proteins such as CNP, PLP, and MBP (Peyron et al., 1997; Timsit et al., 1995). Myelination is most active after birth, and peaks during the second and third weeks of life (Bradl and Lassmann, 2010; Jordan et al., 1989; Rogister et al., 1999; Rowitch, 2004; Verity and Campagnoni, 1988).

AKT and mTORC1 signaling promote myelination *in vivo* (Flores et al., 2008; Narayanan et al., 2009; Tyler et al., 2009a). Expression of a constitutively active AKT in pre-oligodendrocytes promotes hyper-myelination through at least 10 months postnatal, without altering OL proliferation or death. AKT signaling promotes myelination through activation of mTORC1, which in turn promotes transcription of myelin proteins such as MBP and PLP (Narayanan et al., 2009; Tyler et al., 2009a).

### PDGF-AA/ $\alpha\alpha$ , cilia, and oligodendrocytes

Cilia are essential for OLP specification, in so far that specification of the pMN domain requires cilia-dependent Shh signaling. Response to PDGF-AA/ $\alpha\alpha$  signaling

appears to require primary cilia *in vitro*, but whether cilia are important for PDGF-AA/ $\alpha$  signaling of OLP development is unknown. OLIG1 and PDGFR $\alpha$ + OLPs have cilia as late as p7 in the developing mouse brain, as do oligodendroglial-like cells found in tumors (Cenacchi et al., 1996; Gangal and Fuchs, 2009). Adult OLPs expressing NG2 rarely display cilia, which suggests that cilia are important for early, not late, OL development (Gangal and Fuchs, 2009).

### **1.8 Introduction to PP2A**

*PP2A is a serine-threonine phosphatase involved in the regulation of dozens of pathways. In this chapter, I discuss PP2A subunit composition and regulation, and the role of PP2A in cilia. Finally, I focus on the roles of PP2A in regulation of the PI3K/AKT, mTOR, and Hh/Shh signaling pathways.*

#### Structure and regulation of PP2A

Protein phosphatase 2 A (PP2A) is a heterotrimeric phosphatase composed of structural (PP2Aa), regulatory (PP2Ab), and catalytic (PP2Ac) subunits. A single PP2A holoenzyme contains a PP2Aa, PP2Ab, and PP2Ac subunit. In mammals, both PP2Aa and PP2Ac have an  $\alpha$  and  $\beta$  isoform, while PP2Ab subunits come from the structurally unrelated B, B', B'', and B''' families (**Figure 1.8**). There are at least twenty-three isoforms from the combined regulatory B subunit families, and over 90 holoenzyme combinations are proposed to exist (Sents et al., 2013). The isoforms of PP2Aa, PP2Ab, and PP2Ac differ greatly in tissue expression, abundance, subcellular localization, and in binding to one another and to substrates (Hemmings et al., 1990; Khew-Goodall et al., 1991; Zhou et al., 2003). These differences,

combined with the multitude of holoenzyme compositions, facilitate the fine tuning of PP2A activity and substrate specificity.

PP2Ac and PP2Ab associations are partially regulated by reversible methylation and phosphorylation on several residues of the carboxy-terminal tail of PP2Ac. Methylation of PP2Ac does not alter overall PP2A catalytic activity, but is required for holoenzyme assembly with the PP2Ab B family (Ikehara et al., 2007; Yu et al., 2001). PP2Aa and the remaining PP2Ab families (B', B'', and B''') do not absolutely require PP2Ac methylation, although methylation may facilitate association with PP2Ab B' isoforms (Evans and Hemmings, 2000; Tolstykh et al., 2000; Yu et al., 2001). Leucine carboxyl methyltransferase (LCMT1) and protein phosphatase methylesterase (PME-1) add and remove the methyl group on PP2Ac at L309, respectively (De Baere et al., 1999; Favre et al., 1994; Lee and Stock, 1993; Lee et al., 1996; Leulliot et al., 2004; Ogris et al., 1999; Xie and Clarke, 1993). LCMT1 and PME-1 have distinct subcellular localizations, which correspond to localization of methylated and demethylated PP2Ac. Methylated PP2Ac is found primarily in the cytoplasm, where the majority of LCMT1 is localized, while PME-1 and demethylated PP2Ac predominate the nucleus (Longin et al., 2008). Less is known about PP2A phosphorylation, except that phosphorylation of one residue, T304, may inhibit assembly with PP2Ab B family subunits, and phosphorylation of another, Y307, may interfere with PP2Ab B' subunit assembly (Chen et al., 1992; Chung et al., 1999; Schmitz et al., 2010).

PI3K/AKT/mTOR signaling

PP2A is a negative regulator of the PI3K/AKT signaling pathway and is also negatively regulated by AKT signaling through mTORC1. PP2A negatively regulates AKT by dephosphorylation of P-AKT<sup>T308</sup>, and mTORC1 inhibits PP2A by promoting PP2A complex formation with its negative regulator  $\alpha 4$  (Du et al., 2013; Edelstein and Rockwell, 2012; Inui et al., 1998; Smetana et al., 2006). However, inhibition of mTORC1 through rapamycin does not fully ablate P-Akt<sup>T308</sup>, despite increasing the activity of PP2A (Li et al., 2013). This is due to the loss of a negative feedback loop, whereby mTORC1 represses PI3K signaling through downregulation of RTKs. In the absence of this feedback inhibition, RTKs/PI3Ks continue to facilitate phosphorylation of Akt<sup>T308</sup> and establish a new basal level of P-Akt<sup>T308</sup>.

#### Hh/Shh signaling

In *D. melanogaster*, PP2A is a regulator of Hh signaling activity (Casso et al., 2008; Nybakken et al., 2005). Like the vertebrate Gli proteins, Ci is phosphorylated by PKA, GSK3 $\beta$ , and CK1 and then proteolytically processed into Ci repressor (Ci<sup>R</sup>) to inhibit Hh target gene transcription. The fly PP2Ab subunit Twins (Tws) regulates dephosphorylation of Ci, and thus inhibits proteolytic processing of Ci<sup>FL</sup> and promotes formation of Ci activator (Ci<sup>A</sup>) (Jia et al., 2009; Uemura et al., 1993). Another fly PP2Ab subunit, Widerborst (Wdb), dephosphorylates CKI phosphorylated Smo to maintain Hh activity at an intermediate threshold (Jia et al., 2009; Su et al., 2011). Furthermore, PP2A is shown to dephosphorylate the CK1 sites on Smo, again promoting an intermediate range of Hh activity (Jia et al., 2009; Su et al., 2011).

In mammalian Shh signaling, PP2A may dephosphorylate GLI3<sup>FL</sup>, as inhibition of PP2A decreases the electrophoretic mobility of GLI3<sup>FL</sup> *in vitro*, indicative of hyperphosphorylated Gli3 (Wen et al., 2010). In the developing cerebellum, Shh signaling upregulates expression of the PP2Ab subunit B56 $\gamma$  to promote dephosphorylation of S6K and to maintain proliferation of cerebellar granule neuron precursors (CGNPs) (Chizhikov et al., 2007; Mainwaring and Kenney, 2011; Spassky et al., 2008; Wechsler-Reya and Scott, 1999).

### PP2A and cilia

In *C. reinhardtii*, both PP2Ac and a regulatory B subunit (most conserved to the PP2Ab B family) localize to the outer doublet of the flagellar axoneme, and are required for flagellar motility (Elam et al., 2011; Yang et al., 2000). In non-ciliated mammalian HeLa cells, PP2Aa, PP2Ac, and the PP2Ab B56 $\alpha$  subunits localize to centrosomes, although this localization has only been studied in the context of cell division (Andersen et al., 2003; Flegg et al., 2010; Horn et al., 2007; Lange et al., 2013). Most interestingly, the PP2A inhibitor, I2PP2A/SET, localizes to cilia of human diploid retinal epithelial (ARPE-19) cells (Wang and Brautigan, 2008). All together, there is great precedent for a role of PP2A in signaling pathway linked to primary cilia in mammals.

### **1.9 Outstanding questions and preview**

Cells which lack primary cilia have decreased PDGFR $\alpha$  expression and fail to respond to PDGF-AA ligand stimulation (Schneider et al., 2005, 2010). Given that different alterations in IFT and cilia trafficking proteins affect Shh signaling in distinct, tissue-specific ways, it is possible that the relationship between PDGF-AA/ $\alpha$  and IFT is similarly complex. However, PDGF-AA/ $\alpha$  signaling has only been

investigated in the context of IFTB mutants and in fibroblast cells. It remains unknown how, or if, other IFTs and cilia trafficking proteins regulate PDGF-AA/ $\alpha$  signaling, and if primary cilia are essential for PDGF-AA/ $\alpha$  signaling of other cell types *in vivo*. PDGF-AA/ $\alpha$  signaling is essential for OL development and myelination, however defects in myelination are not a symptom of ciliopathies and only in rare cases has delayed or hypomyelination been reported in patients with the ciliopathy Joubert syndrome (Fruttiger et al., 1999; Harting et al., 2011; Klinghoffer et al., 2002a; Quisling et al., 1999; Schneider et al., 2005, 2010; Senocak et al., 2010). The lack of response to PDGF-AA stimulation in *Ift88<sup>orpk</sup>* MEFs predicts that loss of cilia in OLs would be detrimental for their development, as OLs absolutely require PDGF-AA/ $\alpha$  signaling *in vivo*.

Given that OLs require PDGF-AA/ $\alpha$  signaling, and that PDGF-AA/ $\alpha$  signaling is thought to require primary cilia, I asked if cilia are required for OL development, *in vivo*. In chapter 3, I address this question and present the results of my work where cilia were either crippled or ablated *in vivo* in OLs. In chapter 4, I address whether several cilia transport proteins regulate response to PDGF-AA stimulation *in vitro*. For these experiments, I used fibroblast cell lines of the cilia transport mutants outlined in section 1.3. Chapter 4 also discusses the relationship between cilia trafficking and PP2A activity, and how it relates to regulation of PDGF-AA/ $\alpha$ , PI3K/AKT, and mTORC1 signaling.

## **Chapter 2: Materials and Methods**

### Brain tissue lysis

Brain tissues and optic nerves used for Western blot analysis were processed as follows: Brains and optic nerves were dissected in ice cold PBS, and desired tissues (optic nerve, brainstem) were placed in 1.5ml tubes and flash frozen on dry ice and ethanol. Samples were labeled and stored at -80°C until required.

Samples were removed from dry ice and placed on wet ice for lysis. Optic nerve samples were rehydrated in 5ul of phosphate buffered saline (PBS; 37 mM NaCl, 10 mM Phosphate, 2.7 mM KCl in water, pH 7.4) and sonicated 2x (5 seconds) in 50ul of homogenization buffer with protease inhibitors (5mM Tris pH8, 0.32M sucrose, 1mM PMSF, 1ug/ml each of aprotinin, leupeptin, and pepstatin A in water). All other brain tissue samples were minced with a small pair of scissors, homogenized with a pestle in 100ul of homogenization buffer with protease inhibitors (25 strokes for brainstem, 20 strokes for all other brain tissues), and sonicated 2x (5 seconds).

### MEF lysis

MEFs were rinsed with ice cold PBS, scraped off the plate with a cell scraper, and lysed in 150 ul of RIPA buffer (100mM Tris pH7.5, 100mM NaCl, 1% TritonX-100, 0.5% deoxycholate, 0.1% SDS, 0.5mM PMSF in water) supplemented with protease (Roche-1697498001) and phosphatase inhibitors (Sigma-P5726 and Roche-04906845001). MEF lysates were passed through a 25<sup>5</sup>/<sub>8</sub> gauge needle 10 times while on ice, and spun-down at 16,000 rcf (10 min at 4°C), after which the supernatant was transferred to a clean tube.

For experiments to look at demethylated PP2Ac, lysates were prepared as described above, along with an additional treatment to demethylate PP2Ac (Jackson and Pallas, 2012). To demethylate PP2Ac in MEF lysates, supernatant from lysates were treated with an equal volume of 200 mM NaOH (5 minutes on ice) and then neutralized with a volume of neutralization buffer (133.3 mM HCl and 333.3 mM Tris pH 6.8) equal to 3/5 the volume of protein lysate + NaOH.

Base treated and un-treated lysates were aliquoted, flash frozen on dry ice and ethanol, and stored at -80°C until required, or used immediately for protein quantification and Western blot analysis.

#### Protein quantification

Protein concentrations were determined by Coomassie or by the Pierce BCA Protein Assay Kit (cat# 23227). Protein concentrations determined by Coomassie were done as follows: 1-2ul of protein lysate was mixed with 8ul of loading buffer (50 mM Tris-HCl pH 6.8, 2% SDS, 1% glycerol, 1%  $\beta$ -mercaptoethanol, 12.5 mM EDTA, 0.02 % bromophenol blue in water), run on a 6% PAGE until loading dye reached about halfway down glass plate, gel removed from glass plates and placed in plastic dish with enough Coomassie buffer (0.1% w/v Coomassie brilliant blue, 50% v/v methanol, 10% v/v acetic acid, 10% v/v water) to cover gel, covered and microwaved until gel turned blue, rinsed with water, rinsed in enough Coomassie destain buffer (50% v/v methanol, 40% v/v acetic acid, 10% v/v water) to cover gel, and microwaved in Coomassie destain until background blue was gone and blue bands were clearly visible. The intensities of the bands were compared to determine

how much of each sample was required to get close-to equal loading for Western blot analysis.

Protein concentrations determined using the Pierce BCA Protein Assay Kit were done as follows: Albumin standards were made by diluting the provided albumin in PBS to make 20ug, 1ug, 0.5ug, 0.25ug, 0.125ug, 0.625ug, and 0ug albumin standards. Protein samples were diluted 1:20 in PBS. Enough volume is made for each standard and sample to have at least three replicates. 25ul of each albumin standard and protein sample were loaded into a deep dish 96 well plate. Working reagent (WR) was prepared by mixing kit reagents A and B at a ratio of 50 parts A:1 part B. 200ul of WR was added to each well of the 96 well plate. Plates was covered, placed in a black plastic bag, and placed in a 37°C incubator for 25 minutes.

Following 25 minute incubation, plate was brought over to spectrophotometer (in Li Lab, room 355), and remained covered in black bag. Plate was read at 562nm to obtain protein concentrations of samples.

#### SDS PAGE and Western blotting analysis

Prepared protein lysates (from optic nerve, brain tissue, or MEFs) were mixed with loading buffer, separated by SDS-PAGE on 4–20% Mini-PROTEAN TGX Precast Gels (456-1096EDU) with SDS running buffer (50 mM Tris, 0.384 M glycine, 0.2% SDS in water), and transferred to Trans-Blot Turbo nitrocellulose membranes (Biorad-170-4059) using the Trans-Blot Turbo system (Biorad-170-4155). Transfers were done using the pre-programmed setting “High MW” (10 minutes; 2.5A constant for 2 mini gels or 1.3A constant for 1 mini gel). Membranes were processed as follows: Blocked in Pierce T20 blocking buffer (Pierce-37538) (10 min

at room temperature), incubated with primary antibodies in T20 blocking buffer (overnight at 4°C), 3x washes in 0.1% TBST (20 mM Tris base, 150 mM NaCl, 0.1% Tween-20 in water, pH 7.6) (5 min each at RT), incubated with HRP-conjugated secondary antibodies (GE Healthcare Life Sciences, NA934, and NA931) in 5% w/v non-fat milk in 0.1% TBST (1 hour at room temperature), 3x washes in 0.1% TBST (10 min at room temperature).

After antibody incubations and washes, membranes were prepared for development as follows: Excess 0.1% TBST drained off, membrane placed protein side up on cling wrap, ECL reagent at 1:1 (Amersham ECL Prime, Cat# RPN2232) added to protein side of membrane, membrane covered for 5 minutes at room temperature, ECL drained off membrane, membrane sealed in cling wrap and placed in cassette for developing. Signals detected with autoradiography film (Denville, E3012).

Band intensities were measured with Fiji software and normalized to actin or eIF5 $\alpha$  loading control before averaging (McLean and Bennett, 2013).

### Embryo dissections

e.10.5-e12.5 embryos were dissected in ice cold PBS + 0.4% BSA, fixed in 4% PFA (1 hour on ice), washed 3x in ice cold PBS (30 minutes on ice), and sunk in 30% sucrose (30% w/v sucrose in 0.1M sodium phosphate buffer) (overnight at 4°C). The next day, excess sucrose was removed by washing embryos in Tissue-TEK OCT (VWR-25608-930) (2x, 30 minutes at room temperature). Embryos were embedded in Tissue-TEK OCT in plastic cubes, placed on a metal block surrounded by dry ice to freeze, and stored at -80°C or -20°C.

### Perfusion

Perfusion was performed, as follows, on mice p7 and older for collection of brain tissue to be used for immunofluorescence. All steps, unless indicated, were performed under a fume hood. Mice were anesthetized through administration of isoflurane by inhalation, and tested for full anesthetization by absence of reflex after firm pinching of the foot with forceps. Fully anesthetized mice were placed with the ventral side facing up and all four limbs pinned onto a Styrofoam block. Anesthetization was maintained by placing a Kimwipe dipped in isoflurane over the nose of the mouse. Dissection proceeded as follows: Ethanol sprayed on ventral side, scissors used to cut skin, skin removed, diaphragm cut, ribcage cut and removed to reveal heart, right atrium of heart cut to permit blood flow, perfusion needle placed in left ventricle and held in place during perfusion. For perfusion, 5-10mLs of ice cold PBS was used to clear the body of blood (in some cases, more PBS was used until drainage from right ventricle was primarily clear), 10-20 mL of 4%PFA was used for fixation. Successful perfusion was determined by stiff limbs and tail. Heads were cut off with scissors, brain tissue was removed, washed in PBS (3x, 30 minutes, on ice), and sunk in a minimum of 10mL of 30% sucrose in a 15mL conical vial (overnight at 4°C). The next day, excess sucrose was removed by washing brains in Tissue-TEK OCT (2x, 30 minutes at room temperature). Brains were embedded in Tissue-TEK OCT in plastic cubes, placed on a metal block surrounded by dry ice to freeze, and stored at -80°C or -20°C.

### Sectioning

Frozen embryos and brain tissues embedded in Tissue-TEK OCT were removed from plastic cubes and sectioned on a Leica CM 1850 cryostat. e10.5-e12.5 embryos were sectioned at 10 $\mu$ M and e16.5-e18.5 embryos and p5-p21 brains were

sectioned at 20 $\mu$ M. Slides with sectioned tissues air dried for several hours at room temperature, and were stored in plastic slide boxes at -80°C or -20°C.

### Immunofluorescence

Before incubation with primary antibodies, glass slides with embryo sections were permeabilized in antibody wash buffer (PBS, 0.1% TritonX-100, 1% heat-inactivated sheep serum) (10 minutes at room temperature). Glass coverslips with MEFs were rinsed with cold PBS, fixed with 4% paraformaldehyde (PFA) (10 min at room temperature), and then permeabilized in antibody wash buffer (10 minutes at room temperature) before incubating with primary antibodies..

For primary antibody staining, all samples were incubated with primary antibodies diluted in antibody wash buffer (overnight at 4°C), washed 3x in antibody wash buffer (20 minutes at room temperature), incubated with secondary antibodies (Alexa Fluors®) diluted in antibody wash buffer (1 h at room temperature), washed 2x in antibody wash buffer (30 minutes at room temperature), and mounted with ProLong Gold Antifade (Invitrogen-P36930). Coverslips sat at room temperature for 10 minutes before the edges were sealed with nail polish, and given another 10 minutes to dry before storage at 4°C in a dark box.

Fluorescence was visualized on either an Olympus FluoView 100 confocal IX81 inverted microscope, Nikon Structured Illumination Microscope, or a Leica DM600B upright microscope. Images were processed using Fiji software (Schindelin et al., 2012).

### Mouse strains and genotyping

The following mouse strains were used: *Olig1-Cre (Olig1<sup>tm1</sup>(cre)Rth*, from D. Rowitch; MGI:2179311), *Nestin-Cre (Tg(Nes-cre)1Kln*; JAX 003771; MGI:2176173), *PLP-GFP* (from Y. Feng), *Arl13b<sup>flox</sup>* (*Arl13b<sup>tm1Tc</sup>*; MGI:4948239), *Ift88<sup>flox</sup>* (*Ift88<sup>tm1.1Bky</sup>*, from B. Yoder; MGI:3710186), and *Arl13b<sup>hennin</sup>* (*Arl13b<sup>hnn</sup>*; MGI:3578151).

Mouse strains used for MEFs were: *Ift172<sup>wimple</sup>* (*Ift172<sup>wim</sup>*; MGI:2682066), *Ift172<sup>atrioventricular canal 1</sup>* (*Ift172<sup>avc1</sup>*, from K. Anderson; MGI:4821824), *Ift122<sup>sister of open brain</sup>* (*Ift122<sup>sopb</sup>*, from J. Eggenschwiler; MGI:3578529), *Arl13b<sup>hennin</sup>* (*Arl13b<sup>hnn</sup>*), *Dync2h1<sup>ling-ling</sup>*. (*Dync2h1<sup>ln</sup>*, from K. Anderson; MGI:3578144).

DNA for genotyping was obtained from ear punches, tail snips, or yolk sacs. Ear punches and tail snips were digested in Direct lysis buffer (Viagen 102-T) with 4mg/ml proteinase K at 55°C, overnight, boiled at 85°C for 45 minutes to inactivate proteinase K, and stored at 4°C. Yolk sacs were digested in PCR lysis buffer (50mM Tris pH8.8, 0.5% Tween 20 in water), boiled at 85°C to inactivate proteinase K for 15 minutes, and stored at 4°C. DNA samples were diluted 1:10 in sterile water for PCR genotyping. Primers and PCR conditions are described below:

All genotyping was performed with Choice Taq (Denville Scientific Inc, CB4050-3.), except for PLP-GFP and Ift88 conditional PCR programs, which used AmpliTaq Gold (Roche, N12338). Primers were stored at a 100uM working stock in sterile water in -20°C. Working stock primer solutions were composed of 5uM of both forward and reverse primer (10uM combined) in sterile water, except for the Ift88 conditional PCR program (5uM of “Shared Forward”, 2.5uM each of “Flox & WT

Reverse” and “Deleted Reverse”). Per PCR reaction, 5.1175ul PCR mix (2x Denville PCR buffer, 0.4M each of dATP, dCTP, dGTP, dTTP, 3mM MgCl<sub>2</sub> in sterile water), 0.575ul working stock primers, and 0.08ul taq mix were used.

**Cre PCR program for *Olig1-Cre*, and *Nestin-Cre* lines:** 94°C, 3 min; (94°C, 30 sec, 60°C, 1 min, 72°C, 1 min)x 35 repeats; 72°C, 4 min; 21°C, ∞.

oIMR1084 (Cre TG Forward primer): GCG GTC TGG CAG TAA AAA CTA TC

oIMR1085 (Cre TG Reverse primer): GTG AAA CAG CAT TGC TGT CAC TT

oIMR0042 (Control Forward primer): CTA GGC CAC AGA ATT GAA AGA TCT

oIMR0043 (Control Reverse primer): GTA GGT GGA AAT TCT AGC ATC ATC C

Use Cre TG and Control primers separately.

Expected bands: For Cre TG primers, one band if Cre+, no band if Cre-. For Control primers, one band (for Cre+ and Cre-).

**Eppitaq PCR program for *Arl13b<sup>hmn</sup>* allele:** 94°C, 2 min; (94°C, 20 sec; 55°C, 30sec; 72°C, 45sec)x 55 repeats; 72°C, 7 minutes; 21°C, ∞.

hnn147 Forward: AAT GCC TCA AGT GCC TCT TT

hnn147 Reverse: GGG ACT CAT CTT TGG GAA CA

hnn174 Forward: TGT GGG TGG CAT ATG TAG GA

hnn174 Reverse: GCT AGC TAT TTT CTG TTG CTG GA

Use hnn147 and hnn174 primers separately.

**PLP-GFP program for *PLP-GFP* allele:** 94°C, 12 min; (95°C, 30sec; 58°C, 30 sec; 72°C, 30sec)x 35 repeats; 72, 10min; 22°C, ∞.

PLP-GFP Forward-ACG TAA ACG GCC ACA AGT TC

PLP-GFP Reverse-GGG GTG TTC TGC TGG TAG TG

Expected band: ~500bp for presence of GFP, no band if GFP is not present.

**Ift88 conditional PCR program for *Ift88<sup>floxed</sup>* allele:** 94°C, 12 min; (95°C, 30sec; 58°C, 30 sec; 72°C, 30sec)x30 repeats; 72°C, 5min; 21°C, ∞.

Shared Forward-GCC TCC TGT TTC TTG ACA ACA GTG

Flox & WT Reverse-GGT CCT AAC AAG TAA GCC CAG TGT T

Deleted Reverse-CTG CAC CAG CCA TTT CCT CTA AGT CAT GTA

Expected bands: Floxed allele ~370bp, WT allele ~350bp, deleted allele ~270bp.

**Arl13b conditional PCR program for *Arl13b<sup>floxed</sup>* allele:**

Conditional Forward: AGG ACG GTT GAG AAC CAC TG

Conditional Reverse: AAG GCC AGC TTG GGT TAT TT

Expected bands: *Arl13b<sup>floxed</sup>* allele 679 bp, WT allele 526 bp, deleted allele 109 bp.

### MEF preparation

MEFs were prepared from e12.5 *Arl13b<sup>hnn</sup>* embryos, e11.5 *Ift172<sup>wim</sup>* embryos, and e11.5 *Ift122<sup>sopb</sup>* embryos. Embryos were dissected and placed in ice cold PBS + 0.4% BSA on ice. Individual embryos were dissected in dishes with fresh ice cold

PBS, head and visceral organs removed, yolk sacs saved for genotyping, and remaining tissue sucked into a syringe, capped with an 18 gauge needle and stored on ice until all embryos from a litter were processed. Embryos in syringe were brought on ice to the tissue culture hood, and syringes were sprayed down with ethanol before placing in hood. Tissues were homogenized in 1mL of pre-warmed DMEM high glucose (Corning-10-013) supplemented with 10% heat-inactivated fetal bovine serum (FBS; Corning-35-010) and 1% penicillin/streptomycin (P/S; Corning 30-002). Homogenized embryos were plated into tissue culture treated dishes that were pre-coated with 0.1% gelatin for at least one hour prior to plating embryo homogenates, and maintained in either DMEM high glucose supplemented with 10% FBS and 1% P/S or in DMEM/F12 (Corning-10-092) supplemented with 10% FBS and 1% P/S.

#### PDGF-AA, LY294002, rapamycin, okadaic acid, and FTY720 treatments

MEFs were grown until confluent on plates pre-coated with 0.1% gelatin and then serum-starved in DMEM/F12 for 48 h prior to treatments and subsequent processing for Western blot analysis. Individual treatments with the indicated substances were performed in the tissue culture hood as follows: 50 ng/ml PDGF-AA (dissolved in sterile 4mM HCl; R&D Systems 221-AA) treatment for 10 minutes; 50  $\mu$ M LY294002 (dissolved in DMSO; Cell Signaling 9901) treatment for 1 hour; 10 nM rapamycin (dissolved in DMSO; MP Biomedicals-159346) treatment for 24 hours; 200nM okadaic acid (dissolved in DMSO; Cell Signaling 5934) treatment for 3 hours; 10 $\mu$ M FTY720 (Sigma SML0700-5MG) treatment for 5 hours.

For dual PDGF-AA and LY294002 treatment, cells were treated with 50  $\mu$ M LY294002 for 1 hour, and then with 50 ng/ml PDGF-AA for the final 10 minutes of the LY294002 treatment. For dual okadaic acid and LY294002 treatment, cells were treated with 200nM okadaic acid for 3 hours, and then with 50  $\mu$ M LY294002 for the final hour of okadaic acid treatment. For dual PDGF-AA and rapamycin treatment, cells were treated with 10 nM rapamycin for 24 hours, and then with 50 ng/ml PDGF-AA for the final 10 minutes of the rapamycin treatment.

#### PP2A activity assay

The PP2A activity assay kit was purchased from Millipore (17-313). Before beginning experiment, all reagents were checked for contamination with phosphate by mixing 2-5ul of each reagent with 100ul of the Malachite Green Phosphate Detection Solution. Mixtures that turned green indicated contamination with phosphate and were not used for experiment. Phosphate standards were made for the following concentrations, using the phosphate standard provided by the kit, diluted in water: 2000pM, 1800pM, 1600pM, 1400pM, 1200pM, 1000pM, 800pM, 600pM, 400pM, 200pM, and 0pM.

The PP2A activity assay was performed following the manufacturer's protocol with protein lysates from WT, *Ift172<sup>wim</sup>*, *Ift122<sup>sopb</sup>*, and *Arl13b<sup>hnn</sup>* MEFs. At least three 10cm dishes of fully confluent MEFs, serum starved for 48 hours prior to lysis, were pooled together and used for each reaction (a total of 500ul of lysis buffer was used for three dishes). To prepare, MEFs were washed 3x with 10mL of TBS, lysed in the recommended lysis buffer (20mM imidazole-HCl, 2mM EDTA, 2mM EGTA in sterile water pH 7.0, to which 10 $\mu$ g/ml each of aprotinin, leupeptin,

pepstatin, 1mM benzamidine, and 1mM PMSF were added), sonicated for ten seconds (Li lab sonicator), spun down at 4°C for 5 minutes at 2000g, and supernatant transferred to clean 1.5mL tubes. To test for phosphate contamination, 2ul from each sample was added to 100ul of the Malachite Green Phosphate Detection Solution (if mixture turns green, sample is contaminated with phosphate and can not be used). Concentration of supernatants was determined using the Pierce BCA Protein Assay Kit, as described in Protein Quantification.

To each 500ug of sample lysate, the following were added: 4ug of anti-PP2Ac subunit (clone 1D6), 40ul of Protein A agarose slurry, and enough pNPP Ser/Thr Assay Buffer to bring the final volume up to 500ul. Samples were incubated at 4°C for 2 hours on an end-to-end, revolving, rotating, tube mixer (in 4°C cold room across from room 375). Beads were washed with 700ul TBS on ice and spun down briefly to pellet beads (2000g for 5 minutes) for a total of 3 rounds (wash, spin; wash, spin; wash, spin), followed by a final wash with 500ul Ser/Thr Assay Buffer, spin, and removal of buffer. To beads, 60ul of diluted phosphopeptide and 20ul of Ser/Thr Assay Buffer were added (for some samples, 1μM okadaic acid was added to the mixture during the phosphopeptide incubation to serve as a negative control), sealed tubes were placed in a covered beaker, incubated at 30°C in shaking incubator (in room with the ice machine, between the break room and room 355) for 10 minutes, and centrifuged briefly to pellet beads (2000g for 10 seconds). 25ul of supernatant from each sample was transferred into a well of the microtiter plate included in the kit (in triplicate), 100ul of Malachite Green Phosphate Detection Solution was added to each well, the mixture was incubated for 15 minutes at room

temperature, and the plate was read at 650nm using a spectrophotometer (in Li Lab, room 355). Absorbance of samples were determined based on the phosphate standard curve generated from the phosphate standards.

**Chapter 3: The role of Arl13b and Ift88 in oligodendrocyte development *in vivo***

### 3.1 Summary

*Arl13b<sup>hnn</sup>* embryos have an expanded intermediate level of Shh activity in the caudal neural tube, corresponding to an expansion of the pMN domain (Caspary et al., 2007). Both MNs and OLPs are specified from the pMN domain, and while there is an expansion of MNs, no PDGFR $\alpha$ <sup>+</sup> OLPs are seen by the time *Arl13b<sup>hnn</sup>* embryos die around e13.5. This raises the possibility that Arl13b has a role in OLP specification or development.

To circumvent the neonatal lethality of *Arl13b<sup>hnn</sup>* embryos and decipher a role for Arl13b in OL development, I deleted *Arl13b* at two time points using two tissue-specific Cre lines. *Olig1-Cre* at e8.5 in the pMN domain, and *Nestin-Cre* at e10.5 in neural stem cell precursors (NSC) (Lu et al., 2002; Tronche et al., 1999). To determine if intact cilia are required for OL specification or development, I used a conditional allele of *Ift88* to ablate cilia in the pMN domain and in NSC.

In both *Arl13b <sup>$\Delta$ Olig1-Cre</sup>* and *Arl13b <sup>$\Delta$ Nestin1-Cre</sup>*, I did not observe changes in OL development consistent with a model where cilia are essential for OL development *in vivo*. Similarly, *Ift88 <sup>$\Delta$ Olig1-Cre</sup>* and *Ift88 <sup>$\Delta$ Nestin1-Cre</sup>* failed to show deficits in OL development. With *Arl13b <sup>$\Delta$ Olig1-Cre</sup>* embryos, I also provide support for a model (discussed in section 1.5) where progenitors of the pMN domain are generated sequentially by neural stem cells (NSCs).

### 3.2 Introduction

OLs are the myelinating glia of the vertebrate central nervous system (Bunge and Glass, 1965; Wood and Bunge, 1991). PDGF-AA/ $\alpha$  signaling is indispensable for oligodendrocyte development, and is linked to primary cilia *in vitro* (Fruttiger et al.,

1999; Schneider et al., 2005). In mouse, loss of PDGF-A (*PDGF-A<sup>-/-</sup>*) or of PDGFR $\alpha$  signaling to PI3K/AKT (*PDGFR $\alpha$ <sup>PI3K</sup>*) results in decreased OLPs and OLs during prenatal development and in severe hypomyelination postnatally (Fruttiger et al., 1999; Klinghoffer et al., 2002b).

OLPs must migrate throughout the CNS before myelination of axons begins, and PDGF-AA is a powerful chemoattractant for OLs. The optic nerve is one of the final regions reached by migrating OLs. In *PDGF-A<sup>-/-</sup>* mice, the optic nerve it is one of the most hypomyelinated regions of the CNS, and *Ift88<sup>orpk</sup>* MEFs fail to migrate towards PDGF-AA ligand (Fruttiger et al., 1999; Schneider et al., 2010).

Arl13b is a small, putative GTPase that localizes to cilia and has a role in trafficking of Shh components and in building the axoneme.. *Arl13b<sup>hnn</sup>* mice are null for Arl13b and have defects in the ultrastructure of cilia and in Shh signaling. The cilia of *Arl13b<sup>hnn</sup>* mice are short and stubby, and the B tubule fails to connect to the A tubule in the outer doublets. Shh signaling components are misdistributed within the cilia of *Arl13b<sup>hnn</sup>* MEFs, and cells are unresponsive to Shh ligand, and instead have a constitutive moderate level of Shh activity. Ift88 is a component of the IFTB complex, which is required for anterograde trafficking of ciliary cargo. Loss of Ift88 leads to loss of cilia and an absence of Shh signaling activity.

Loss of either Arl13b or Ift88 is lethal; embryos die at e13.5 and e10.5, respectively, preventing investigation of OL specification or development. To circumvent the embryonic lethality, I used conditional alleles of *Arl13b* and *Ift88* to either cripple or ablate cilia in specific cell lineages (Caspary et al., 2007; Huangfu et al., 2003). *Olig1-Cre* restricts deletion to Olig1 expressing cells (*Arl13b<sup>ΔOlig1-Cre</sup>* and

*Ift88<sup>ΔOlig1-Cre</sup>*), while *Nestin-Cre* induces deletion in the NSC which give rise to the entire CNS (*Arl13b<sup>ΔNestin1-Cre</sup>* and *Ift88<sup>ΔNestin1-Cre</sup>*). Deletion in the pMN versus the entire CNS allows me to address whether cilia have a cell autonomous or non-autonomous role in OL specification and development. Both Cre lines are expressed before OLP specification; Cre expression is initiated at e8.5 in *Arl13b<sup>ΔOlig1-Cre</sup>* and *Ift88<sup>ΔOlig1-Cre</sup>* mice, and at e10.5 in *Arl13b<sup>ΔNestin1-Cre</sup>* and *Ift88<sup>ΔNestin1-Cre</sup>* mice.

### 3.3 Results

#### 3.3.1 Generation of *Arl13b<sup>ΔOlig1-Cre</sup>* mice, birth incidence, and post-natal weight

I crossed females homozygous for the conditional allele of *Arl13b* (*Arl13b<sup>lox/lox</sup>*) to *Arl13b<sup>+</sup>/Arl13b<sup>hnn</sup>*; *Olig1-Cre* males to generate *Arl13b<sup>lox</sup>/Arl13b<sup>hnn</sup>*; *Olig1-Cre* (*Arl13b<sup>ΔOlig1-Cre</sup>*) mutants. The *Arl13b<sup>hnn</sup>* allele and *Olig1-Cre* allele are linked and segregate together 85% of the time (recombination rate of 15%). Thus, 85% of progeny from the above cross will be *Arl13b<sup>lox</sup>/Arl13b<sup>+</sup>* or *Arl13b<sup>lox</sup>/Arl13b<sup>hnn</sup>*; *Olig1-Cre* (no recombination between the *Arl13b<sup>hnn</sup>* and *Olig1-Cre* alleles), while 15% will be *Arl13b<sup>lox</sup>/Arl13b<sup>hnn</sup>* or *Arl13b<sup>lox</sup>/Arl13b<sup>+</sup>*; *Olig1-Cre* (due to recombination between the *Arl13b<sup>hnn</sup>* and *Olig1-Cre* alleles). This predicts that the mutant will appear 42.5% of the time ( $\frac{1}{2} \times 85\% = 42.5\%$ ), while any of the three wild type genotypes will appear 57.5% of the time ( $15\% + \frac{1}{2} \times 85\% = 57.5\%$ ).

Half of the embryos with *Olig1-Cre* are wild type (*Arl13b<sup>lox</sup>/Arl13b<sup>+</sup>*; *Olig1-Cre*), and half are mutants (*Arl13b<sup>lox</sup>/Arl13b<sup>hnn</sup>*; *Olig1-Cre*). As previously reported in our lab, approximately 5% of *Olig1-Cre* positive embryos have leaky, ubiquitous Cre expression (Su, 2011). Thus, leaky Cre expression will occur in 2.5% of wild type

(*Arl13b<sup>flox</sup>/Arl13b<sup>+</sup>; Olig1-Cre*) embryos, and in 2.5% of mutant (*Arl13b<sup>flox</sup>/Arl13b<sup>hnn</sup>; Olig1-Cre*) embryos. Loss of *Arl13b* in all tissues is embryonic lethal, so 2.5% of *Arl13b<sup>flox</sup>/Arl13b<sup>hnn</sup>; Olig1-Cre* embryos will die during midgestation due to leaky Cre expression. This adjusts the predicted frequency of mutants to 40% (42.5% - 2.5% = 40%), and the predicted frequency of wild type to 60% (57.5% + 2.5% = 60%). I outline these calculations in **Figure 3.1A**. I observed *Arl13b<sup>ΔOlig1-Cre</sup>* pups 38.67% of the time at birth, which is not significantly different from the expected adjusted ratio of 40% (**Figure 3.1A, B**;  $p=0.7913$ ). Thus, deletion of *Arl13b* in the pMN domain at e8.5 is not embryonic lethal.

To determine if *Arl13b<sup>ΔOlig1-Cre</sup>* mice mimic the phenotype of *PDGF-A<sup>-/-</sup>* mice, I monitored seven *Arl13b<sup>ΔOlig1-Cre</sup>* mice and twelve wild type (WT) littermates over three months for survival, weight, and development of a tremor. A majority of *PDGF-A<sup>-/-</sup>* mice die around p14 (others survive to 6 weeks of age at most), present with a tremor that is indicative of myelination defects by p21, and become “increasingly runted” as they age (Fruttiger et al., 1999). Over this time, *Arl13b<sup>ΔOlig1-Cre</sup>* mice survived as long as WT littermates, and failed to present with a tremor, which is inconsistent with *Arl13b* being required for OL development (**Figure 3.1C**). While there was a trend towards decreased weight from p5-p21, no significant difference was observed between weights at the specified ages, and *Arl13b<sup>ΔOlig1-Cre</sup>* mice continued to gain weight with age (**Figure 3.1D**). These data demonstrate that loss of *Arl13b* in the pMN domain of *Arl13b<sup>ΔOlig1-Cre</sup>* mice is not lethal in embryos or young adults, nor does it mimic the postnatal phenotype of *PDGF-A<sup>-/-</sup>* mice.

### 3.3.2 Deletion of *Arl13b* in *Arl13b<sup>ΔOlig1-Cre</sup>* embryos

*Olig1-Cre* expression begins at e8.5, and *in vivo* turnover of Arl13b takes approximately 42 hours (Su et al., 2012). This predicts absence of Arl13b from the pMN domain of *Arl13b<sup>ΔOlig1-Cre</sup>* embryos by e10.5. To determine the timing of Arl13b turnover in the pMN domain of *Arl13b<sup>ΔOlig1-Cre</sup>* embryos, I stained neural tube sections of e10.5 embryos for Olig2 to mark the pMN domain and for Arl13b. By e10.5, deletion of Arl13b is complete in *Arl13b<sup>ΔOlig1-Cre</sup>* mice, shown by an absence of Arl13b staining in the Olig2+ pMN domain (**Figure 3.2 A-F**).

### 3.3.3 *Arl13b<sup>ΔOlig1-Cre</sup>* embryos and pups fail to display phenotypes indicative of disrupted OL development

To determine if Arl13b is required for migration and maturation of OLPs in the optic nerve, I looked at expression of PDGFR $\alpha$ + at p7 and of MBP at p11 in the optic nerves of WT and *Arl13b<sup>ΔOlig1-Cre</sup>* pups. At p7, PDGFR $\alpha$ + OLPs reach the optic nerve, and at p11 myelination in the optic nerve is reaching its peak (Foran and Peterson, 1992; Mudhar et al., 1993a; Wolswijk, Guus, Noble, 1995). At p11, there is no significant difference in MBP expression from protein lysates of WT and *Arl13b<sup>ΔOlig1-Cre</sup>* optic nerves (Figure 3.3). These data indicate that Arl13b is not required for myelination of the optic nerve in *Arl13b<sup>ΔOlig1-Cre</sup>* mice.

To determine if Arl13b is required for earlier stages of OLP migration and maturation in the neural tube, I looked at expression of Olig2, which marks OLPs at various stages of development, and at expression of MBP. At e16.5, when OLPs are actively migrating, Olig2+ OLPs are seen throughout the rostral and caudal neural tube of both WT and *Arl13b<sup>ΔOlig1-Cre</sup>* embryos (**Figure 3.4 B, D, F, H**). Furthermore, MBP is expressed in the rostral neural tube of both WT and *Arl13b<sup>ΔOlig1-Cre</sup>* embryos

(**Figure 3.4 A, E**). As MBP is expressed in both the neural tube and optic nerve of *Arl13b<sup>ΔOlig1-Cre</sup>* mutants, this suggests that Arl13b is not essential for the expression of MBP at the observed stages and locations. Thus, in the absence of Arl13b, OLP maturation into pre-myelinating OLs is on-track, and that OLs are able to migrate outward from the pMN domain where they are specified. Together, these data suggest that Arl13b is not essential for migration and maturation of OLPs in either the neural tube at e16.5, or to the optic nerve at p11.

### 3.3.4 Repopulation of the pMN domain with Arl13b expressing Olig2+ progenitors (in *Arl13b<sup>ΔOlig1-Cre</sup>* embryos at e12.5)

OLPs are specified from Olig1/2+ progenitors of the pMN domain at e12.5. To determine if Arl13b is required for earlier stages of OL development, I looked at the neural tubes of e12.5 embryos. Although I observe loss of Arl13b at e10.5 in the pMN domain of *Arl13b<sup>ΔOlig1-Cre</sup>* embryos, Arl13b is again present in the pMN domain and along the VZ of the pMN domain at e12.5 (**Figure 3.5 A-D**). This indicates that an Arl13b+, Olig1/2- population of cells continually specifies Olig1/2+ progenitors of the pMN domain. Thus, any time Olig1/2- cells give rise to new Olig1/2+ progenitors, the cycle of Arl13b deletion and turnover begins again. As such, the lack of observable OL phenotype in *Arl13b<sup>ΔOlig1-Cre</sup>* mutants may be due to presence of Arl13b at right period of time in order for OLP development to continue smoothly.

### 3.3.5 Generation and characterization of *Ift88<sup>ΔOlig1-Cre</sup>* mice

To determine if cilia are required for OL development, I generated *Ift88<sup>lox/lox</sup>*, *Olig1-Cre (Ift88<sup>ΔOlig1-Cre</sup>)* mice by the following cross: *Ift88<sup>lox/lox</sup>* females to *Ift88<sup>Δlox/+</sup>*,

*Olig1-Cre* males. As with *Arl13b<sup>ΔOlig1-Cre</sup>* embryos, approximately 5% of *Olig1-Cre* positive embryos have leaky, ubiquitous Cre expression. As such, 2.5% of *Ift88<sup>ΔOlig1-Cre</sup>* mutant embryos will recapitulate the *Ift88* null phenotype and die during midgestation. Adjusting for leaky *Olig1-Cre* expression, I observed *Ift88<sup>ΔOlig1-Cre</sup>* mutants at birth at the expected adjusted ratio (32 observed vs. 26.78 expected;  $p=0.3009$ ) (**Figure 3.6**). Thus, deletion of *Ift88* in the pMN domain at e8.5 is not lethal.

I crossed females homozygous for the conditional allele of *Ift88* (*Ift88<sup>fllox/fllox</sup>*) to *Ift88<sup>+</sup>/Ift88<sup>fllox</sup>*, *Olig1-Cre* males to generate *Ift88<sup>fllox</sup>/Ift88<sup>fllox</sup>; Olig1-Cre* (*Ift88<sup>ΔOlig1-Cre</sup>*) mutants. From this cross, mutants are generated 25% of the time. As with *Arl13b<sup>ΔOlig1-Cre</sup>* embryos, approximately 5% of *Olig1-Cre* positive embryos have leaky, ubiquitous Cre expression. As such, 2.5% of *Ift88<sup>ΔOlig1-Cre</sup>* mutant embryos will recapitulate the *Ift88* null phenotype and die during midgestation. The predicted frequency of *Ift88<sup>ΔOlig1-Cre</sup>* mutants is thus re-adjusted to 22.5% (25% - 2.5% = 22.5%). I observed *Ift88<sup>ΔOlig1-Cre</sup>* pups in 26.9% of live births, which is not significantly different from the expected adjusted ratio of 22.5% (**Figure 3.6A, B**;  $p=0.3009$ ). Thus, deletion of *Ift88* in the pMN domain at e8.5 is not embryonic lethal.

To determine the timing of *Ift88* turnover in the pMN domain of *Ift88<sup>ΔOlig1-Cre</sup>* embryos, I stained neural tube sections of e12.5 embryos for *Olig2* to mark the pMN domain, for *Arl13b* to mark cilia, and for *Ift88*. At e12.5, both *Ift88* and *Arl13b<sup>+</sup>* cilia are present in the *Olig2<sup>+</sup>* pMN domain of *Ift88<sup>ΔOlig1-Cre</sup>* neural tubes (**Figure 3.7 A-C**). This observation halted further investigation of OL development in *Ift88<sup>ΔOlig1-Cre</sup>*

mice, as *Ift88* is present at the onset of OLP specification. Thus, a role for *Ift88* in early stages of OL development can not be discerned from this model.

To determine if *Ift88* is required for maintenance of OLs, and of myelin, in adults, I monitored two adult *Ift88<sup>ΔOlig1-Cre</sup>* males over a period of six months, after which they were euthanized. Neither male displayed any phenotype indicative of demyelination, which indicates that maintenance of OLs and of myelin in adults does not require *Ift88*.

### 3.3.6 Rational for *Nestin-Cre*

To overcome the issues with *Olig1-Cre*, I switched to *Nestin-Cre* to drive deletion of *Arl13b* and *Ift88* in the neural stem cell (NSC) population. *Nestin* is a marker of NSCs, and *Nestin-Cre* expression is present by e10.5 (Graus-Porta et al., 2001; Lendahl et al., 1990; Tronche et al., 1999). Among other neuronal cell types, *Nestin+* NSCs give rise to the *Olig1/2* pMN domain, and thus to OLPs (Kessar et al., 2008; Lu et al., 2002; Zhou and Anderson, 2002). By inducing deletion in the NSC we can avoid the continual repopulation of the pMN domain with *Arl13b+* or *Ift88+* cells.

### 3.3.7 Generation of *Arl13b<sup>ΔNestin1-Cre</sup>* mice and turnover of *Arl13b* in the neural tube

I generated *Arl13b<sup>flox/hnn</sup>, Nestin-Cre (Arl13b<sup>ΔNestin1-Cre</sup>)* mutants by the following cross: *Arl13b<sup>flox/flox</sup>* females to *Arl13b<sup>+/hnn</sup>, Nestin-Cre* males. *Arl13b<sup>ΔNestin1-Cre</sup>* mutants are born at near expected ratios (*Arl13b<sup>ΔNestin1-Cre</sup>*-18.58% observed vs. 25% expected,  $p=0.1426$ ) (**Figure 3.8 A**). To determine if *Arl13b* turnover is complete by e12.5, I stained e12.5 neural tube sections of *Arl13b<sup>ΔNestin1-Cre</sup>* embryos for *Arl13b* and showed that *Arl13b* is absent at e12.5 (**Figure 3.9 A, D**). To show that cilia

remain present in the absence of Arl13b, I stained e12.5 neural tube sections with Ift88. The presence of Ift88 in the neural tube at e12.5 indicates that cilia remain **(Figure 3.9 B, E)**.

### 3.3.8 *Arl13b*<sup>ΔNestin1-Cre</sup> mice do not display defects in prenatal OL development or early postnatal myelination

To determine if loss of Arl13b in *Arl13b*<sup>ΔNestin1-Cre</sup> embryos affects OLP specification and migration, I looked at expression of Olig2 and PDGFRα OLPs in the neural tube of e14.5 embryos. At this stage, Olig2+ OLPs are present throughout the neural tube of both WT and *Arl13b*<sup>ΔNestin1-Cre</sup> embryos, which suggests that OLP migration is not impaired in *Arl13b*<sup>ΔNestin1-Cre</sup> mutants **(Figure 3.10 A, B)**.

Furthermore, expression of PDGFRα in *Arl13b*<sup>ΔNestin1-Cre</sup> embryos is grossly indistinguishable from WT littermates **(Figure 3.10 C, D)**. Thus, Arl13b is not essential for the specification of PDGFRα OLPs or for OLP migration in the neural tube at e14.5.

To follow OLP maturation into pre-myelinating OLs, I monitored expression of a *PLP-GFP* transgene in WT and *Arl13b*<sup>ΔNestin1-Cre</sup> embryos at e14.5. PLP is a component of myelin and a marker of maturing, pre-myelinating OLs. To assay the intensity and pattern of *PLP-GFP* expression at e14.5, images of whole embryos were taken under a GFP filter. *Arl13b*<sup>ΔNestin1-Cre</sup> embryos and WT littermates have no discernable difference in either intensity or pattern of PLP-GFP at e14.5 **(Figure 3.11 A, B)**. Both genotypes expressed PLP-GFP throughout the spinal cord and in the same regions of the brain at similar intensities, although *Arl13b*<sup>ΔNestin1-Cre</sup> embryos did appear smaller on average compared to WT littermates. Overall, these

data support a model where *Arl13b* is not essential for prenatal stages of OL development, including PDGFR $\alpha$  OLP specification, OLP migration throughout the neural tube, and OLP maturation into pre-myelinating OLs.

### 3.3.9 *Arl13b* <sup>$\Delta$ Nestin1-Cre</sup> mice do not display defects in postnatal myelination and develop cystic kidneys

Nestin+ cells also give rise to cells in the kidney, and alterations in cilia *in vivo* are known to promote development of cystic kidneys (Boehlke et al., 2010; Lin et al., 2003; Pazour et al., 2002; Qin et al., 2001; Trapp et al., 2008). *Arl13b* <sup>$\Delta$ Nestin1-Cre</sup> mice develop cystic kidneys early during postnatal development and die young (p12.29  $\pm$  5.24). Kidney failure is a likely cause of death in these mice, given the development of severely cystic kidneys during postnatal development.

Because the cystic kidneys and overall poor health of *Arl13b* <sup>$\Delta$ Nestin1-Cre</sup> mice could contribute to defects in OL development, analysis of postnatal OL development was restricted to p7 (Kikusui and Mori, 2009; Yusuf et al., 1981). This was several days before pups died, on average, and is also the time by which OLs reach the optic nerve and begin myelination (Foran and Peterson, 1992; Fruttiger et al., 2000; Mudhar et al., 1993b). To determine if loss of *Arl13b* affects OL migration to the optic nerve by p7, I looked at expression of PDGFR $\alpha$  and Olig2. At this time-point, there is no difference between expression of PDGFR $\alpha$  and Olig2 in the optic nerves of *Arl13b* <sup>$\Delta$ Nestin1-Cre</sup> mice and their WT littermates (**Figure 3.12 A, B**). These data suggest that *Arl13b* is not essential for OL migration to the optic nerve at p7.

### 3.3.10 Generation and characterization of *Ift88* <sup>$\Delta$ Nestin1-Cre</sup> mice

I crossed *Ift88<sup>flox/flox</sup>* females to *Ift88<sup>+ /flox</sup>, Nestin-Cre* males to generate *Ift88<sup>flox/flox</sup>, Nestin-Cre (Ift88<sup>ΔNestin1-Cre</sup>)* mutants. *Ift88<sup>ΔNestin1-Cre</sup>* mutants are born at near expected ratios (9 observed vs. 9.75 expected,  $p=0.9203$ ) (**Figure 3.8 B**). *Ift88<sup>ΔNestin1-Cre</sup>* embryos maintain cilia and continue to express Ift88 as late at e18.5 (**Figure 3.10 A-C**). Thus, I restricted analysis of OL development to later postnatal stages in these mice in order to give enough time for loss of Ift88 to have an effect.

To determine if Ift88 is required for late stages of OL development, I compared expression of Olig2, PDGFR $\alpha$ , and CNP, markers of OLs, OLPs, and myelinating OLs respectively, at p21 in the optic nerve. This is the last region of the CNS to be myelinated, and is a good place to look for defects in OL migration and differentiation in myelinating OLs (Baumann and Pham-Dinh, 2001). Both *Ift88<sup>ΔNestin1-Cre</sup>* mice and their WT littermates have no significant difference in expression of these markers at p21 in the optic nerve (**Figure 3.13 D**). These data suggest that Ift88 is not required for later stages of OL development and myelination in the optic nerve.

Like the *Arl13b<sup>ΔNestin1-Cre</sup>* mice, *Ift88<sup>ΔNestin1-Cre</sup>* mice also developed cystic kidneys, and survive slightly longer than *Arl13b<sup>ΔNestin1-Cre</sup>* mice ( $p14.25 \pm 1.89$ ). Since Ift88 turnover takes longer than Arl13b turnover, the most likely explanation is that *Arl13b<sup>ΔNestin1-Cre</sup>* mice develop cystic kidneys earlier due to earlier turnover of Arl13b.

### 3.4 Discussion

Based on previous links between PDGF-AA/ $\alpha$  and primary cilia, and because PDGF-AA/ $\alpha$  is essential for OL development, I sought to determine if

primary cilia are essential for OL development *in vivo*. Results from four genetic models where cilia were crippled (*Arl13b*<sup>Δ*Olig1-Cre*</sup> and *Arl13b*<sup>Δ*Nestin-Cre*</sup>) or ablated (*Ift88*<sup>Δ*Olig1-Cre*</sup> and *Ift88*<sup>Δ*Nestin-Cre*</sup>) in OLs fail to support a model where cilia are essential for OL development *in vivo*. Loss of either *Arl13b* or *Ift88* at different stages of OL development had no discernable effect on prenatal or postnatal OL development. The implications of these results are discussed below.

#### 3.4.1 Benefits and disadvantages of *Olig1-Cre* and *Nestin-Cre*

The combination of *Olig1-Cre* and *Nestin-Cre* permit a more comprehensive analysis of OL development; their advantages and drawbacks are summarized in Table 3.1. Briefly, *Olig1-Cre* allows analysis of later stages of OL development and myelination, while *Nestin-Cre* permits analysis of early stages of OL development. Furthermore, in the *Olig1-Cre* models I can ask if cilia are cell autonomous for OL development, while in the *Nestin-Cre* models I can ask if cilia have a non-cell autonomous role in OL development. As deletion of *Arl13b* or *Ift88* through either *Olig1-Cre* or *Nestin-Cre* failed to disrupt OL development, this suggests that cilia do not function in a cell autonomous or non-cell autonomous manner for OL development.

**Table 3.1**

<b>Benefits and disadvantages of <i>Olig1-Cre</i> and <i>Nestin-Cre</i> models</b>	
<b><i>Olig1-Cre</i></b>	<b><i>Nestin-Cre</i></b>
Re-emergence of <i>Arl13b</i> <sup>+</sup> or <i>Ift88</i> <sup>+</sup> cells in pMN domain prevents analysis of prenatal OL development	No re-population of <i>Arl13b</i> or <i>Ift88</i> during OLP specification, permits analysis of prenatal OL development
Normal lifespan permits analysis of later stages of OL development and of prenatal behavior	Mice develop cystic kidneys and die young, precludes analysis of later stages of OL development

### 3.4.2 Arl13b and Ift88 are not essential for OL development *in vivo*

*Arl13b<sup>ΔOlig1-Cre</sup>* mice failed to show defects in OL development or in myelination. The caveat of this conclusion is that Arl13b is present at the time of PDGFR $\alpha$ + OLP specification. *In vitro*, continuous exposure to PDGF-AA is not required for sustained migration of OLPs (Frost et al., 2009). Therefore, it is possible that Arl13b is present at the precise time when OLPs are competent for response to PDGF-AA.

To circumvent the re-emergence of Arl13b, I used *Arl13b<sup>ΔNestin-Cre</sup>* mice to induce deletion of Arl13b in the NSC population. This avoids the repopulation of the pMN domain with Arl13b+ cells that will undergo another round of Arl13b turnover. Unlike *PDGF-A<sup>-/-</sup>* embryos, which have significantly decreased expression of immature and mature OL markers, both *Arl13b<sup>ΔOlig1-Cre</sup>* and *Arl13b<sup>ΔNestin-Cre</sup>* mice had overall normal OL development. This indicates that Arl13b is not essential for prenatal or postnatal OL development *in vivo*.

I limited analysis of OL development in *Ift88<sup>ΔOlig1-Cre</sup>* and *Ift88<sup>ΔNestin-Cre</sup>* mice to postnatal stages, since both models maintain expression of Ift88 through the time at which OLPs are specified. Compared to WT littermates, neither *Ift88<sup>ΔOlig1-Cre</sup>* nor *Ift88<sup>ΔNestin-Cre</sup>* mice show defects in postnatal OL development. Furthermore, in stark contrast to *PDGF-A<sup>-/-</sup>* mice which develop a tremor by p21 and die by 6 weeks of age, *Ift88<sup>ΔOlig1-Cre</sup>* mice failed to present with phenotypes indicative of hypomyelination and lived for several months (Fruttiger et al., 1999). These data suggest that Ift88 is not essential for postnatal OL development *in vivo*.

The lack of OL phenotype in the *Arl13b<sup>ΔOlig1-Cre</sup>*, *Arl13b<sup>ΔNestin-Cre</sup>*, *Ift88<sup>ΔOlig1-Cre</sup>*, and *Ift88<sup>ΔNestin-Cre</sup>* mice implies that cilia and PDGF-AA/α signaling are not linked in oligodendrocytes. However, my data do not rule out a link between cilia and PDGF-AA/α signaling in other cell types *in vivo* or *in vitro*. Alternatively, cilia and PDGF-AA/α signaling are linked in oligodendrocytes, but the limitations of my *in vivo* models preclude an accurate evaluation of this link.

### 3.4.3 Support for a sequential progenitor model from *Arl13b<sup>ΔOlig1-Cre</sup>* embryos

The sequential model of MN/OLP specification proposes that a persistent, self-renewing population of NSCs gives rise to waves of Olig1/2+ precursors at different times during development (**Figure 1.5 B**). Depending on the stage of development, the Olig1/2+ precursors will specify either MNs or OLPs: At e9.5, Olig1/2+ progenitors specify MNs, and by e12.5, NSCs generate another wave of Olig1/2+ precursors that then specify OLPs. The mixed model proposes that the pMN domain is composed of two populations of progenitors: One population specifies MNs and the other specifies OLPs (**Figure 1.5 A**).

My data from *Arl13b<sup>ΔOlig1-Cre</sup>* embryos is consistent with the sequential model. I observe loss of Arl13b in the pMN domain at e10.5, which is consistent with deletion initiating at e8.5 and Arl13b turnover taking approximately 42 hours. At e12.5, the pMN domain is again repopulated with Arl13b+ cells. The loss and re-population of Arl13b+ cells in the pMN domain suggests that an Olig1/2- population gives rise to multiple waves of Olig1/2+ cells in the pMN domain. Upon expression of *Olig1-Cre*, each wave of Olig1/2+ cells begins a round of Arl13b deletion and turnover. In contrast to the sequential model, the mixed model proposes the

existence of a single motor neuron/oligodendrocyte progenitor (MNOP) population of Olig1/2+ cells in the pMN domain. My data do not support the mixed model, as it predicts that we should not see repopulation of the pMN domain with Arl13b+ cells.

**Chapter 4: Cilia transport regulates PDGF-AA/ $\alpha$  signaling via elevated mTOR  
signaling and diminished PP2A activity**

**(as submitted to the Proceedings of the National Academy of Sciences [PNAS]**

**on March 21, 2014)**

## 4.1 Introduction

Primary cilia, the microtubule-based projections found on the eukaryotic cell surface, are linked to a number of signaling pathways (Goetz and Anderson, 2010). Primary cilia are built and maintained by intraflagellar transport (IFT), whereby the two IFT complexes, IFTA and IFTB, carry cargo via kinesin and dynein motors for anterograde and retrograde transport, respectively. Many signaling pathways, including Sonic hedgehog (Shh), Wnt, PDGF, and mTORC1, are linked to primary cilia since mutations in IFTA, IFTB, kinesins, or dyneins alter the signaling response (Boehlke et al., 2010; Huangfu et al., 2003; Schneider et al., 2005). The relationship between IFT and signaling can be complex; for example, Shh response is reduced in IFTB, dynein, and kinesin mutants, but elevated in IFTA mutants (Huangfu et al., 2003; May et al., 2005; Tran et al., 2008).

Altering IFT leads to distinct changes in cilia structure, depending on which IFT or motor protein function is disrupted. For example, primary cilia do not form when anterograde transport is abolished via loss of IFTB or kinesin components. In contrast, cilia become swollen when either IFTA or dynein components are lost, preventing retrograde IFT (Goetz and Anderson, 2010). Several other classes of proteins play roles in trafficking and ciliary structure, including the small GTPase, ADP-ribosylation factor-like 13B (ARL13B) (Larkins et al., 2011). Loss of ARL13B disrupts the microtubule structure of primary cilia, as well as disrupting the localization and distribution of proteins within cilia (Caspary et al., 2007; Larkins et al., 2011).

Distinct signaling pathways require cilia for their activity. The best characterized of these is Shh signal transduction, which does not occur in the absence of cilia; dynamic ciliary movement of the Shh receptor and other pathway components is necessary to elicit a Shh response (Corbit et al., 2005; Haycraft et al., 2005; May et al., 2005; Rohatgi et al., 2007). The relationship between PDGF signaling and cilia is less understood. PDGF-AA acts through Defray homodimers to activate downstream targets, including Akt kinase. PDGFRs is upregulated and enriched in primary cilia in growth-arrested fibroblasts (Tucker et al., 1979), and PDGF-AA/ $\alpha$  signaling is critical to induce G0 cells into the cell cycle (Greenberg and Ziff; Pledger et al., 1981; Stiles et al., 1979). Moreover, PDGF-AA cannot signal in fibroblasts lacking cilia, suggesting ciliary localization of the receptor may be critical to its function. However, cells lacking cilia display decreased PDGFRs protein levels, which could also explain the lowered signaling (Schneider et al., 2005, 2010).

Akt is fully activated via phosphorylation of threonine 308 (P-Akt<sup>T308</sup>) and serine 473 phosphorylation (P-Akt<sup>S473</sup>). Dephosphorylation of P-Akt<sup>T308</sup> is mediated by the phosphatase, PP2A. PP2A regulates the activity of a variety of additional substrates and is negatively regulated by the mammalian target of rapamycin complex 1 (mTORC1) (Andjelković et al., 1996; Boehlke et al., 2010; Jackson and Pallas, 2012; McBride et al., 2010; Vereshchagina et al., 2008; Zhao et al., 2003). Interestingly, the activities of both Akt and mTORC1 are linked to primary cilia (Boehlke et al., 2010; Schneider et al., 2005, 2010). Here, using mouse embryonic fibroblasts (MEFs), we demonstrate a role for cilia transport in the regulation of PP2A activity. We explore the connections among diminished PP2A activity and

misregulation of mTORC1 and PDGF-AA/ $\alpha$  signaling pathways in cilia transport mutants. Our data reveal that the role of cilia transport in PDGF-AA/ $\alpha$  signaling is due to elevated mTORC1 signaling. Furthermore, we show that cilia transport regulates PP2A activity and propose that misregulation of PP2A contributes to the disruption of cilia-linked signaling pathways.

## 4.2 Results

### 4.2.1 PP2Ac Localizes to the Basal Body of MEFs

We examined the subcellular localization of PP2A relative to the primary cilium in serum-starved, ciliated mouse embryonic fibroblasts (MEFs). PP2A is composed of a structural subunit (subunit A), a regulator subunit (subunit B), and a catalytic subunit (subunit C). While there are dozens of B subunits, there are only two isoforms of the A and C subunits, which are 85% and 97% identical at the protein level, respectively (Arino et al., 1988; Green et al., 1987; Hemmings et al., 1990; Virshup and Shenolikar, 2009). Using immunofluorescence, we found PP2Ac concentrated at the base of the cilium. By co-staining with  $\gamma$  tubulin and Arl13b, we determined PP2Ac localized to the basal body (Fig. 4.1A and B). The connection between PP2Ac and cilia is further supported by data from *Chlamydomonas reinhardtii* that show PP2Ac in flagella (Yang et al., 2000).

Previous work showed P-Akt<sup>S473</sup> and Akt<sup>T308</sup> localized to the basal body of MEFs, where we saw PP2Ac (Schneider et al., 2010; Zhu et al., 2009). Since P-Akt<sup>T308</sup> is a PP2A substrate, we examined its localization relative to cilia and found P-Akt<sup>T308</sup> localized to a single centriole of the basal body of WT MEFs (Fig. S1). Thus, PP2Ac and its substrate, P-Akt<sup>T308</sup>, localize to the basal body of ciliated WT MEFs. Notably,

we saw no change in PP2Ac or P-Akt<sup>T308</sup> localization at the basal body when we examined MEFs carrying mutations in specific proteins critical for cilia transport (Fig. 4.1A, Fig. S1).

#### 4.2.2 P-Akt<sup>T308</sup> is Increased in Cilia Transport Mutant MEFs

Because several regions at the cilium base, including the basal body (a modified centriole), play roles in regulating protein traffic in and out of the cilium, we tested whether PP2A and P-Akt<sup>T308</sup> at the basal body might interact with cilia transport mechanisms (Garcia-Gonzalo et al., 2011). We derived MEFs from mouse embryos with mutations in the following genes encoding cilia proteins important for transport: *Ift172<sup>wim</sup>* and *Ift172<sup>avc</sup>*, an IFTB component; *Ift122<sup>sopb</sup>*, an IFTA component; and *Arl13b<sup>hnn</sup>*, a small, ciliary GTPase (Caspary et al., 2007; Friedland-Little et al., 2011; Huangfu et al., 2003; Qin et al., 2011). *Ift172<sup>wim</sup>* and *Ift172<sup>avc</sup>* represent null and hypomorphic alleles, respectively, in an IFT B complex protein, so *Ift172<sup>wim</sup>* MEFs lack cilia, while *Ift172<sup>avc</sup>* MEFs have truncated cilia; *Ift122<sup>sopb</sup>* MEFs have disrupted retrograde transport and display swollen or bulgy cilia; and *Arl13b<sup>hnn</sup>* MEFs have short cilia with abnormal ultrastructure and mislocalized ciliary proteins. With the exception of *Ift172<sup>wim</sup>* MEFs, which cannot form cilia, the other MEFs can be induced to form cilia through serum starvation. We grew WT, *Ift172<sup>wim</sup>*, *Ift172<sup>avc</sup>*, *Ift122<sup>sopb</sup>*, and *Arl13b<sup>hnn</sup>* MEFs in serum-supplemented media until confluent, serum-starved them for 48 h, and then harvested the cells. Western blot revealed increased levels of P-Akt<sup>T308</sup> in *Ift172<sup>wim</sup>*, *Ift172<sup>avc</sup>*, *Ift122<sup>sopb</sup>*, and *Arl13b<sup>hnn</sup>* MEFs compared to WT MEFs (Fig. 4.1C and E).

Because Akt phosphorylation is stimulated through PI3 kinase (PI3K) signaling (Andjelković et al., 1996), to determine whether the increased P-Akt<sup>T308</sup> levels were PI3K dependent, we pretreated the MEFs with the PI3K inhibitor, LY294002. We could not detect P-Akt<sup>T308</sup> in LY294002-treated WT, *Ift172<sup>avc</sup>*, *Ift122<sup>sopb</sup>*, or *Arl13b<sup>hnn</sup>* MEFs, confirming the T308 phosphorylation we saw was PI3K-dependent (Fig. 4.1C and E). P-Akt<sup>T308</sup> remained elevated in *Ift172<sup>wim</sup>* MEFs after LY294002 treatment (Fig. 4.1C and E). This could be due either to a PI3K-independent pathway phosphorylating P-Akt<sup>T308</sup> or to a lack of P-Akt<sup>T308</sup> dephosphorylation, mediated by PP2A. Our observation that *Ift172<sup>avc</sup>*, *Ift122<sup>sopb</sup>*, and *Arl13b<sup>hnn</sup>* MEFs are LY294002-sensitive while *Ift172<sup>wim</sup>* MEFs are insensitive is consistent with the disruption of cilia transport decreasing P-Akt<sup>T308</sup> dephosphorylation.

#### 4.2.3 PP2A Function is Disrupted in Cilia Transport Mutant MEFs

To determine whether the loss of P-Akt<sup>T308</sup> we saw in WT, *Ift172<sup>avc</sup>*, *Ift122<sup>sopb</sup>*, and *Arl13b<sup>hnn</sup>* MEFs after LY294002 treatment is PP2A dependent, we pharmacologically inhibited PP2A. Okadaic acid (OA) is a PP2A inhibitor, and treatment with OA increases P-Akt<sup>T308</sup> in a variety of cell lines in vitro (Cohen et al., 1989; Edelstein and Rockwell, 2012; Li et al., 2013). We performed our analysis in the presence of OA alone or in the presence of both OA and LY294002. Under either treatment, we detected P-Akt<sup>T308</sup> in WT, *Ift172<sup>wim</sup>*, *Ift172<sup>avc</sup>*, *Ift122<sup>sopb</sup>*, and *Arl13b<sup>hnn</sup>* MEFs (Figures 4.1B and 1D), indicating that the loss of P-Akt<sup>T308</sup> we saw in LY294002-treated *Ift172<sup>avc</sup>*, *Ift122<sup>sopb</sup>*, and *Arl13b<sup>hnn</sup>* MEFs was due to PP2A activity. P-Akt<sup>T308</sup> in *Ift172<sup>wim</sup>* MEFs treated with OA remained unchanged. These

results indicate PP2A activity is disrupted in *Ift172<sup>avc</sup>*, *Ift122<sup>sopb</sup>*, and *Arl13b<sup>hmn</sup>* MEFs and ablated in *Ift172<sup>wim</sup>* MEFs.

PP2A activity is regulated by endogenous inhibitors, such as I2PP2A/SET, which localizes to primary cilia in human retinal pigment epithelial cells (Li et al., 1996; Saddoughi et al., 2013; Wang and Brautigan, 2008). To directly ask whether loss of PP2A activity is responsible for the persistence of P-Akt<sup>T308</sup> in *Ift172<sup>wim</sup>* MEFs, we treated the cells with FTY720, the inhibitor of I2PP2A/SET, thereby functioning as a PP2A agonist. We found P-Akt<sup>T308</sup> levels in *Ift172<sup>wim</sup>* MEFs with FTY720 treatment were equivalent to those in WT MEFs, indicating that the defect in *Ift172<sup>wim</sup>* MEFs is due to lack of PP2A activity (Figure 4.1D). Taken together, our data argue that lack of anterograde transport, as in *Ift172<sup>wim</sup>* MEFs, results in an absence of PP2A activity, whereas diminished anterograde transport, as in the *Ift172<sup>avc</sup>* MEFs, or abnormal transport, as in the *Ift122<sup>sopb</sup>* and *Arl13b<sup>hmn</sup>* MEFs, leads to decreased PP2A activity (Fig. 4.1E). The LY294002 sensitivity of *Ift172<sup>avc</sup>* MEFs compared to the insensitivity of *Ift172<sup>wim</sup>* MEFs suggests that the kinetics of cilia transport may be critical in regulating PP2A activity.

Additionally, we examined *Dync2h1<sup>ln</sup>* MEFs, which carry a null allele of the retrograde dynein motor. *Dync2h1<sup>ln</sup>* MEFs do not survive in serum-free conditions, requiring us to grow the cells in 0.5% serum, which introduces confounding signaling (Ocbina and Anderson, 2008; Ocbina et al., 2011) (Fig.S2A). Nevertheless, P-Akt<sup>T308</sup> was absent following PI3K inhibition (LY294002) and present following PP2A inhibition (OA) (Fig. S2A). We investigated the *Dync2h1<sup>ln</sup>* MEFs in all subsequent assays and found the results were consistent with results from

*Ift122<sup>sopb</sup>*, the other mutant that primarily affects retrograde transport (Fig. S2). Since *Ift122<sup>sopb</sup>* cells grow in the absence of sera, we focused on them.

#### 4.2.4 Total PP2A Activity is Similar in WT and Cilia Transport Mutant MEFs

PP2A has dozens of substrates that belong to a variety of pathways (Basu, 2011; Janssens and Goris, 2001). To determine whether overall PP2A activity is altered in the cilia transport mutant MEFs, we used two distinct assays: 1) a commercially available PP2A activity assay and 2) Western blot analysis of the inactive, unmethylated PP2A pool. For the phosphatase activity assay, PP2A is immunoprecipitated from the cell lysates and its activity monitored on a specific phosphopeptide substrate (K-R-pT-I-R-R) (Saddoughi et al., 2013). While our control showed reduced PP2A activity by inhibiting with OA in WT and cilia transport mutant lysates (Figure 4.2A), we found no difference in PP2A activity towards the phosphopeptide in any of the cilia transport mutant MEFs compared to WT MEFs. For the second assay, we monitored the methylation state of PP2Ac. Active PP2Ac is methylated, so unmethylated PP2Ac represents inactive PP2A (Jackson and Pallas, 2012; Turowski et al., 1995). We measured both total and unmethylated PP2Ac expression by Western blot and found no difference in the level of total or unmethylated PP2Ac expression in WT, *Ift172<sup>wim</sup>*, *Ift122<sup>sopb</sup>*, and *Arl13b<sup>hnn</sup>* MEFs (Fig. 4.2B). These data indicate that cilia transport does not alter overall PP2A activity, but rather a specific pool of PP2A activity.

#### 4.2.5 mTORC1 Pathway Activity is Increased in Cilia Transport Mutant MEFs

mTORC1 signaling negatively regulates PP2A activity, and loss of cilia can result in increased mTORC1 signaling (Boehlke et al., 2010; Peterson et al., 1999).

Thus, we wanted to determine whether mTORC1 signaling is increased in the cilia transport mutant MEFs and determine whether it could contribute to the inactivation of PP2Ac.

We assayed mTORC1 pathway activity by monitoring phosphorylation of the mTORC1 subunit, mTOR (P-mTOR<sup>S2448</sup>), and mTORC1's substrate, p70 S6K (P-p70 S6K<sup>T389</sup>), through Western analysis. mTOR is the core component of mTORC1 and is phosphorylated on serine 2448 (P-mTOR<sup>S2448</sup>) via Akt signaling (Inoki et al., 2002). Active mTORC1 phosphorylates p70 S6K (P-p70 S6K<sup>T389</sup>) (Ballou, 1988; Burnett et al., 1998; Ferrari et al., 1991; Isotani et al., 1999; Jenou, 1988). Notably, P-p70 S6K<sup>T389</sup> is a PP2A substrate (Ballou et al., 1988). We found elevated expression of P-mTOR<sup>S2448</sup> and of P-p70 S6K<sup>T389</sup> in *Ift172<sup>wim</sup>*, *Ift172<sup>avc</sup>*, *Ift122<sup>sopb</sup>*, and *Arl13b<sup>hnn</sup>* MEFs compared to WT, indicating mTORC1 signaling is upregulated when cilia transport is disrupted (Fig. 4.3).

#### 4.2.6 Abnormal Response to PDGF Signaling in Cilia Transport Mutant MEFs

mTORC1 signaling can inhibit PDGFR $\alpha$  levels, thus decreasing PDGF-AA/ $\alpha$  signaling. Normally, PDGF-AA/ $\alpha$  stimulation induces P-Akt<sup>T308</sup> and P-Akt<sup>S473</sup>. In *Ift88<sup>orpk</sup>* MEFs carrying a hypomorphic mutation in the IFTB component, P-Akt<sup>S473</sup> induction is lower than in WT MEFs upon PDGF-AA/ $\alpha$  stimulation (Schneider et al., 2005, 2010). As P-Akt<sup>T308</sup> facilitates phosphorylation of S473, the decreased P-Akt<sup>S473</sup> following PDGF-AA stimulation is difficult to reconcile with the elevated P-Akt<sup>T308</sup> levels we saw in *Ift172<sup>wim</sup>*, *Ift122<sup>sopb</sup>*, and *Arl13b<sup>hnn</sup>* MEFs (Bellacosa et al., 1998). Therefore, we investigated the link between cilia transport, PDGF-AA/ $\alpha$  signaling, and phosphorylation of Akt.

Initially, we examined P-Akt<sup>S473</sup> levels in serum-starved WT, *Ift172<sup>wim</sup>*, *Ift122<sup>sopb</sup>*, and *Arl13b<sup>hnn</sup>* MEFs. Similar to the published results in *Ift88<sup>orpk</sup>* MEFs, we found low P-Akt<sup>S473</sup> levels when cilia transport was disrupted (Fig. 4.4A). Next, we assessed P-Akt<sup>T308</sup> and P-Akt<sup>S473</sup> induction upon PDGF-AA stimulation in the cilia transport mutant MEFs. We found PDGF-AA stimulation increased levels of P-Akt<sup>T308</sup> and P-Akt<sup>S473</sup> in WT and *Arl13b<sup>hnn</sup>* MEFs; however, we detected no change in P-Akt<sup>T308</sup> and P-Akt<sup>S473</sup> in *Ift172<sup>wim</sup>* or *Ift122<sup>sopb</sup>* MEFs (Fig. 4.4A). These data indicate that WT and *Arl13b<sup>hnn</sup>* MEFs are PDGF-AA responsive, whereas *Ift172<sup>wim</sup>* and *Ift122<sup>sopb</sup>* MEFs are not.

Next we analyzed additional steps in PDGF-AA/ $\alpha$  signal transduction. PDGFR $\alpha$ , the PDGF-AA receptor, is phosphorylated at tyrosine 742 and activated upon PDGF-AA binding (Yu et al., 1991, 1994). We found overall PDGFR $\alpha$  levels and activated P-PDGFR $\alpha$ <sup>Y742</sup> levels were reduced in *Ift172<sup>wim</sup>* and *Ift122<sup>sopb</sup>* MEFs, whereas they appeared to be at WT levels in *Arl13b<sup>hnn</sup>* MEFs without serum (Fig. 4.4A). These data are consistent with the observation that mTORC1 signaling is elevated in the cilia transport mutant MEFs since mTORC1 is known to inhibit PDGFR $\alpha$  levels (Zhang et al., 2007). The published analysis of *Ift88<sup>orpk</sup>* MEFs also showed low PDGFR $\alpha$  and low P-PDGFR $\alpha$ <sup>Y742</sup> levels, raising the possibility that the defects in PDGF response could be due to the low levels of receptor (Schneider et al., 2005, 2010).

#### 4.2.7 Rapamycin Treatment Restores PDGFR $\alpha$ Levels and Response to PDGF-AA Stimulation

To test whether the aberrant PDGF response in *Ift172<sup>wim</sup>* and *Ift122<sup>sopb</sup>* MEFs was the result of increased mTORC1 inhibiting PDGFR $\alpha$  levels, we treated the cells with the mTORC1 inhibitor, rapamycin, and examined PDGFR $\alpha$  expression and PDGF-AA response. We found PDGFR $\alpha$  expression levels were restored by rapamycin in *Ift172<sup>wim</sup>* MEFs, and that *Ift172<sup>wim</sup>* MEFs remain un-ciliated in the presence of rapamycin (Fig. 4.4B and C, S3). We also saw induction of P-PDGFR $\alpha$ <sup>Y742</sup>, P-Akt<sup>T308</sup>, and P-Akt<sup>S473</sup> expression upon PDGF-AA stimulation, indicating that limited PDGFR $\alpha$  levels could explain the low PDGF-AA/ $\alpha$  response of IFT mutants. The increased basal P-Akt<sup>T308</sup> in rapamycin-treated, WT MEFs highlights the feedback among mTORC1 signaling, PP2A activity, and PDGF-AA/ $\alpha$  signaling. P-Akt<sup>T308</sup> levels reflect the relative activities of PDGF-AA/ $\alpha$ -induced phosphorylation of Akt and of PP2A-mediated dephosphorylation of Akt. Previous reports showed that rapamycin can induce Akt phosphorylation (as loss of mTORC1 signaling increases PDGFR $\alpha$  protein expression and downstream signaling) and can increase PP2A activity (via loss of mTORC1's inhibition of PP2A) (Li et al., 2013; Rodrik-Outmezguine et al., 2011). Indeed, when we treated WT MEFs with rapamycin and increasing concentrations of PDGFR $\alpha$  blocking antibody, and then stimulated with PDGF-AA, the P-Akt<sup>T308</sup> levels dropped as PDGFR $\alpha$  blocking antibody concentration increased. This is consistent with the known feedback between mTORC1 and PDGF-AA/ $\alpha$  signaling. Based on our finding that loss of *Ift172* ablates PP2A activity, we next tested whether the feedback equilibrium depends on IFT172 by repeating this treatment regimen in *Ift172<sup>wim</sup>* MEFs. In contrast to WT MEFs, we found P-Akt<sup>T308</sup> levels were unchanged, indicating that despite rapamycin treatment, PP2A is unable

to dephosphorylate P-Akt<sup>T308</sup> (Fig. 4.4D). Together these data argue that the role of mTORC1 signaling in regulating the phosphorylation of Akt via PDGF-AA/ $\alpha$  signaling and PP2A activity depends on Ift172.

### 4.3 Discussion

Here we clarify the relationship between primary cilia and PDGF-AA/ $\alpha$  signaling in the context of mTORC1 signaling and PP2A activity. Although we see an inhibited response to PDGF-AA and decreased PDGFR $\alpha$  protein levels in the cilia transport mutant MEFs, we find that rapamycin treatment restores both PDGFR $\alpha$  protein levels and response to PDGF-AA stimulation in cilia transport mutant MEFs. Consistent with our observations, others have shown that mTORC1 signaling is increased in anterograde mutants and that rapamycin treatment increases PDGFR $\alpha$  protein expression in vitro (Boehlke et al., 2010; Zhang et al., 2007). Taken together, these data indicate that the inhibited response to PDGF-AA in cilia transport mutant MEFs is an indirect effect of increased mTORC1 signaling causing decreased PDGFR $\alpha$  protein. That PDGF-AA/ $\alpha$  signaling is restored in MEFs lacking cilia (*Ift172<sup>wim</sup>*) treated with rapamycin indicates that PDGFR $\alpha$ , although normally localized to cilia in vitro, need not be there to function. Since other receptors localize to cilia, it will be interesting to see whether their function requires such localization.

We also show P-Akt<sup>T308</sup> levels are abnormally elevated in MEFs with aberrant cilia transport, indicating disrupted PP2A activity toward P-Akt<sup>T308</sup>, with the most severe PP2A activity disruption in cells lacking anterograde transport. We rescue P-Akt<sup>T308</sup> levels with a PP2A agonist that blocks the function of an endogenous PP2A inhibitor. Several feed-forward and feedback loops between mTORC1 signaling and

PP2A highlight the intricate connections between the pathways. Our data raise the question of whether the primary defect in the cilia transport mutants is the increase in mTORC1 signaling or the diminished PP2A activity. The most parsimonious model favors the notion that disruption of cilia transport leads to deregulation of PP2A activity, which in turn indirectly increases mTORC1 signaling. Normally, mTORC1 signaling results in phosphorylation of p70 S6K<sup>T389</sup>, and P-p70 S6K<sup>T389</sup> is a PP2A substrate (Ballou et al., 1988; Hahn et al., 2010). Thus, diminished PP2A activity can explain the increased mTORC1 signaling and the aberrant P-Akt<sup>T308</sup> levels we see in cilia transport mutant MEFs. The alternative model, that the increased mTORC1 signaling causes the decreased PP2A activity, predicts that total PP2A activity would be lowered. Because total PP2A activity is not decreased in *Ift172<sup>wim</sup>* MEFs, where elevated P-Akt<sup>T308</sup> levels are constant, this model is less likely.

Our data argue that only a subset of PP2A activity in the cell is regulated by cilia transport since we found no evidence that total PP2A activity is regulated by cilia transport. Rather, we see problems with dephosphorylation of substrates linked to signaling pathways regulated by primary cilia: Akt and mTORC1 (Boehlke et al., 2010; Hahn et al., 2010; Kuo et al., 2008; Schneider et al., 2005). Experiments manipulating cilia transport or PP2A in vivo also indicate that some PP2A functions are spared in cilia transport mutants. PP2A  $C\alpha^{-/-}$  embryos die around e6.5 and fail to form mesoderm, underscoring the essential role of PP2A early in development (Götz et al., 1998). In contrast, *Ift172<sup>wim</sup>*, *Ift172<sup>avc</sup>*, *Ift122<sup>sopb</sup>*, *Arl13b<sup>hnn</sup>*, and *Dync2h1<sup>lln</sup>* embryos form mesoderm and survive through midgestation (Casparly et al., 2007; Friedland-Little et al., 2011; Huangfu et al., 2003; Ocbina and Anderson, 2008; Qin et

al., 2011). There are over 20 isoforms of the regulatory B subunit of PP2A, making possible at least 80 different combinations of all three PP2A subunits (Haesen et al., 2012; Jackson and Pallas, 2012). The various B subunits have different developmental, subcellular, and tissue-specific expression patterns and play a large role in determining PP2A substrate specificity and activity (Janssens and Goris, 2001). Together, these data suggest cilia transport regulates the activity of the PP2Ac pool seen at the ciliary base.

Several possibilities could explain how cilia transport regulates PP2A activity. PP2A subunits or the assembled holoenzyme may require cilia transport to be activated either by being physically brought into the cilium for activation, or by an activator being transported into the cilium; however, our observation that PP2Ac remained at the basal body in all cilia transport mutant MEFs suggests the entire holoenzyme is not transported into the cilium. Alternatively, it is possible that an inhibitor of PP2A activity is regulated by cilia transport. The rescue of P-Akt<sup>T308</sup> dephosphorylation in *Ift172<sup>wim</sup>* MEFs upon treatment with FTY720 is consistent with this possibility since FTY720 inhibits an endogenous inhibitor of PP2A, I2PP2A/SET (Li et al., 1996; Saddoughi et al., 2013).

Our data show aberrant P-Akt<sup>T308</sup> levels when cilia transport is disrupted, with the most severe defects in MEFs deficient for anterograde transport (*Ift172<sup>wim</sup>*). Indeed, in the presence of the PI3K inhibitor, LY294002, the anterograde mutants show P-Akt<sup>T308</sup> levels consistent with complete inhibition of PP2A activity. However, these cells lack cilia, making it impossible to distinguish whether the lack of cilia or the absence of anterograde traffic underlies the diminished PP2A activity. In the

remaining cilia transport mutant MEFs, PP2A is active, albeit less efficient than WT. Indeed, *Ift172<sup>avc</sup>*, *Ift122<sup>sopb</sup>*, *Arl13b<sup>hnn</sup>*, and *Dync2h1<sup>lln</sup>* MEFs required PI3K inhibition for T308 to be completely dephosphorylated as in WT MEFs. Our observations, combined with the known ciliary localization of the endogenous PP2A inhibitor, I2PP2A/SET, raise the possibility that cilia transport controls the kinetics of I2PP2A/SET inhibition of PP2A, thereby regulating PP2A activity.

## Chapter 5: Perspectives

## 5.1 Arl13b and Ift88 in oligodendrocyte development

The results presented in chapter three, *The role of Arl13b and Ift88 in oligodendrocyte development in vivo*, suggest that Arl13b is not required for OL development *in vivo*. Deletion of Arl13b in either Olig1+ pMN cells or in Nestin+ NSC had no effect on OLP specification or on OL development. How then, do *Arl13b<sup>hnn</sup>* embryos fail to specify PDGFR $\alpha$ + OLPs when loss of Arl13b in either oligodendrocytes or in the entire CNS has no effect on PDGFR $\alpha$ + OLP specification? One possibility is that specification of PDGFR $\alpha$ + OLPs in *Arl13b<sup>hnn</sup>* embryos is delayed beyond the point of embryo survival. That is, if *Arl13b<sup>hnn</sup>* embryos survived longer, PDGFR $\alpha$ + OLPs may eventually appear, and OL development may be delayed. However, the timing of OL development in *Arl13b<sup>\Delta Nestin-Cre</sup>* embryos is normal, which suggests that OL development is not delayed in *Arl13b<sup>hnn</sup>* embryos. Another possibility is that *Arl13b<sup>hnn</sup>* OLPs (if at all present) express PDGFR $\alpha$ + at low levels that are not detectable by immunofluorescence, as I show that *Arl13b<sup>hnn</sup>* MEFs express less PDGFR $\alpha$  than WT MEFs. In this case, other markers that recognize OLPs, such as Sex Determining Region Y-Box (Sox10), NG2, or A2B5, should reveal the presence of OLPs (Fredman et al., 1984; Kuhlbrodt et al., 1998; Nishiyama et al., 1996). Alternatively, there may be precocious differentiation of pMN cells into MNs instead of OLPs, and thus other OLP markers are not expected to be present.

Deletion of Ift88 in either pMN or NSCs had no effect on OL development, with the caveat that Ift88 was present all through prenatal development in *Ift88<sup>\Delta Nestin-Cre</sup>* mice. Therefore, I can not rule out a role for Ift88 in specification of OLPs or in prenatal OL development based on results from either *Ift88<sup>\Delta Olig1-Cre</sup>* or

*Ift88*<sup>ΔNestin-Cre</sup> mice. However, based on the work of others and on my own *in vitro* observations, I predict that cilia transport is not essential for OL development *in vivo*. The lack of a hypomyelination phenotype in either *Ift88*<sup>ΔOlig1-Cre</sup> or *Ift88*<sup>ΔNestin-Cre</sup> mice, or in *Ift88*<sup>orp<sup>k</sup></sup> mice, which are hypomorphs for *Ift88* support a model where *Ift88* is not essential for OLP specification and development *in vivo*.

The data I present in chapter 4 further supports a model where cilia are not essential for OL development, as I demonstrate that even in the absence of a functional response to PDGF-AA stimulation, Akt and mTORC1 appear to remain active in cilia transport mutant MEFs. Both Akt and mTORC1 have important roles in OL development, and their ectopic activation in cilia transport mutants may bypass the requirement of PDGF-AA/ $\alpha\alpha$  signaling and permit “normal” or sufficient OLP development *in vivo* (Cui et al., 2005; Flores et al., 2000, 2008; Narayanan et al., 2009; Tyler et al., 2009b; Vora et al., 2011; Zou et al., 2011). Thus, even if cilia are required for response to PDGF-AA, cilia transport mutant OLPs may be able proliferate and mature as a result of inappropriate activation of Akt and mTORC1. It would be interesting to see if either Akt or mTORC1 are increased in other cilia transport mutant cell types, both *in vivo* and *in vitro*.

## 5.2 PP2A and cilia trafficking

The results presented in chapter four, *Cilia trafficking regulates the activity of PP2A*, present a novel link between primary cilia and the serine-threonine phosphatase PP2A. Here, I provide the first published evidence that the catalytic subunit of PP2A, PP2Ac, localizes to the basal body of ciliated MEFs. I then show that phosphorylation of two PP2A substrates, P-Akt<sup>T308</sup> and P-p70 S6K<sup>T389</sup>, is increased

in cilia transport mutant MEFs (*Ift172<sup>wim</sup>*, *Ift122<sup>sopb</sup>*, and *Arl13b<sup>hnn</sup>*), which indicates decreased PP2A activity towards these substrates upon cilia transport disruption. Furthermore, I show that dephosphorylation of P-Akt<sup>T308</sup> is restored in cilia-null *Ift172<sup>wim</sup>* MEFs, following inhibition of I2PP2A/SET, an inhibitor of PP2A that localizes along the length of cilia. As phosphorylation of PP2A substrates is increased, and since I2PP2A/SET inhibition restores dephosphorylation of P-Akt<sup>T308</sup> in cilia transport mutant MEFs, I propose that cilia transport regulates I2PP2A/SET activity towards PP2A, such that absence of functional cilia transport promotes I2PP2A/SET inhibition of PP2A.

I further propose that multiple cilia-related signaling pathways are linked to primary cilia in vertebrates through PP2A. PP2A regulates dephosphorylation of Hh components in *Drosophila*, and may regulate dephosphorylation of Gli proteins and other Shh components in vertebrates (Casso et al., 2008; Jia et al., 2009; Krauss et al., 2008, 2009; Mainwaring and Kenney, 2011; Nybakken et al., 2005; Su et al., 2011; Wen et al., 2010). In vertebrate Shh, the Gli family of transcription factors acts to promote or repress expression of Shh target genes. Unphosphorylated, full length Gli (Gli<sup>FL</sup>) proteins are processed into activators (Gli<sup>A</sup>), while phosphorylated Gli proteins are processed into repressors (Gli<sup>R</sup>) (Pan et al., 2006; Wang et al., 2000a). Multiple IFT mutants display decreased Gli<sup>R</sup> (suggesting inhibited phosphorylation), which could be accounted for through decreased PP2A activity towards a negative regulator of PKA called RII (Caspary et al., 2007; Haycraft et al., 2005; Huangfu et al., 2003; Isensee et al., 2013; Liem et al., 2012; Liu et al., 2005; May et al., 2005; Qin et al., 2011; Tran et al., 2008). PKA phosphorylates Gli<sup>FL</sup>, and phosphorylation of Gli<sup>FL</sup>

is required for its processing into Gli<sup>R</sup> (Chen et al., 2011; Riobó et al., 2006; Tuson et al., 2011; Wen et al., 2010). In mammalian cells, PP2A dephosphorylation inactivates a negative regulator of PKA called RII (Isensee et al., 2013). It is tempting to speculate that misregulation of PP2A in cilia transport mutants could promote hyperphosphorylation of RII, contributing to decreased PKA activity and thus decreased Gli<sup>FL</sup> phosphorylation and subsequently decreased Gli<sup>R</sup>. As discussed in section 1.4, the absence of anterograde IFT would prevent formation of Gli<sup>A</sup> (Huangfu and Anderson, 2005; Tran et al., 2008).

Shh activity in the vertebrate neural tube establishes an opposing gradient of Gli<sup>A</sup> and Gli<sup>R</sup>, and the ratio of Gli<sup>A</sup>:Gli<sup>R</sup> is important for proper cell fate specification along the dorsal/ventral axis. In *Arl13b<sup>hnn</sup>* mutants, there is an intermediate level of Shh activity in the neural tube instead of a gradient, and Gli<sup>A</sup>, but not Gli<sup>R</sup>, activity is inhibited (Caspary et al., 2007). Normal Gli<sup>R</sup> activity suggests that there is sufficient phosphorylation and processing of Gli<sup>FL</sup> into Gli<sup>R</sup>, and lowered Gli<sup>A</sup> activity suggests that dephosphorylation of Gli<sup>FL</sup> is inhibited. As PP2A activity does not appear as severely inhibited in *Arl13b<sup>hnn</sup>* mutants as it is in *Ift172<sup>wim</sup>* mutants (based on comparisons of P-Akt<sup>T308</sup> levels in *Arl13b<sup>hnn</sup>* and *Ift172<sup>wim</sup>* MEFs), *Arl13b<sup>hnn</sup>* mutants may have sufficient PP2A activity to permit PKA phosphorylation of Gli<sup>FL</sup>, and thus allow for processing of phosphorylated Gli<sup>FL</sup> into Gli<sup>R</sup>. Furthermore, some amount of Gli<sup>FL</sup> dephosphorylation is likely to occur, thus accounting for the low levels of Gli<sup>A</sup> and intermediate level of Shh activity in the neural tubes of *Arl13b<sup>hnn</sup>* embryos (Caspary et al., 2007).

My results have implications for inhibition of I2PP2A/SET as a novel treatment option for ciliopathy patients, if PP2A activity is indeed regulated by IFT. The I2PP2A/SET inhibitor FTY720 (Fingolimod, Gilenya®) is already approved for treatment of multiple sclerosis in humans, and multiple pre-clinical models, in mouse and in patient tissue samples, support use of FTY720 as a treatment in colorectal cancer, leukemia, and Huntington disease (Henault et al., 2013; Kappos et al., 2006; Nagahashi et al., 2013; Neviani et al., 2013; Oaks et al., 2013; Di Pardo et al., 2013; Rosa et al., 2013; Saddoughi et al., 2013; Thomas and Ziemssen, 2013). Loss of primary cilia can promote formation of medulloblastoma, a malignant tumor that derives from the cerebellum and is the most common solid tumor in children under four years of age (McKean-Cowdin et al., 2013; Mueller and Chang, 2009; Patel et al., 2013). Over-activation of several cilia-linked signaling pathways (Shh, PI3K/AKT, mTOR) are observed in mouse and human medulloblastoma, and FTY720 treatment could further improve patient outcomes, as PP2A regulates aspects of all three pathways (Bhatia et al., 2009; Buonamici et al., 2010; Hambardzumyan et al., 2008; Józwiak et al., 2011; Włodarski et al., 2006). Thus, it is of great relevance to investigate the role of IFT in regulation of PP2A and I2PP2A/SET in mammalian cilia-dependent signaling pathways.

### **5.3 PDGF-AA/ $\alpha$ , Akt, and mTORC1**

The results from chapter 4 also demonstrate that decreased PDGFR $\alpha$  protein levels in cilia transport mutant MEFs is a side effect of mTORC1 upregulation, and that inhibition of mTORC1 restores response to PDGF-AA stimulation in the absence of functional cilia transport. Prior to my work, PDGF-AA/ $\alpha$ , Akt, and mTORC1

signaling were only described in the context of anterograde IFT, and studies on PDGF-AA/ $\alpha$  in *Ift88<sup>orpk</sup>* MEFs analyzed P-Akt<sup>S473</sup>, which regulates substrate specificity, but not P-Akt<sup>T308</sup>, which regulates Akt kinase activity (Alessi et al., 1996; Calleja et al., 2007; Guertin et al., 2006; Jacinto et al., 2006; Moore et al., 2011; Vincent et al., 2011). My work fine tunes our understanding of the relationship between PDGF-AA, Akt, mTORC1, and cilia *in vitro*.

As mentioned in section 5.2, P-Akt<sup>T308</sup> levels are increased in cilia transport mutant MEFs, but do not increase upon PDGF-AA stimulation in *Ift172<sup>wim</sup>* and *Ift122<sup>sopb</sup>* MEFs, which also have low levels of PDGFR $\alpha$  protein. Through inhibition of mTORC1 in *Ift172<sup>wim</sup>* and *Ift122<sup>sopb</sup>* MEFs, I restore PDGFR $\alpha$  protein expression levels, which in turn restores response to PDGF-AA stimulation. This observation highlights the role of cilia as a signaling hub that regulates a multitude of interconnected pathways in vertebrates and the importance of considering how cilia-dependent pathways interact with one another when investigating the links between any one pathway and cilia. Importantly, it demonstrates that cilia need not be present for response to PDGF-AA stimulation, as previously thought.

Signaling pathways do not function in isolation, as shown by the connections between PDGFR $\alpha$ , Akt, mTORC1, and PP2A (**Figure 5.3**). Activated PDGFR $\alpha$  signals to activate Akt, which consists of phosphorylation on both Akt T<sup>308</sup> and Akt S<sup>473</sup> (**Figure 5.3A**). Phosphorylated Akt promotes activation of mTORC1, leading to phosphorylation of substrates such as p70 S6K (**Figure 5.3B**). mTORC1 mediated inhibition of PP2A inhibits dephosphorylation of Akt and keeps the pathway “on,” while mTORC1 also signals to downregulated expression of PDGFR $\alpha$ , thus turning

the pathway “off” (**Figure 5.3C, D**). As PDGFR $\alpha$  decreases, phosphorylation of Akt decreases, activation of mTORC1 decreases, and inhibition of PP2A is relieved, thus leading to dephosphorylation of Akt and a “shutting down” of the pathway (**Figure 5.3E**).

#### **5.4 Final summary**

In summary, this thesis presents data that further our understanding of the role of cilia in signaling, particularly in PDGF-AA/ $\alpha$  signaling, show that Arl13b is not required for OL development *in vivo*, and that decreased PDGFR $\alpha$  expression and response to PDGF-AA is a result of increased mTORC1 signaling in cilia mutant MEFs. Furthermore, the manuscript within this thesis introduces PP2A as a novel, basal-body associated phosphatase in vertebrates, shows that IFT regulates PP2A activity towards specific substrates, and provides precedent for further study of PP2A as a regulator of Shh, a well described cilia-dependent signaling pathway.

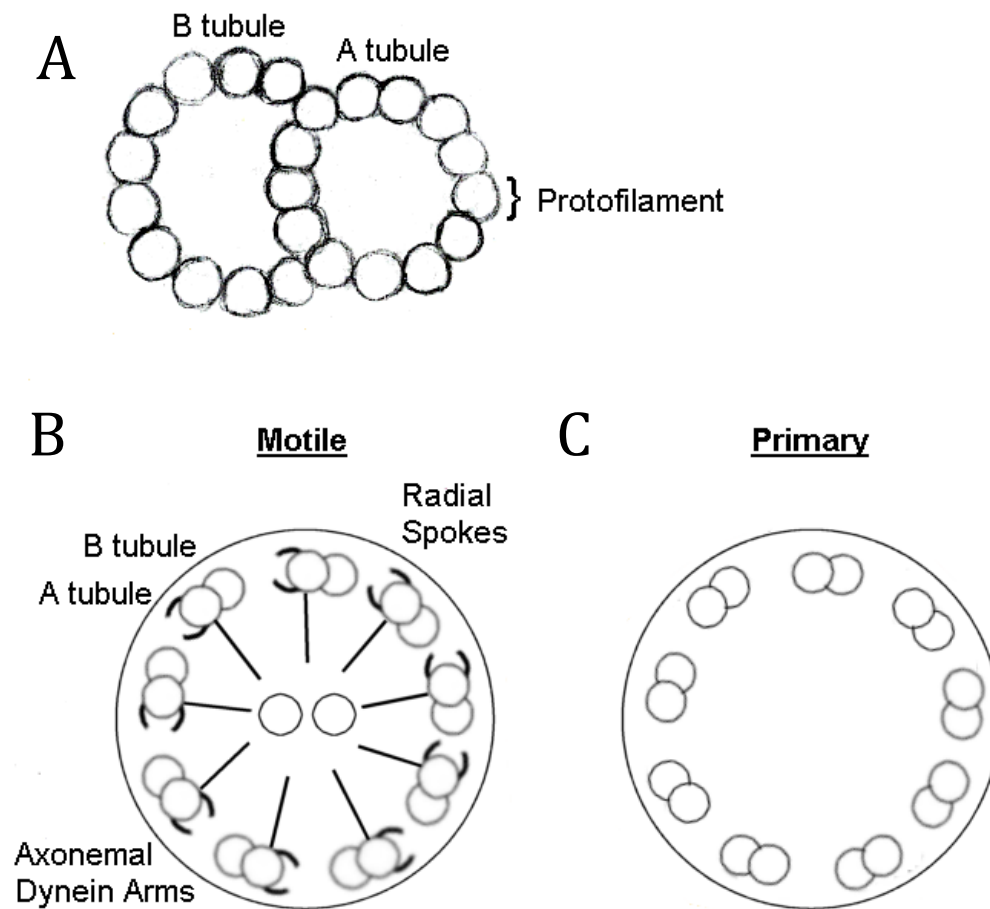


Figure 1.2.1-The ciliary axoneme consists of an outer ring with nine microtubule doublets, and may or may not have a central pair of microtubules.

A-The microtubule doublets of the outer ring are composed of a 13 protofilament A tubule connected to an 11 filament B tubule.

B-Motile cilia contain a central pair of microtubule singlets, as well as radial spokes and axonemal dynein arms, all which help to generate motility.

C-Primary cilia lack a central pair of microtubules, as well as radial spokes and axonemal dyneins.

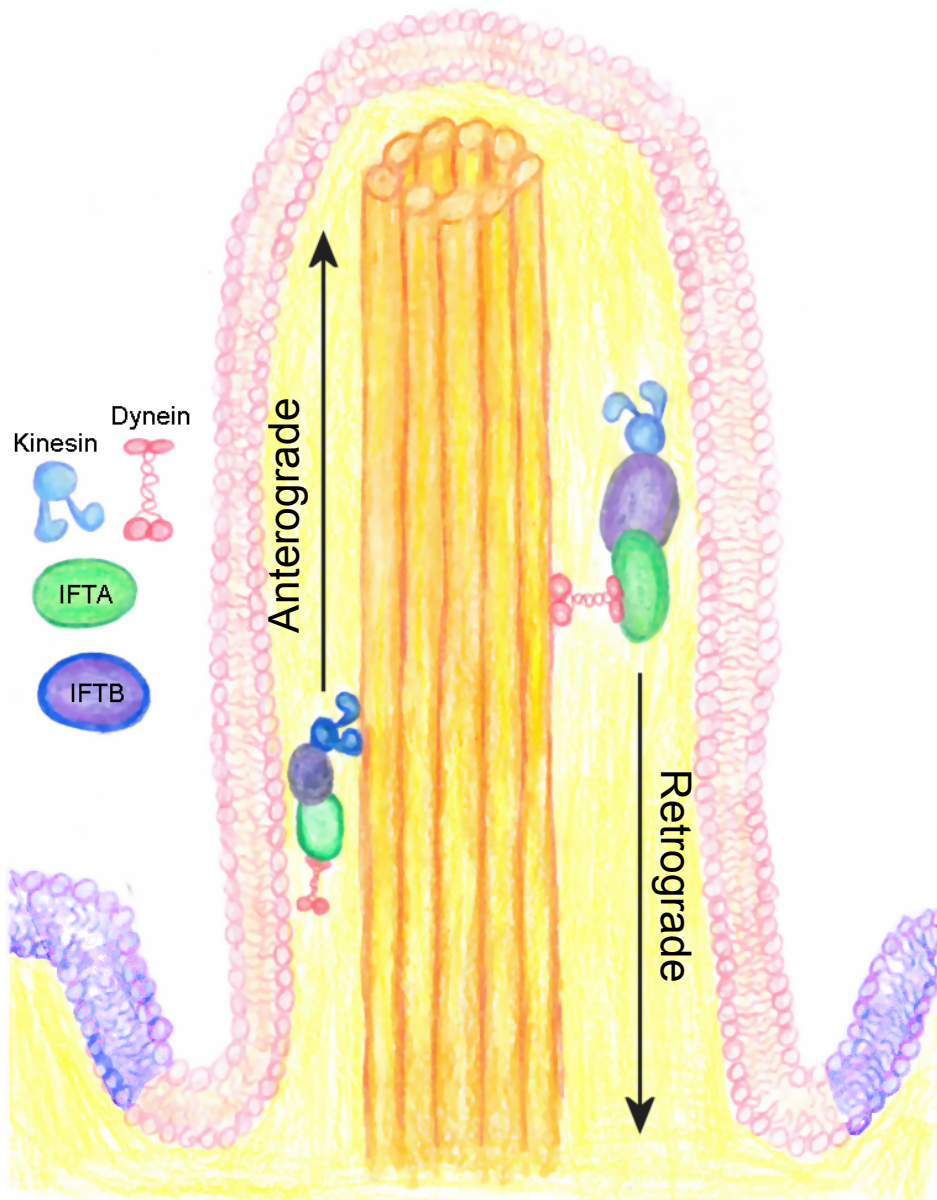


Figure 1.2.2-Cargo transport into and out of the cilium is regulated by IFT.

Kinesin and dynein motors move along the microtubule doublets of the outer ring for anterograde and retrograde transport, respectively. The IFTB complex and kinesin motors carry cargo for anterograde transport, and the IFTA complex and dynein motors regulate retrograde transport of cargo.

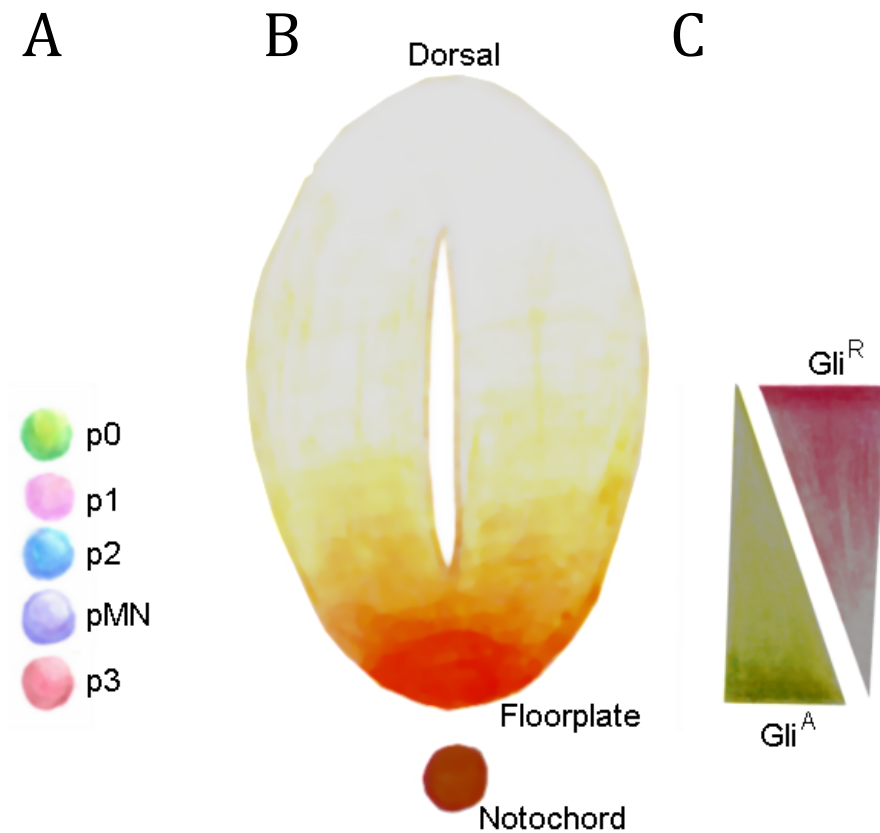


Figure 1.4-Five distinct cell fates are specified in the ventral neural tube by an opposing gradient of Gli<sup>A</sup> and Gli<sup>R</sup>, established by diffusion of Shh ligand from the notochord and floorplate.

A-A gradient of Shh is required for the establishment of five ventral cell fates. The more ventral fates require higher levels of Shh activity, while the more dorsal fates are specified at lower levels of Shh activity.

B-Shh ligand from the notochord and floorplate establishes a gradient of Shh activity, such that the most ventral regions of the neural tube have the greatest Shh activity, and more dorsal regions have less.

C- Gli<sup>A</sup> activity is greatest in the most ventral regions of the neural tube, and decreasing going dorsally. Gli<sup>R</sup> activity is at the lowest in the most ventral regions of the neural tube, and increases more dorsally.

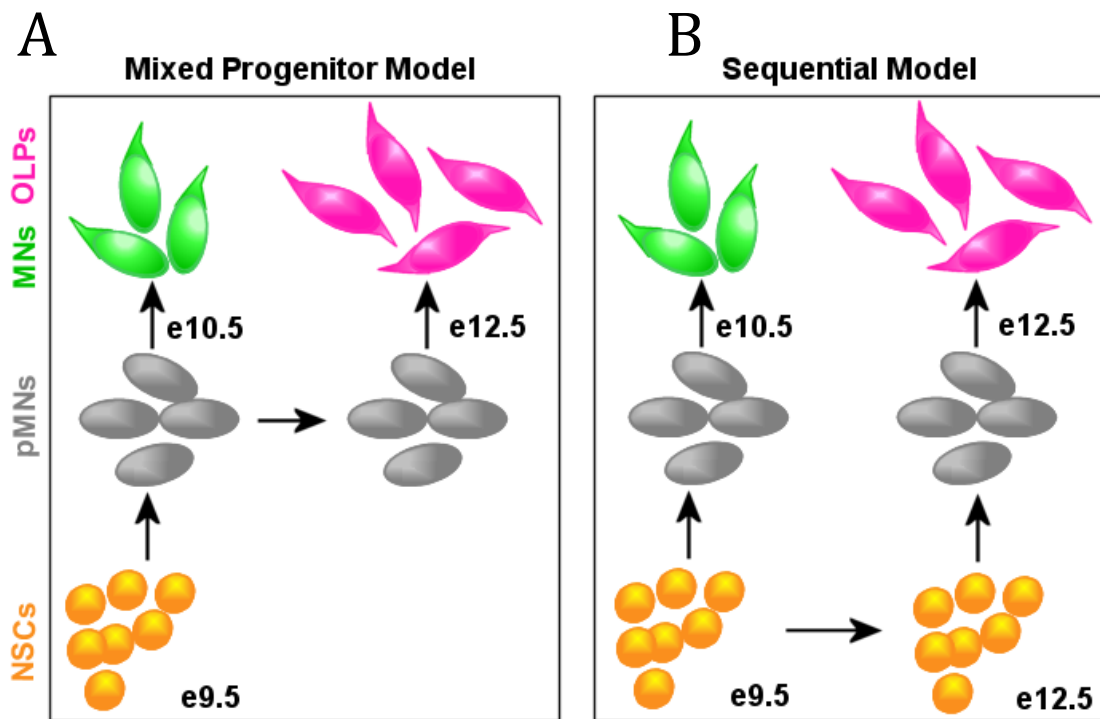


Figure 1.5-The mixed progenitor model and sequential model of pMN domain specification. These two models, the mixed progenitor and sequential models, propose how MNs and OLPs are specified from the pMN domain.

These cartoons illustrate two models of MN and OLP specification from NSCs. NSCs are in orange, pMNs in gray, MNs in green, and OLPs in hot pink. Arrows indicate “where” the different cell types come from (For example, in the left panel, the gray pMN cells give rise to green MNs. Some gray pMNs remain as pMNs, and at e12.5 these pMNs produce pink OLPs).

A-The mixed progenitor model proposes that the pMN domain is composed of a mixed population of cells. One population gives rise to MNs at e10.5, while the other gives rise to OLPs at e12.5.

B-The sequential model proposes that the pMN domain is consistently replenished by NSCs. At e10.5, the first “waves” of pMN cells give rise to MNs. Later, at e12.5, NSCs specify another wave of pMN cells. These pMN cells give rise to OLPs.

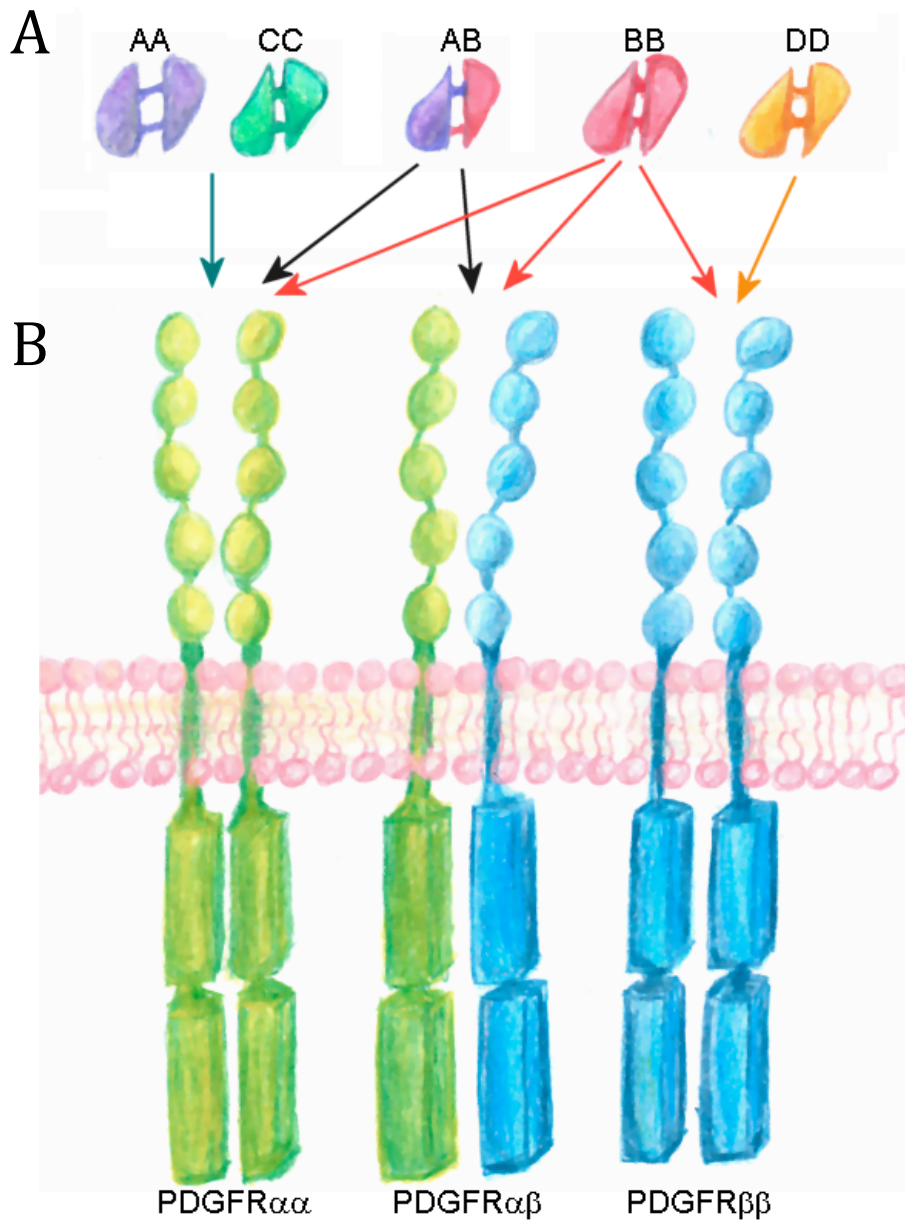


Figure 1.6-The three PDGF receptor dimers bind different homo and heterodimers of PDGF ligand.

A-There are four PDGF ligands: A, B, C, and D. A and B forms homodimers and a heterodimer with each other. C and D only form heterodimers.

B-There are two PDGF receptors:  $\alpha$  and  $\beta$ . PDGFR $\alpha\alpha$  binds PDGF-AA, CC, AB, and BB dimers. PDGFR $\alpha\beta$  binds PDGF-AB and BB dimers. PDGFR $\beta\beta$  binds PDGF-BB and DD dimers.

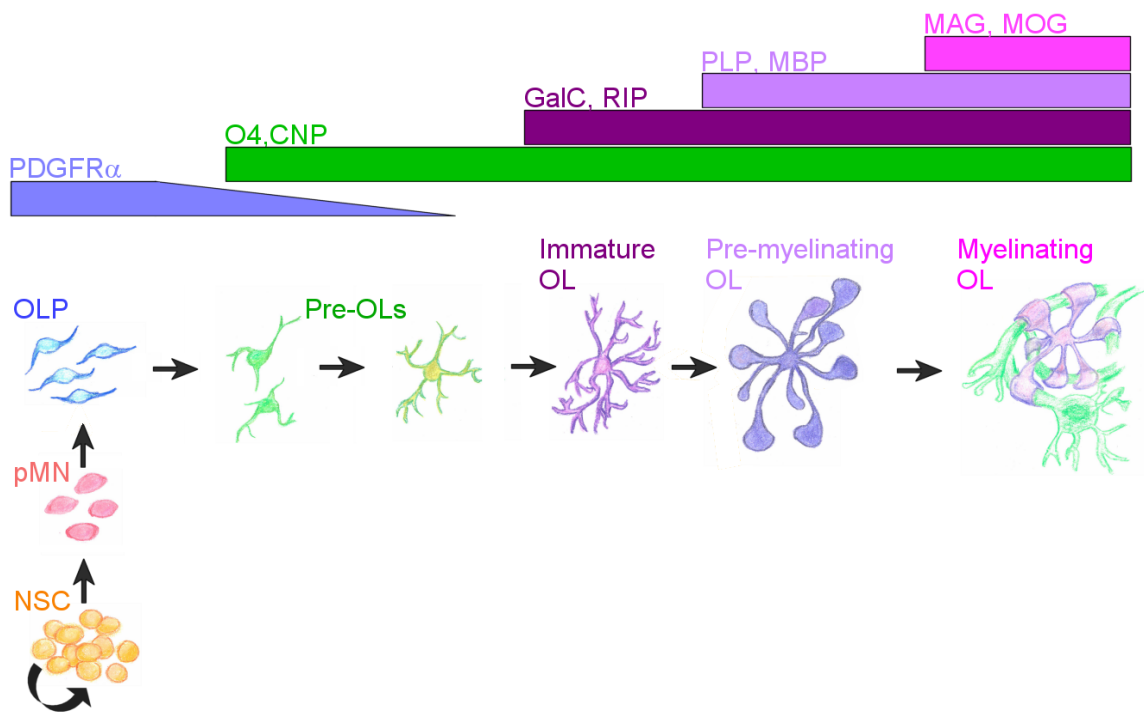


Figure 1.7.1-OLs undergo the same developmental steps from OLPs into mature, post-mitotic, myelinating OLs.

In the mouse neural tube, the NSC population gives rise to the pMN domain, which then specifies OLPs. The stages of OL development are characterized by morphology and by the expression of stage-specific markers. OLPs are bipolar, express PDGFR $\alpha$ , and are actively proliferating and migrating throughout the neural tube. As OLPs become pre-OLs, both expression of PDGFR $\alpha$  and migration decrease. From pre-OLs to immature OLs, the number of extensions increases, as does extension branching. Pre-myelinating OLs are post-mitotic, and are recognized by expression of myelin components and formation of a myelin-like membrane. Fully mature, myelinating OLs wrap extensions of the plasma membrane around the axons of multiple neurons.

Abbreviations: NSC-Neural Stem Cell, pMN-precursor Motor Neuron, MN-Motor Neuron, OLP-Oligodendrocyte Progenitor, OL-Oligodendrocyte, CNP-, GalC-Galactosylceramides, PLP-proteolipid protein (PLP), MBP-Myelin Basic Protein, MAG-myelin-associated glycoprotein, MOG- myelin/oligodendrocyte glycoprotein.

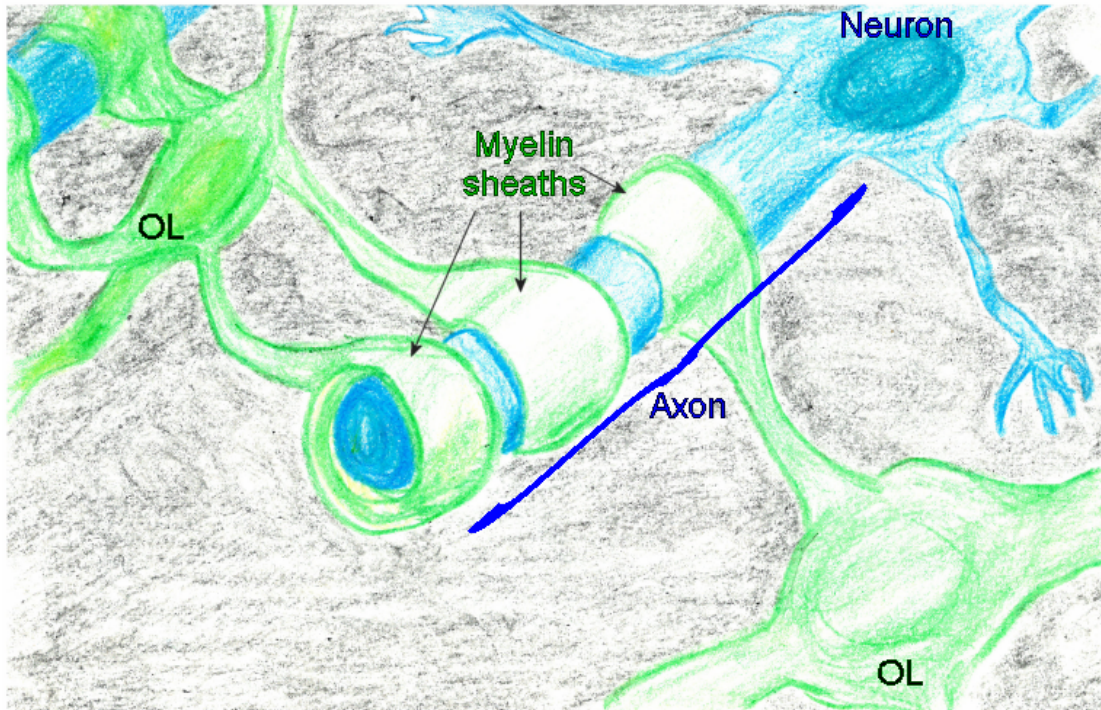


Figure 1.7.2- Mature OLs myelinate multiple axons by wrapping axon segments in multilayered sheaths of myelin.

Myelin is primarily composed of fats, and provides insulation to neurons to facilitate smooth and rapid signal transduction. Immature OLs begin to produce myelin proteins during gestation, while the process of myelination is greatest after birth. In the CNS, a single OL can myelinate multiple axons.

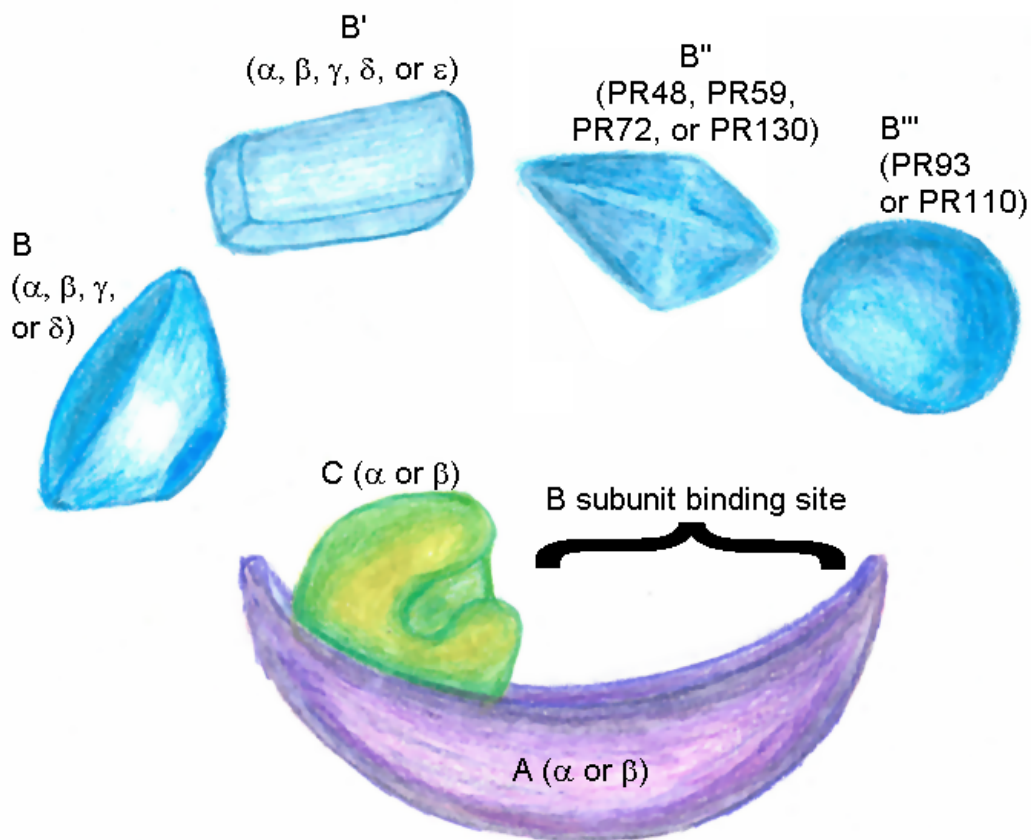
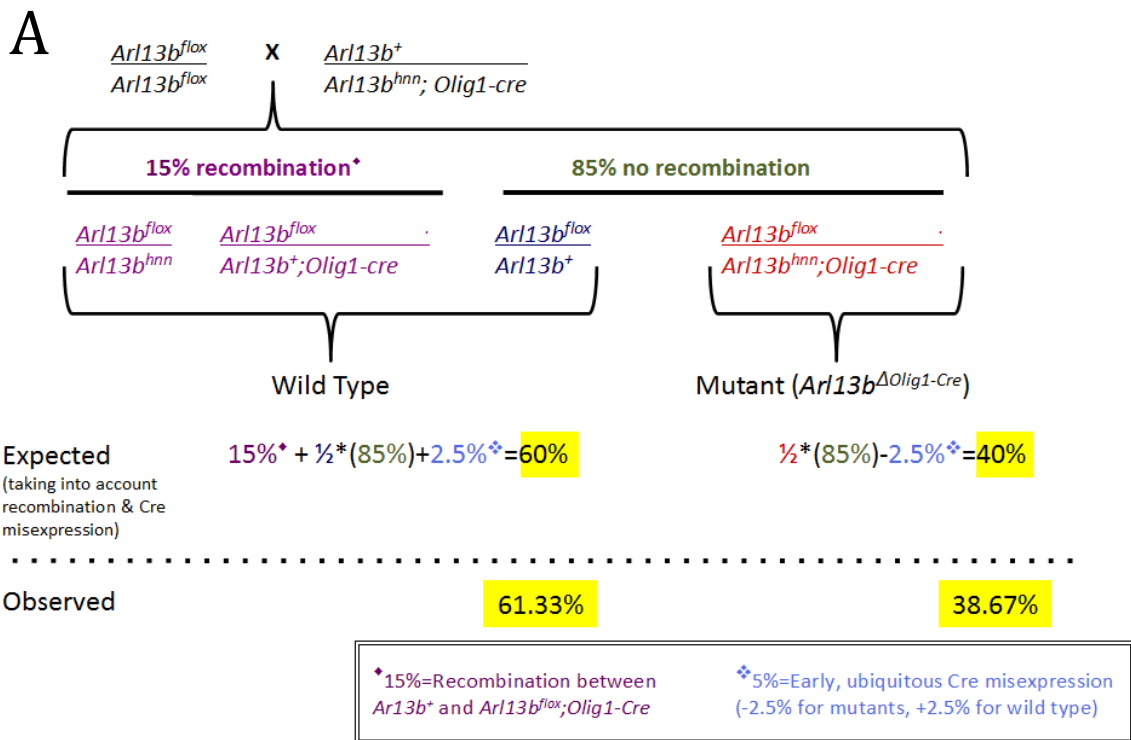


Figure 1.8-PP2A is composed of a structural (A), regulatory (B), and catalytic (C) subunit.

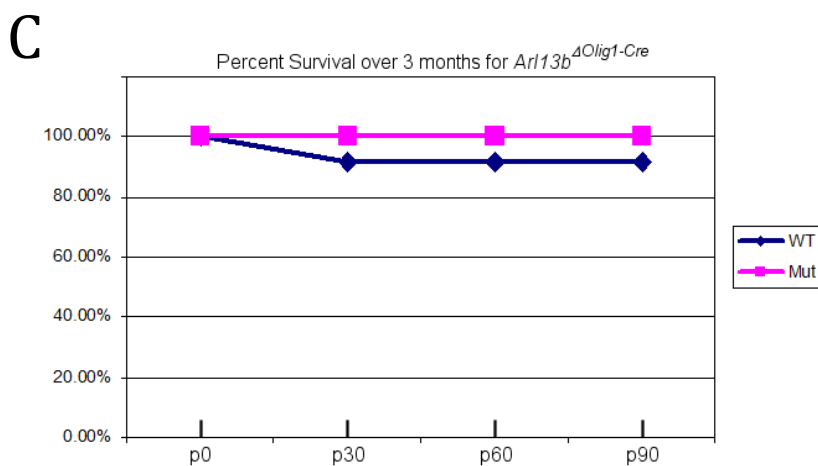
The structural A subunit, and the catalytic C subunit each have  $\alpha$  and  $\beta$  isoforms. The regulatory B subunit comes from one of four unrelated B subunit families, which contain fifteen different proteins that can form up to twenty-three isoforms combined. The B subunit family contains B $\alpha$ , B $\beta$ , B $\gamma$ , and B $\delta$  proteins. The B' family contains B' $\alpha$ , B' $\beta$ , B' $\gamma$ , B' $\delta$ , and B' $\epsilon$ . The B'' family contains PR48, PR59, PR72, and PR130. The B''' family contains proteins PR93 and PR110.



**B**

**Observed vs. expected (Live births)**

	WT	$Arl13b^{\Delta Olig1-Cre}$
Expected	60.00%	40.00%
Observed	61.33%	38.73%



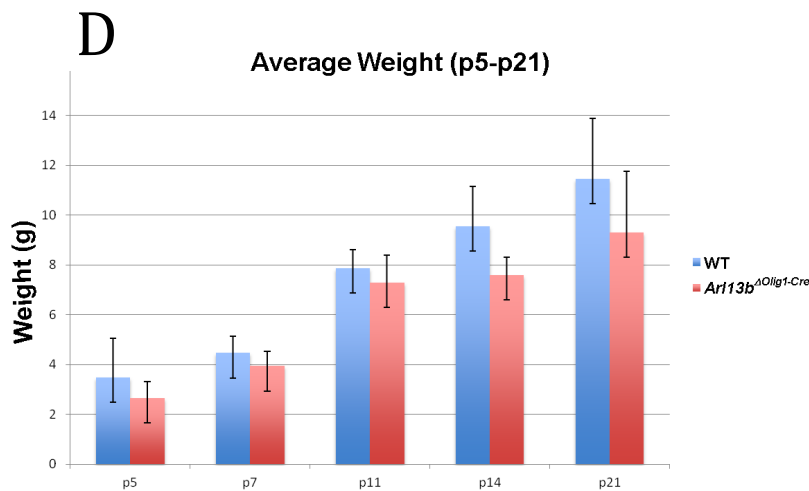


Figure 3.1 A, B-Observed vs. expected ratios of *Arl13b<sup>ΔOlig1-Cre</sup>* pups. C-Percent survival over 3 months for *Arl13b<sup>ΔOlig1-Cre</sup>* and WT littermates. D-Average weights of *Arl13b<sup>ΔOlig1-Cre</sup>* pups at p5, p7, p11, p14, and p21.

A-The *Arl13b<sup>hnn</sup>* allele is linked to *Olig1-Cre*, and recombination between the two is observed 15% of the time. This produces genotypes *Arl13b<sup>lox</sup>/Arl13b<sup>hnn</sup>* and *Arl13b<sup>lox</sup>/Arl13b<sup>+</sup>; Olig1-Cre*. The remaining 85% of genotypes will be *Arl13b<sup>lox</sup>/Arl13b<sup>+</sup>* and *Arl13b<sup>lox</sup>/Arl13b<sup>hnn</sup>; Olig1-Cre*. The genotypes of wild type mice are *Arl13b<sup>lox</sup>/Arl13b<sup>hnn</sup>*, *Arl13b<sup>lox</sup>/Arl13b<sup>+</sup>; Olig1-Cre*, and *Arl13b<sup>lox</sup>/Arl13b<sup>+</sup>*. The mutant genotype is *Arl13b<sup>lox</sup>/Arl13b<sup>hnn</sup>; Olig1-Cre*.

5% of *Olig1-Cre* positive embryos have leaky, ubiquitous Cre expression. This is divided between the two genotypes that have *Olig1-Cre*: *Arl13b<sup>lox</sup>/Arl13b<sup>+</sup>; Olig1-Cre* (wild type) and *Arl13b<sup>lox</sup>/Arl13b<sup>hnn</sup>; Olig1-Cre* (mutant). As a result, 2.5% of each *Olig1-Cre* positive genotype has ubiquitous Cre expression. *Arl13b<sup>lox</sup>/Arl13b<sup>hnn</sup>; Olig1-Cre* (mutant) embryos die during midgestation, since ubiquitous loss of Arl13b

is embryonic lethal. *Arl13b<sup>flox</sup>/Arl13b<sup>+</sup>; Olig1-Cre* embryos have a wild type allele of *Arl13b*, and thus survive to birth.

The calculation for mutants expected to survive to birth is  $\frac{1}{2} * (85\%) - 2.5\% = 40\%$ .  $\frac{1}{2}$  of 85% are mutant because half of the 85% non-recombinants genotypes are *Arl13b<sup>flox</sup>/Arl13b<sup>hnn</sup>; Olig1-Cre* (mutant). 2.5% is subtracted since 2.5% of *Arl13b<sup>flox</sup>/Arl13b<sup>hnn</sup>; Olig1-Cre* embryos will die during midgestation due to leaky, ubiquitous *Olig1-Cre* expression.

The calculation for wild type expected to survive to birth is  $15\% + \frac{1}{2} * (85\%) + 2.5\% = 60\%$ . Recombination between the *Arl13b<sup>hnn</sup>* allele and *Olig1-Cre* allele occurs 15% of the time, and the resulting genotypes are wild type.  $\frac{1}{2}$  of 85% are wild type because half of the 85% non-recombinants genotypes are *Arl13b<sup>flox</sup>/Arl13b<sup>+</sup>* (wild type). 2.5% is added to bring the sum to 100%, since 2.5% was subtracted from the mutant calculation. (n=92 WT, and n=58 *Arl13b<sup>ΔOlig1-Cre</sup>*).

B- *Arl13b<sup>ΔOlig1-Cre</sup>* pups are born at the expected ratios (table form of Figure 3.1A).

C-No difference in survival of *Arl13b<sup>ΔOlig1-Cre</sup>* mice compared to their WT littermates over 3 months (n=12 WT, n=7 *Arl13b<sup>ΔOlig1-Cre</sup>*).

D-While there is an overall trend towards lower a lower weight in *Arl13b<sup>ΔOlig1-Cre</sup>* pups at the indicated ages, there is no significant difference between *Arl13b<sup>ΔOlig1-Cre</sup>* pups and their WT littermates (n=12 WT, n=7 *Arl13b<sup>ΔOlig1-Cre</sup>*). Blue bars-WT. Red bars- *Arl13b<sup>ΔOlig1-Cre</sup>*. Error bars show standard deviation.

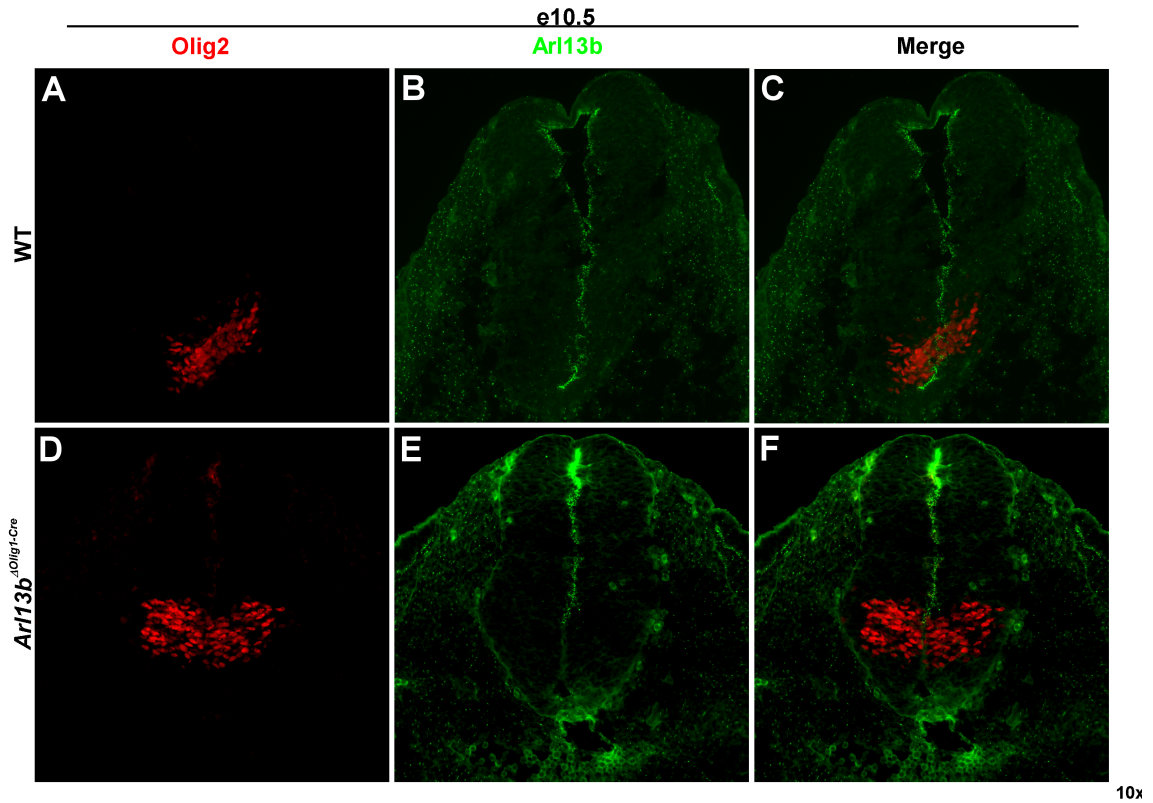


Figure 3.2 Neural tube of WT (A-C) and *Arl13b<sup>ΔOlig1-Cre</sup>* (D-F) e10.5 embryos stained for Olig2 (red; A and D) and Arl13b (green; B and E).

(A-C) WT embryos express Arl13b along the ventricular zone (VZ) of the neural tube at e10.5.

(D-F) At e10.5, expression of Arl13b is absent from the Olig2+ pMN domain of *Arl13b<sup>ΔOlig1-Cre</sup>* embryos, but present in other regions of the neural tube.

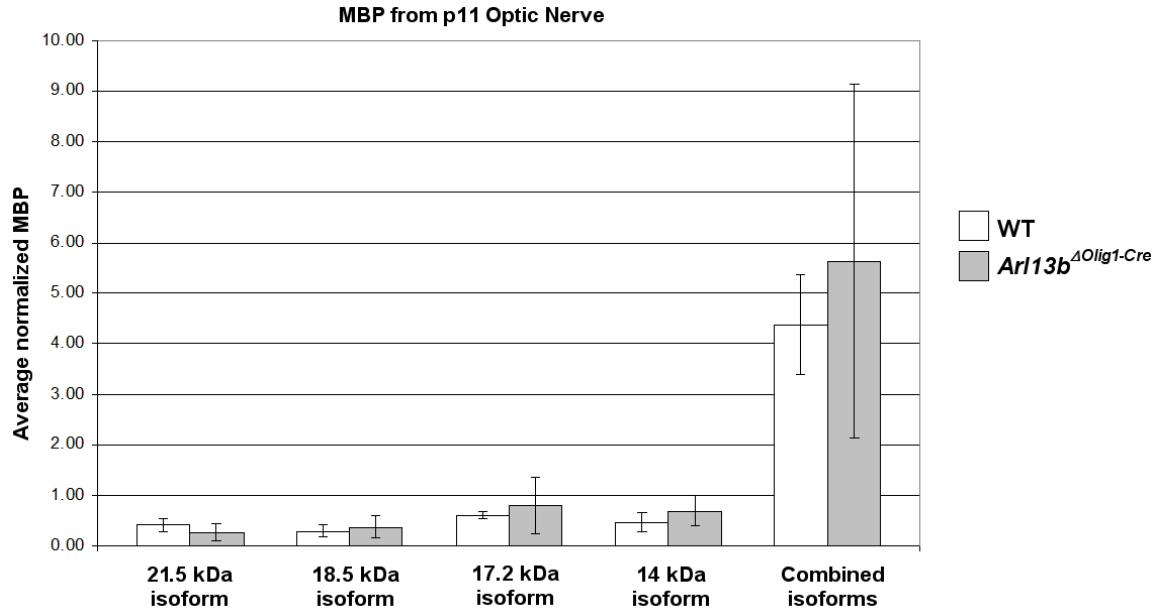


Figure 3.3 Protein levels of MBP, normalized to actin loading controls, from the optic nerves of p7 WT (white bars) and *Arl13b*<sup>ΔOlig1-Cre</sup> (gray bars) pups (n=6 WT, n=4 *Arl13b*<sup>ΔOlig1-Cre</sup>).

At p11, there is no significant difference in MBP expression for any one isoform or for total MBP between *Arl13b*<sup>ΔOlig1-Cre</sup> pups and their WT littermates. Error bars show standard deviation.

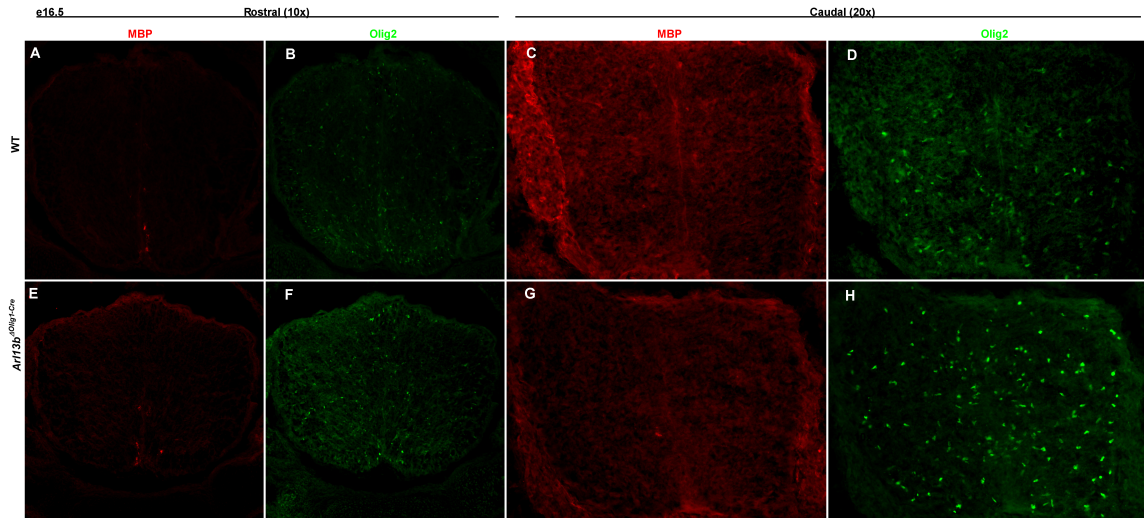


Figure 3.4 Rostral (A-B, E-F) and caudal (C-D, G-H) neural tube of WT (A-D) and *Arl13b $\Delta$ Olig1-Cre* (E-H) e16.5 embryos stained for MBP (red) and Olig2 (green).

(A, E) Expression of MBP in the rostral neural tube is seen at e16.5 in both WT (A) and *Arl13b $\Delta$ Olig1-Cre* (E) embryos.

(B, D, F, H) Olig2+ OLs are specified and found throughout the rostral (B, F) and caudal (D, H) neural tubes of WT (B, D) and *Arl13b $\Delta$ Olig1-Cre* (F, H) e16.5 embryos.

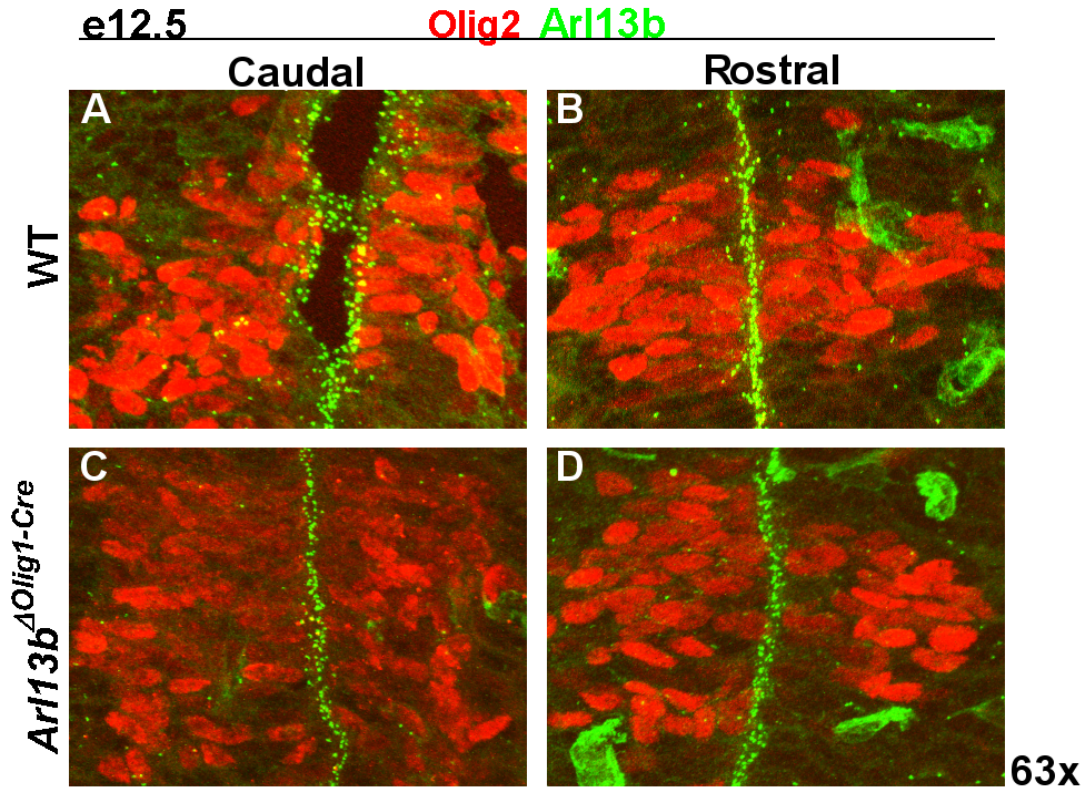
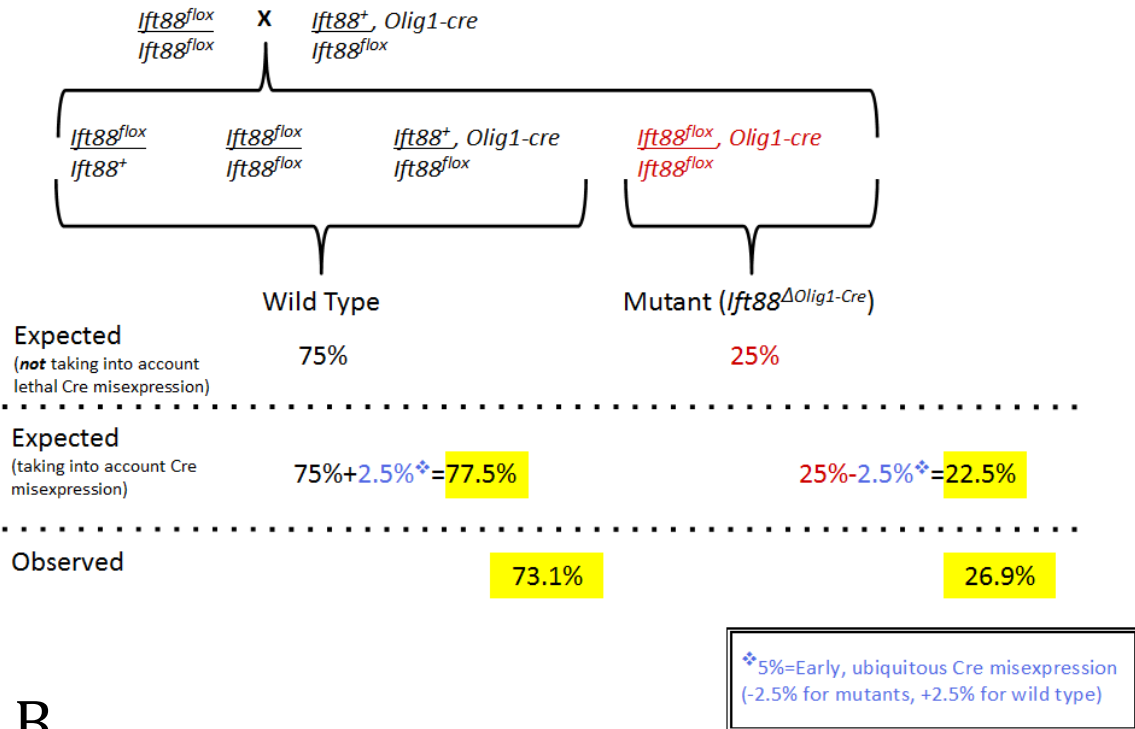


Figure 3.5 Caudal (A, C) and rostral (B, D) neural tube of WT (A-B) and *Arl13b<sup>ΔOlig1-Cre</sup>* (C-D) e12.5 embryos stained for Olig2 (red) and Arl13b (green).

(A-B) WT embryos continue to express Arl13b along the ventricular zone and within the Olig2+ pMN domain of the caudal and rostral neural tube at e12.5.

(C-D) *Arl13b<sup>ΔOlig1-Cre</sup>* re-express Arl13b at e12.5 along the ventricular zone and within the pMN domain of the caudal and rostral neural tube at e12.5.

A



B

Observed vs. expected (Live births)		
	WT	$Ift88^{\Delta Olig1-Cre}$
Observed	73.10%	26.90%
Expected	77.50%	22.50%

Figure 3.6 Observed vs. expected ratios of  $Ift88^{\Delta Olig1-Cre}$  pups.

A- $Ift88^{flox}/Ift88^{flox}$  females were crossed to  $Ift88^{flox}/Ift88^{+}, Olig1-Cre$  males. This cross produces genotypes  $Ift88^{flox}/Ift88^{+}$ ,  $Ift88^{flox}/Ift88^{flox}$ ,  $Ift88^{flox}/Ift88^{+}, Olig1-Cre$ , and  $Ift88^{flox}/Ift88^{flox}, Olig1-Cre$ . The genotypes of wild type mice are  $Ift88^{flox}/Ift88^{+}$ ,  $Ift88^{flox}/Ift88^{flox}$ , and  $Ift88^{flox}/Ift88^{+}, Olig1-Cre$ . The mutant genotype is  $Ift88^{flox}/Ift88^{flox}, Olig1-Cre$ . Wild type genotypes are generated 75% of the time, and the one mutant genotype is generated 25% of the time.

5% of  $Olig1-Cre$  positive embryos have leaky, ubiquitous Cre expression. This is divided between the two genotypes which have  $Olig1-Cre$ :  $Ift88^{flox}/Ift88^{+}, Olig1-Cre$

(wild type) and *Ift88<sup>fllox</sup>/Ift88<sup>fllox</sup>, Olig1-Cre* (mutant). As a result, 2.5% of each *Olig1-Cre* positive genotype has ubiquitous Cre expression. *Ift88<sup>fllox</sup>/Ift88<sup>fllox</sup>, Olig1-Cre* (mutant) embryos die during midgestation, since ubiquitous loss of Ift88 is embryonic lethal. *Ift88<sup>fllox</sup>/Ift88<sup>+</sup>, Olig1-Cre* embryos have a wild type allele of *Ift88*, and thus survive to birth.

The calculation for mutants expected to survive to birth is  $25\% - 2.5\% = 22.5\%$ . 2.5% is subtracted since 2.5% of *Ift88<sup>fllox</sup>/Ift88<sup>fllox</sup>, Olig1-Cre* embryos will die during midgestation due to leaky, ubiquitous *Olig1-Cre* expression.

The calculation for wild type expected to survive to birth is  $75\% + 2.5\% = 77.5\%$ . 2.5% is added to bring the sum to 100%, since 2.5% was subtracted from the mutant calculation. (n=87 WT, and n=32 *Ift88<sup>ΔOlig1-Cre</sup>*).

B-*Ift88<sup>ΔOlig1-Cre</sup>* pups are born at the expected ratios (table form of Figure 3.6A).

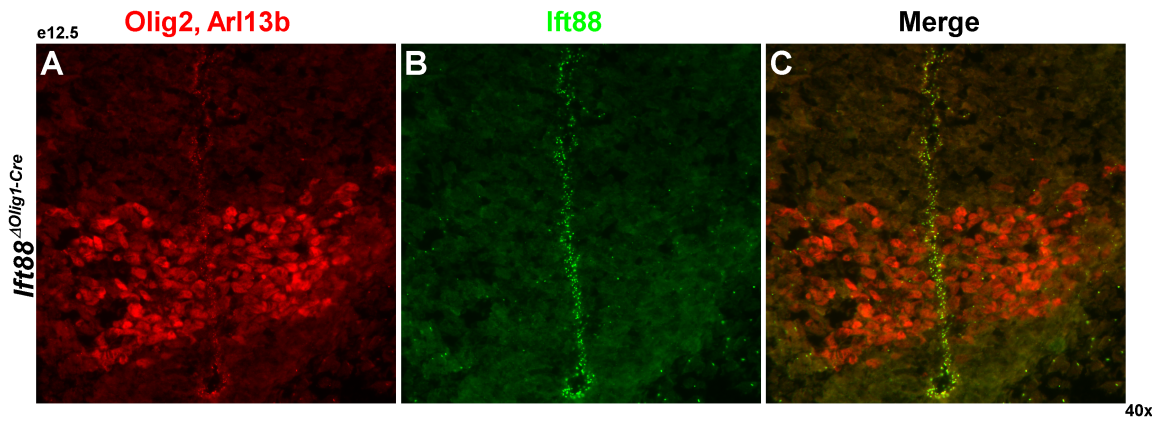


Figure 3.7 Neural tube of *Ift88<sup>ΔOlig1-Cre</sup>* e12.5 embryos stained for Olig2 (red cells), Arl13b (red punctae), and Ift88 (green punctae).

(A) At e12.5, the Olig2+ pMN domain is present. (A-C) Both Arl13b+ cilia and Ift88 persist in the pMN domain and along the ventricular zone of the pMN domain.

A

Observed vs. expected (Live births)		
	WT	<i>Arl13b</i> <sup><math>\Delta</math>Nestin-Cre</sup>
Observed	81.42%	18.58%
Expected	75.00%	25.00%

B

Observed vs. expected (Live births)		
	WT	<i>Ift88</i> <sup><math>\Delta</math>Nestin-Cre</sup>
Observed	76.92%	23.08%
Expected	75.00%	25.00%

Figure 3.8 Observed vs. expected ratios of *Arl13b* <sup>$\Delta$ Nestin-Cre</sup> (A) and *Ift88* <sup>$\Delta$ Nestin-Cre</sup> pups (B).

A-Both *Arl13b* <sup>$\Delta$ Nestin-Cre</sup> pups are born at the expected ratios. (n=92 WT, and n=21 *Arl13b* <sup>$\Delta$ Nestin-Cre</sup>).

B- *Ift88* <sup>$\Delta$ Nestin-Cre</sup> pups are born at the expected ratios. (n=30 WT, and n=9 *Ift88* <sup>$\Delta$ Nestin-Cre</sup>).

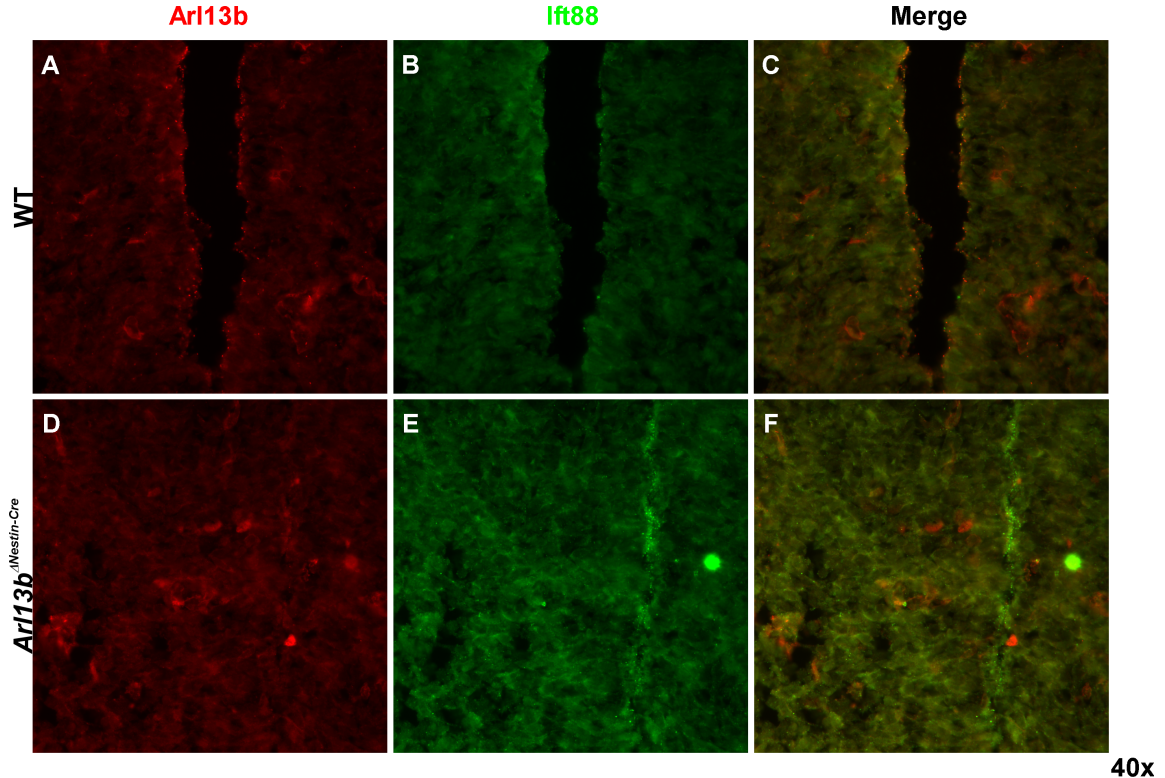


Figure 3.9 Neural tube of WT (A-C) and *Arl13b*<sup>ΔNestin-Cre</sup> (D-F) e12.5 embryos stained for Olig2 (red cells), Arl13b (red punctae; A, D), and Ift88 (green punctae; B, F).

A, D-At e12.5, Arl13b is present in the neural tube of WT, but not *Arl13b*<sup>ΔNestin-Cre</sup> embryos.

B, C, E, F-The presence of Ift88 in both WT and *Arl13b*<sup>ΔNestin-Cre</sup> embryos indicates presence of cilia at e12.5. Loss of Arl13b staining is observed throughout the neural tube of *Arl13b*<sup>ΔNestin-Cre</sup> embryos at e12.5. Thus, *Arl13b*<sup>ΔNestin-Cre</sup> embryos maintain cilia, but lose Arl13b in the neural tube by e12.5.

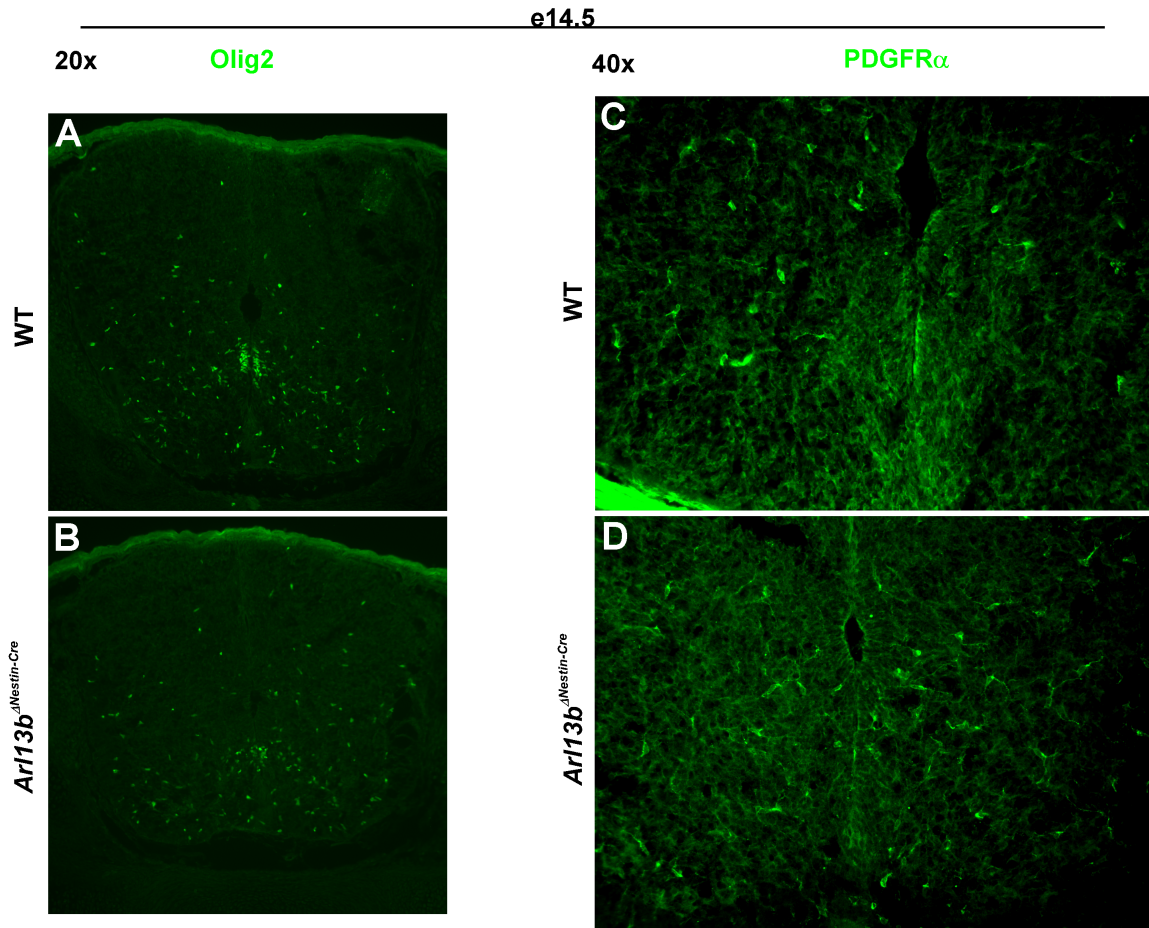


Figure 3.10 Neural tube of WT (A,C) and *Arl13b* <sup>$\Delta$ Nestin-Cre</sup> (B, D) e14.5 embryos stained for Olig2 (A, B; green) and PDGFR $\alpha$  (C, D; green).

(A, B) At e14.5, Olig2+ OLPs are present and migrating throughout the neural tube in both *Arl13b* <sup>$\Delta$ Nestin-Cre</sup> and WT littermates.

(C, D) At e14.5, PDGFR $\alpha$  +OLPs are present and migrating throughout the neural tube in both *Arl13b* <sup>$\Delta$ Nestin-Cre</sup> and WT littermates.

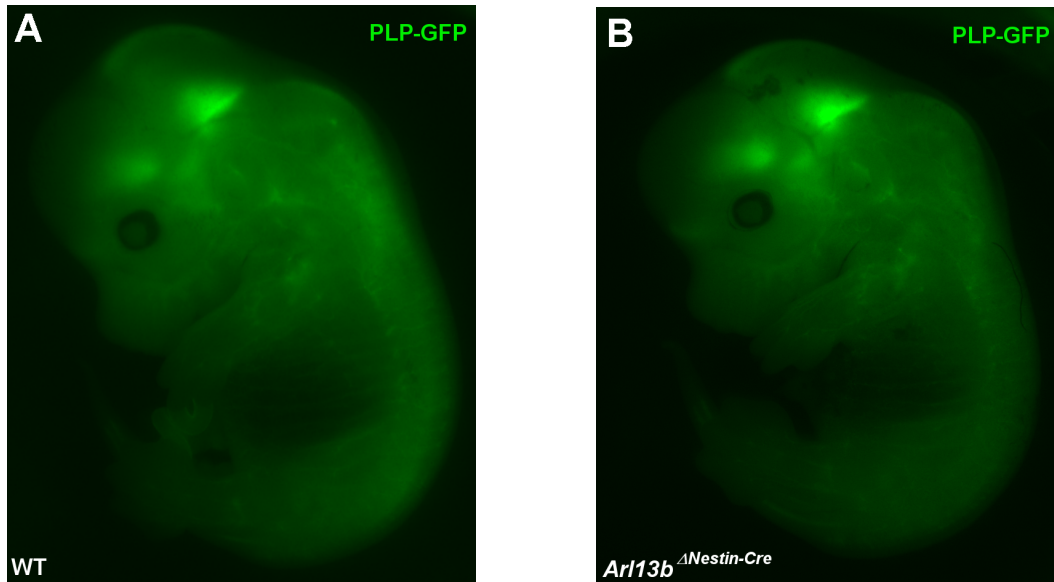


Figure 3.11 Whole embryos of WT (A) and *Arl13b*<sup>ΔNestin-Cre</sup> (B) e14.5 embryos expressing PLP-GFP.

(A, B) Expression of PLP-GFP, a marker of maturing OLS, is present throughout the central nervous system of *Arl13b*<sup>ΔNestin-Cre</sup> (B) and WT (A) e14.5 embryos.

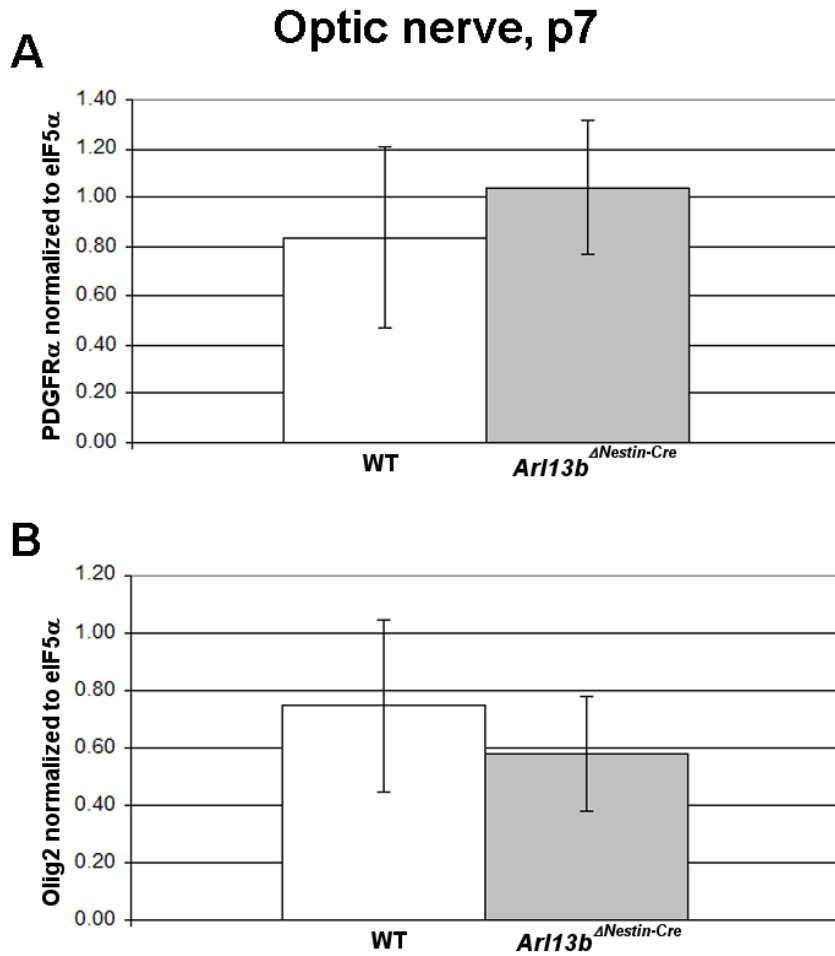


Figure 3.12 Average normalized values of PDGFR $\alpha$  (A) and Olig2 (B) from p7 optic nerves of WT pups (white boxes) and *Arl13b* <sup>$\Delta$ Nestin-Cre</sup> (gray boxes). (n=6 WT, and n=6 *Arl13b* <sup>$\Delta$ Nestin-Cre</sup>).

(A) There is no difference in amount of PDGFR $\alpha$  in the optic nerves of WT (white boxes) and *Arl13b* <sup>$\Delta$ Nestin-Cre</sup> (gray boxes) p7 pups.

(B) There is no difference in amount of Olig2 in the optic nerves of WT (white boxes) and *Arl13b* <sup>$\Delta$ Nestin-Cre</sup> (gray boxes) p7 pups.

Error bars show standard deviation.

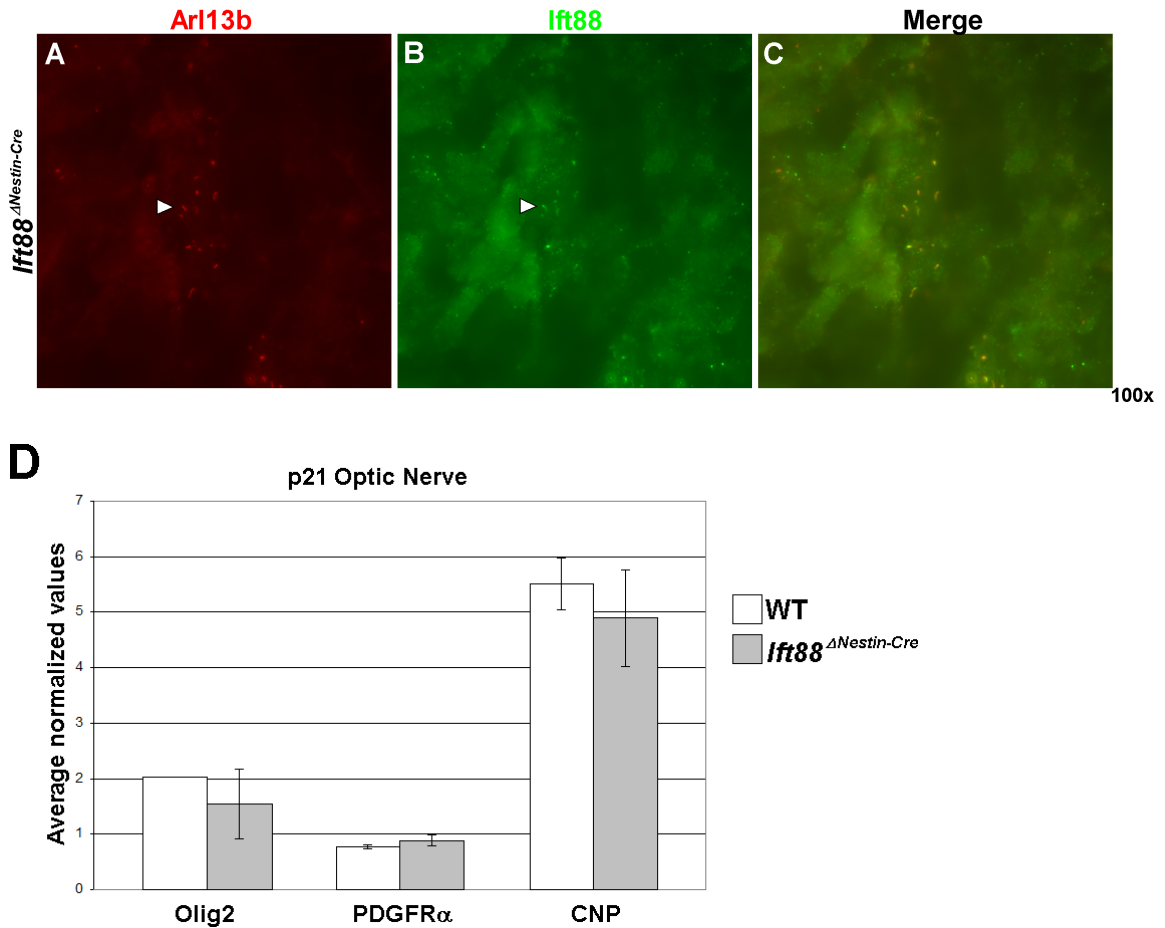


Figure 3.13 Neural tube sections of e18.5 *Ift88<sup>ΔNestin-Cre</sup>* (A-C) embryos stained for Arl13b (A, red) and Ift88 (B, green). Average normalized values of Olig2, PDGFR $\alpha$ , and CNP from p11 optic nerves of WT (white boxes) and *Ift88<sup>ΔNestin-Cre</sup>* (gray boxes) pups.

(A-C) At e18.5, both Arl13b+ cilia (A, C) and Ift88 (B, C) are present in the neural tube of *Ift88<sup>ΔNestin-Cre</sup>* embryos.

(D) At p21, the optic nerves of WT (white boxes) and *Ift88<sup>ΔNestin-Cre</sup>* (gray boxes) pups contain similar levels of Olig2, PDGFR $\alpha$ , and CNP. Error bars show standard deviation. (n=2 WT, and n=2 *Ift88<sup>ΔNestin-Cre</sup>*).

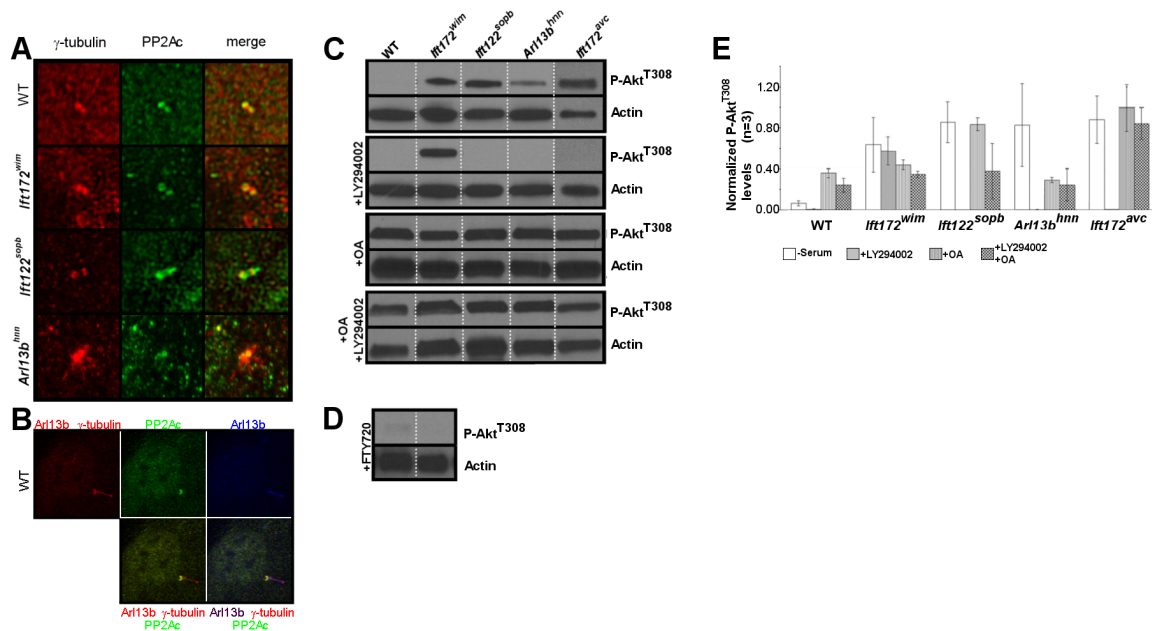


Figure 4.1: PP2Ac localizes to the basal body of WT and cilia transport mutant MEFs, and P-Akt<sup>T308</sup> is increased in cilia transport mutant MEFs.

A: Serum-starved WT and cilia transport mutant MEFs were immunolabeled for the catalytic subunit of PP2A, PP2Ac (green), and for the basal body using  $\gamma$ -tubulin (red).

B: Serum-starved WT MEFs were immunolabeled for the catalytic subunit of PP2A, PP2Ac (green), for the basal body using  $\gamma$ -tubulin (red), and for cilia using Arl13b (red, blue).

C: Serum-starved WT and cilia transport mutant MEFs were lysed and processed for Western blot analysis of P-Akt<sup>T308</sup> under the indicated experimental conditions (no serum, +LY294002, +okadaic acid, and +okadaic acid +LY294002). Note the presence of P-Akt<sup>T308</sup> in *Ift172*<sup>wim</sup> MEFs during LY294002 treatment.

D: Serum-starved WT and *Ift172<sup>wim</sup>* MEFs were treated with a PP2A agonist FTY720, and then lysed and processed for Western blot analysis of P-Akt<sup>T308</sup>. FTY720 agonizes PP2A activity by inhibiting the PP2A inhibitor I2PP2A/SET1. Note the absence of P-Akt<sup>T308</sup> in *Ift172<sup>wim</sup>* MEFs.

E: Average densitometry values of P-Akt<sup>T308</sup> in WT and cilia transport mutant MEFs under the different experimental conditions. Error bars show standard deviation (n=3, p<0.0001).

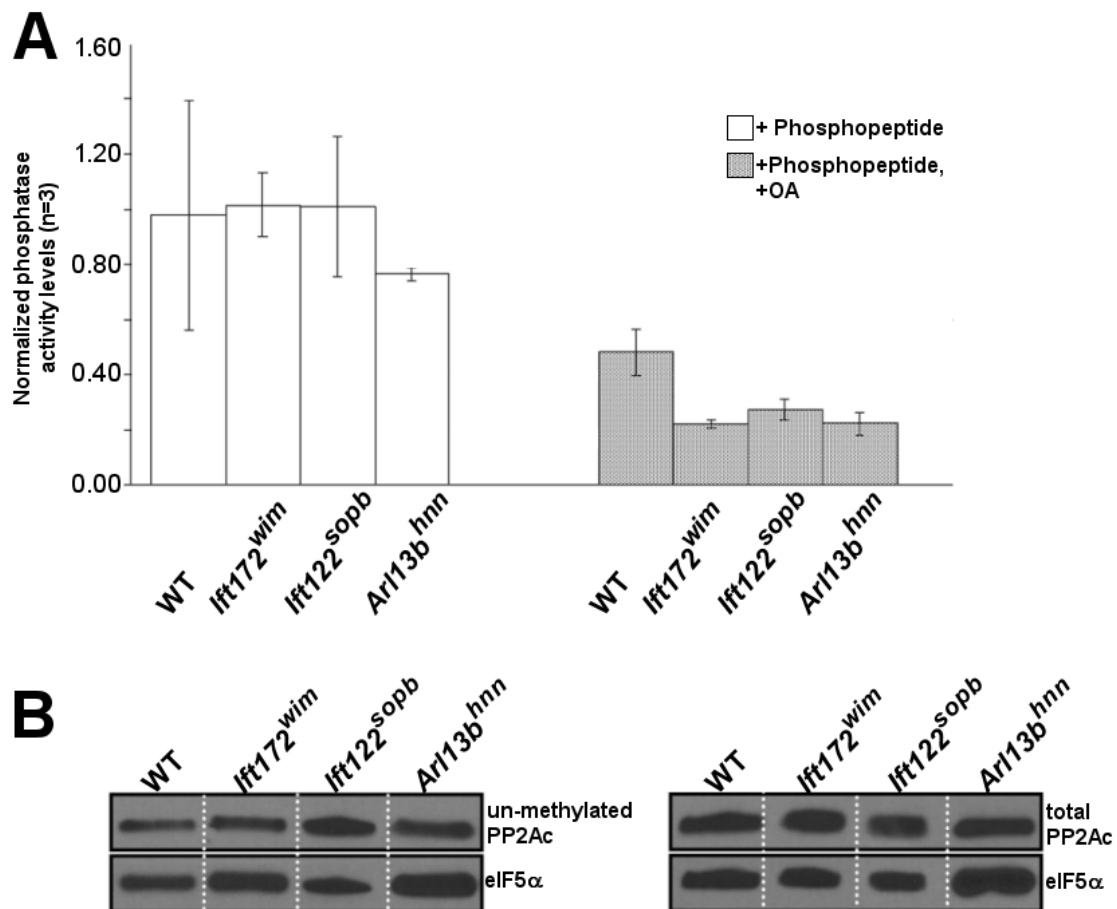


Figure 4.2: PP2A phosphatase activity and levels of total and unmethylated PP2Ac are unchanged in cilia transport mutant MEFs.

A: PP2A activity was measured in WT and cilia transport mutant MEFs. Bars show the average of three independent experiments (n=3). Error bars show standard deviation.

B: Serum-starved WT and cilia transport mutant MEFs were lysed and processed for Western blot analysis of total and unmethylated PP2Ac levels.

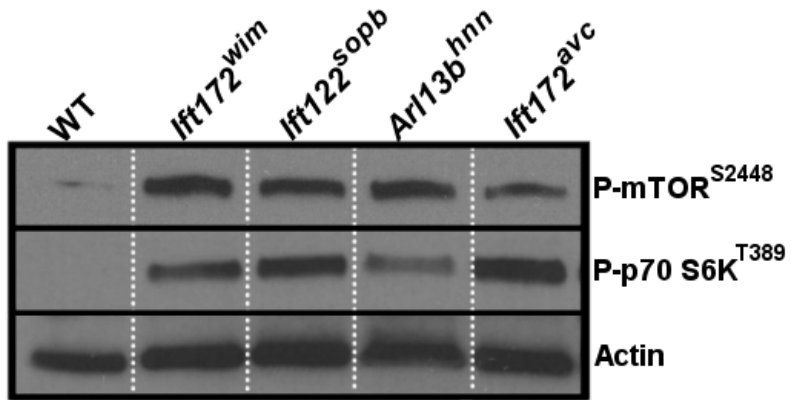


Figure 4.3: mTORC1 signaling is increased in cilia transport mutant MEFs.

Phosphorylation of mTOR (P-mTOR<sup>S2448</sup>) (n=2, p<0.01) and of p70 S6K (P-p70 S6K<sup>T389</sup>) (n=2, p<0.001) are increased in cilia transport mutant MEFs.

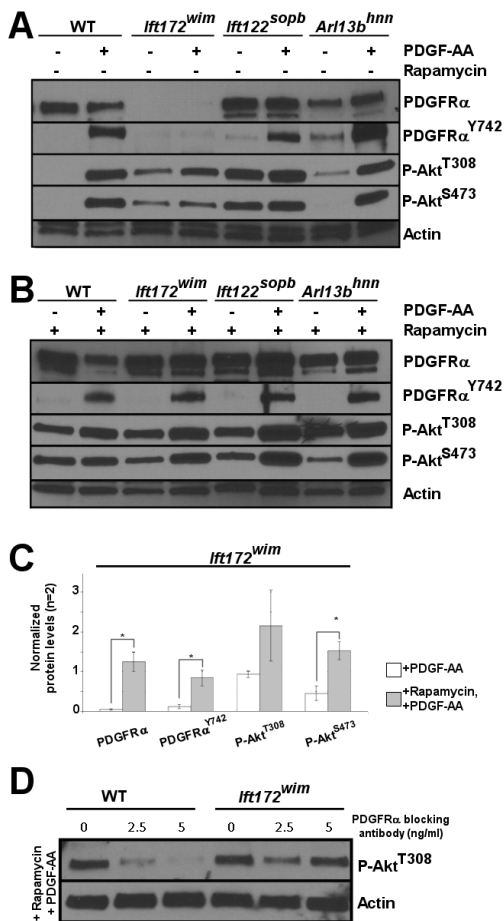


Figure 4.4: Response to PDGF-AA stimulation is inhibited in cilia transport mutant MEFs and is restored by inhibition of mTORC1 with rapamycin.

A: Comparison of PDGFRα, P-PDGFRα<sup>Y742</sup>, P-Akt<sup>T308</sup>, and P-Akt<sup>S473</sup> in WT and cilia transport mutant MEFs in the presence or absence of PDGF-AA ligand stimulation.

B: Rapamycin treatment of WT and cilia transport mutant MEFs in the absence of serum, with or without PDGF-AA ligand stimulation.

C: Average densitometry values of PDGFRα, P-PDGFRα<sup>Y742</sup>, P-Akt<sup>T308</sup>, and P-Akt<sup>S473</sup> in *lft172<sup>wim</sup>* MEFs during PDGF-AA stimulation alone or PDGF-AA stimulation and rapamycin treatment. Error bars show standard deviation (n=2, p<0.05-\*).

D: P-Akt<sup>T308</sup> levels of WT and Ift172<sup>wim</sup> MEFs treated with rapamycin, PDGF-AA, and an increasing concentration of PDGFR $\alpha$  blocking antibody.

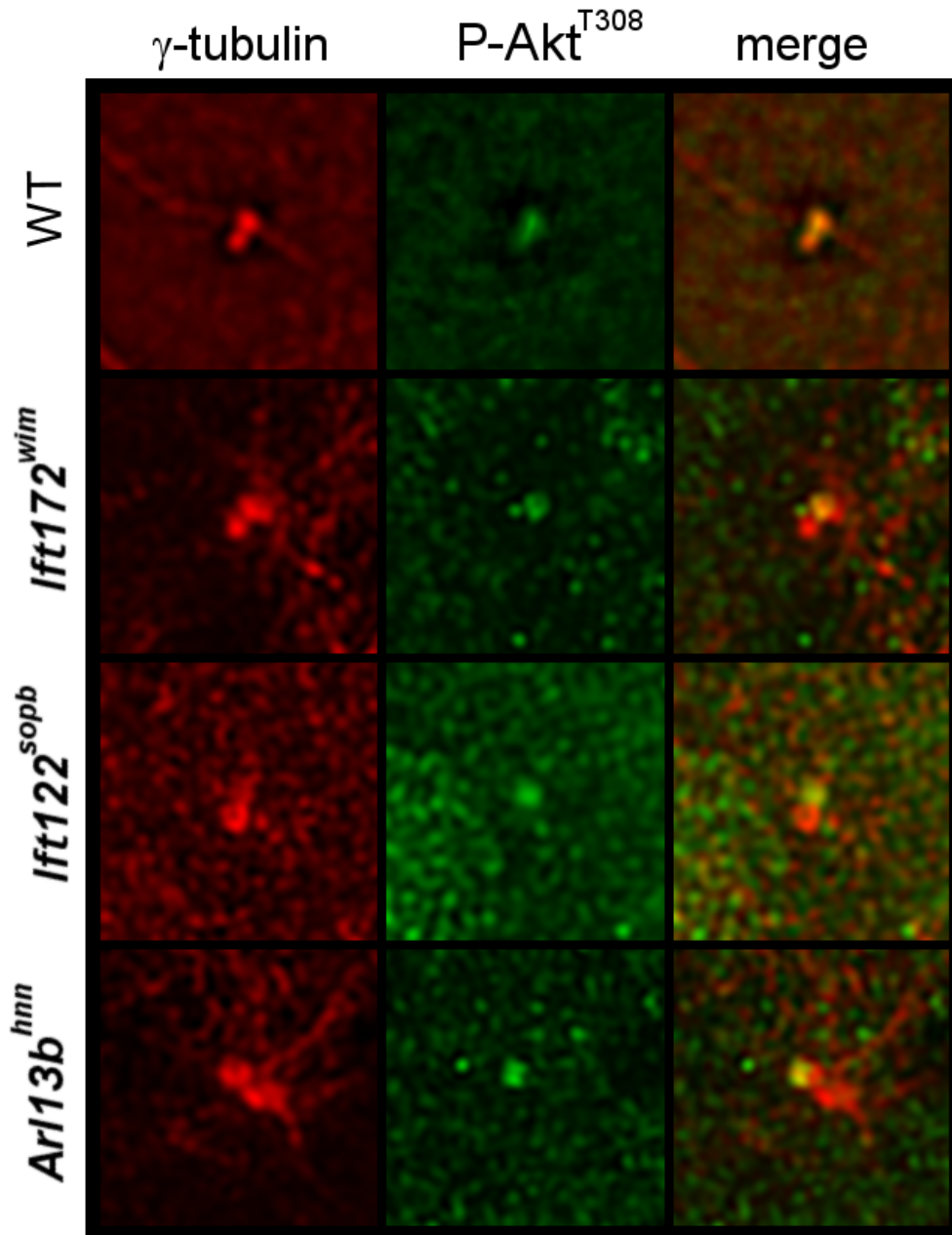


Figure S1: P-Akt<sup>T308</sup> localization in WT and indicated cilia transport mutant MEFs  
Serum starved WT and cilia transport mutant MEFs were immunolabeled for P-Akt<sup>T308</sup> (green) and for the basal body using  $\gamma$ -tubulin (red).

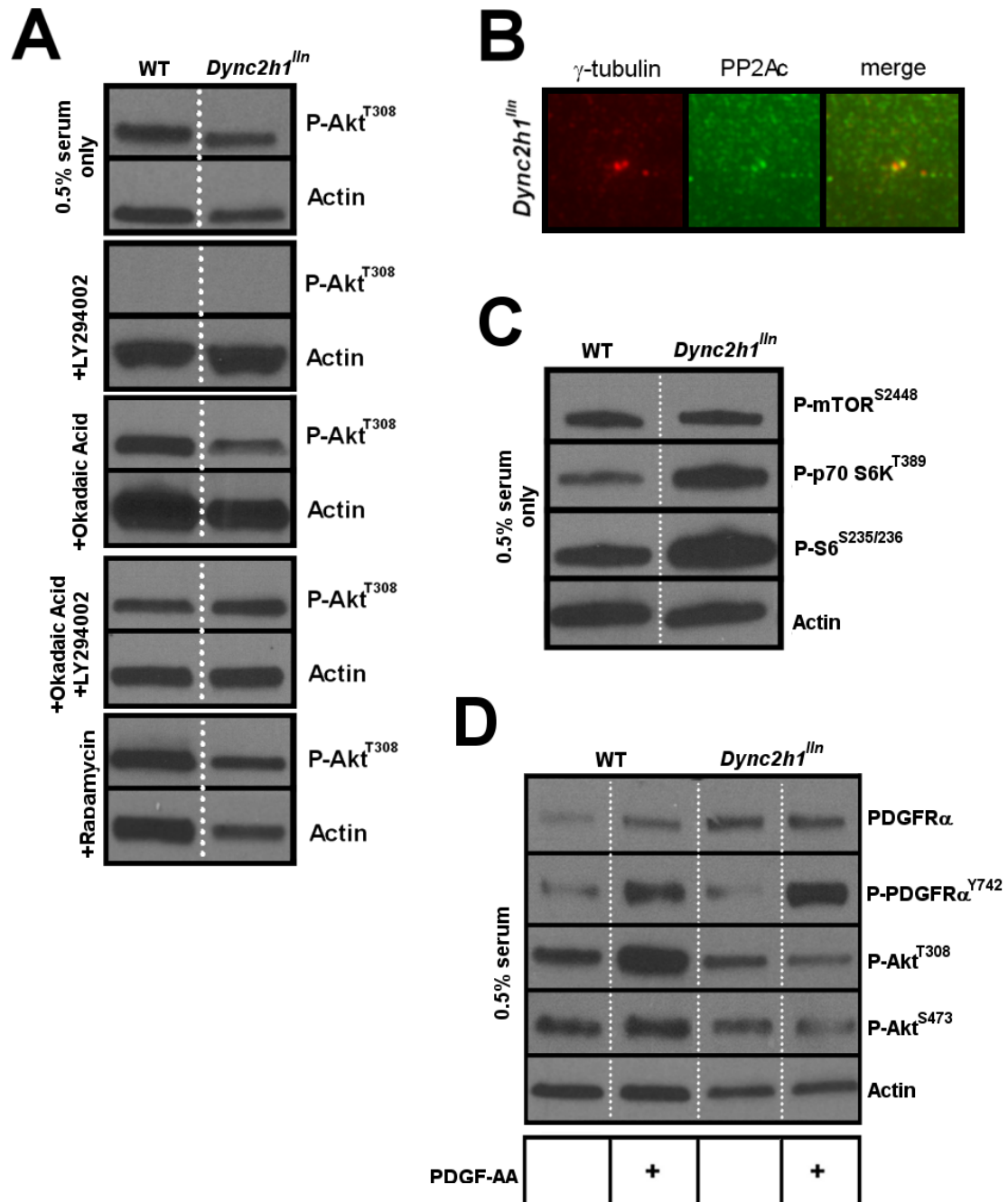


Figure S2: P-Akt<sup>T308</sup> levels of *Dync2h1<sup>fln</sup>* MEFs grown in 0.5% serum

A: WT and *Dync2h1<sup>fln</sup>* MEFs grown in 0.5% serum were lysed and processed for Western blot analysis of P-Akt<sup>T308</sup> under the indicated conditions (0.5% serum only, +LY294002, +okadaic acid, +okadaic acid +LY294002, and +rapamycin).

B: WT and *Dync2h1<sup>ln</sup>* MEFs grown in 0.5% serum were immunolabeled for the catalytic subunit of PP2A, PP2Ac (green), and for the basal body using  $\gamma$ -tubulin (red).

C: WT and *Dync2h1<sup>ln</sup>* MEFs grown in 0.5% serum were lysed and processed for Western blot analysis of phosphorylated mTOR (P-mTOR<sup>S2448</sup>), p70 S6K (P-p70 S6K<sup>T389</sup>), and S6 (S6<sup>S235/236</sup>). Note the increased P-mTOR<sup>S2448</sup> and P-p70 S6K<sup>T389</sup> in *Dync2h1<sup>ln</sup>* MEFs relative to WT MEFs.

D: Comparison of PDGFR $\alpha$ , P-PDGFR $\alpha$ <sup>Y742</sup>, P-Akt<sup>T308</sup>, and P-Akt<sup>S473</sup> in WT and *Dync2h1<sup>ln</sup>* MEFs grown in 0.5% serum with or without stimulation with PDGF-AA ligand.

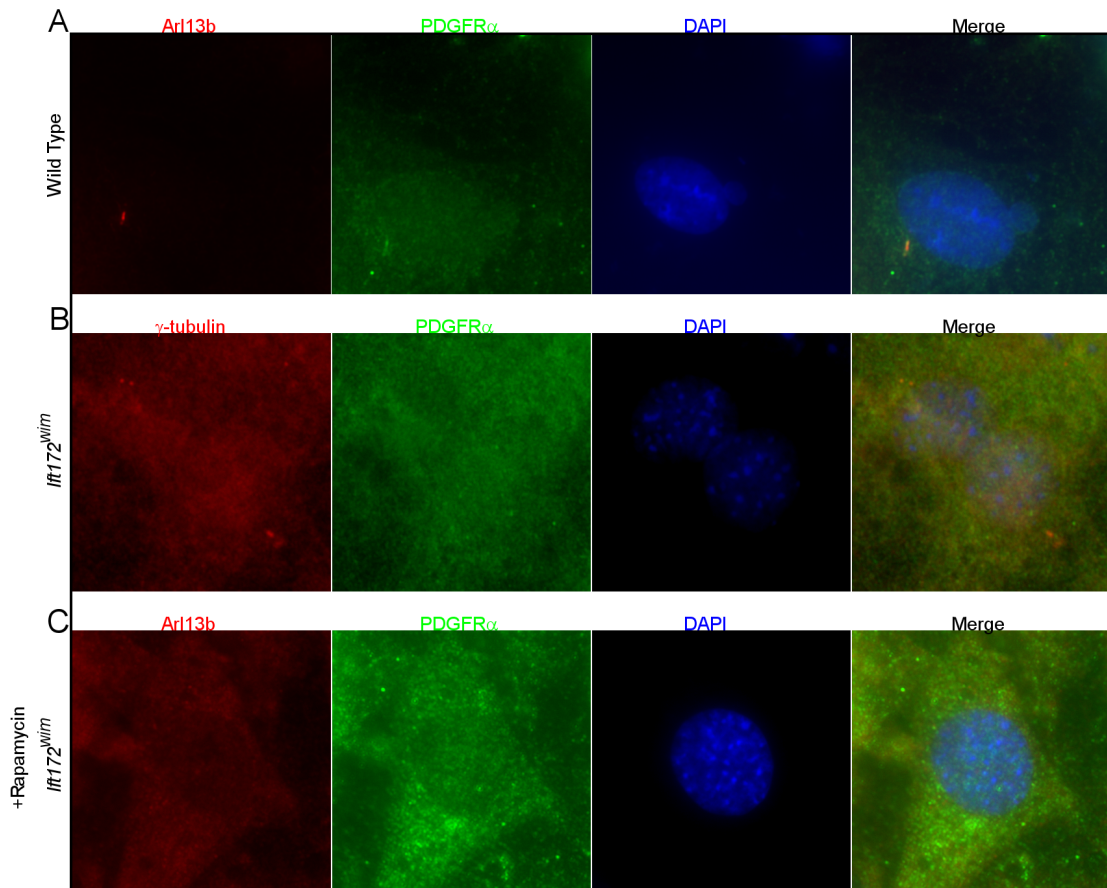


Figure S3: *Ift172<sup>wim</sup>* MEFs do not form cilia during rapamycin treatment.

A: WT MEFs in serum-free media were immunolabeled for Arl13b (red), to mark cilia, and PDGFR $\alpha$  (green).

B: *Ift172<sup>wim</sup>* MEFs in serum-free media were immunolabeled for  $\gamma$ -tubulin (red), to mark the basal body, and PDGFR $\alpha$  (green).

C: *Ift172<sup>wim</sup>* MEFs in serum-free media, treated with rapamycin, were immunolabeled for Arl13b (red), to mark cilia, and PDGFR $\alpha$  (green).

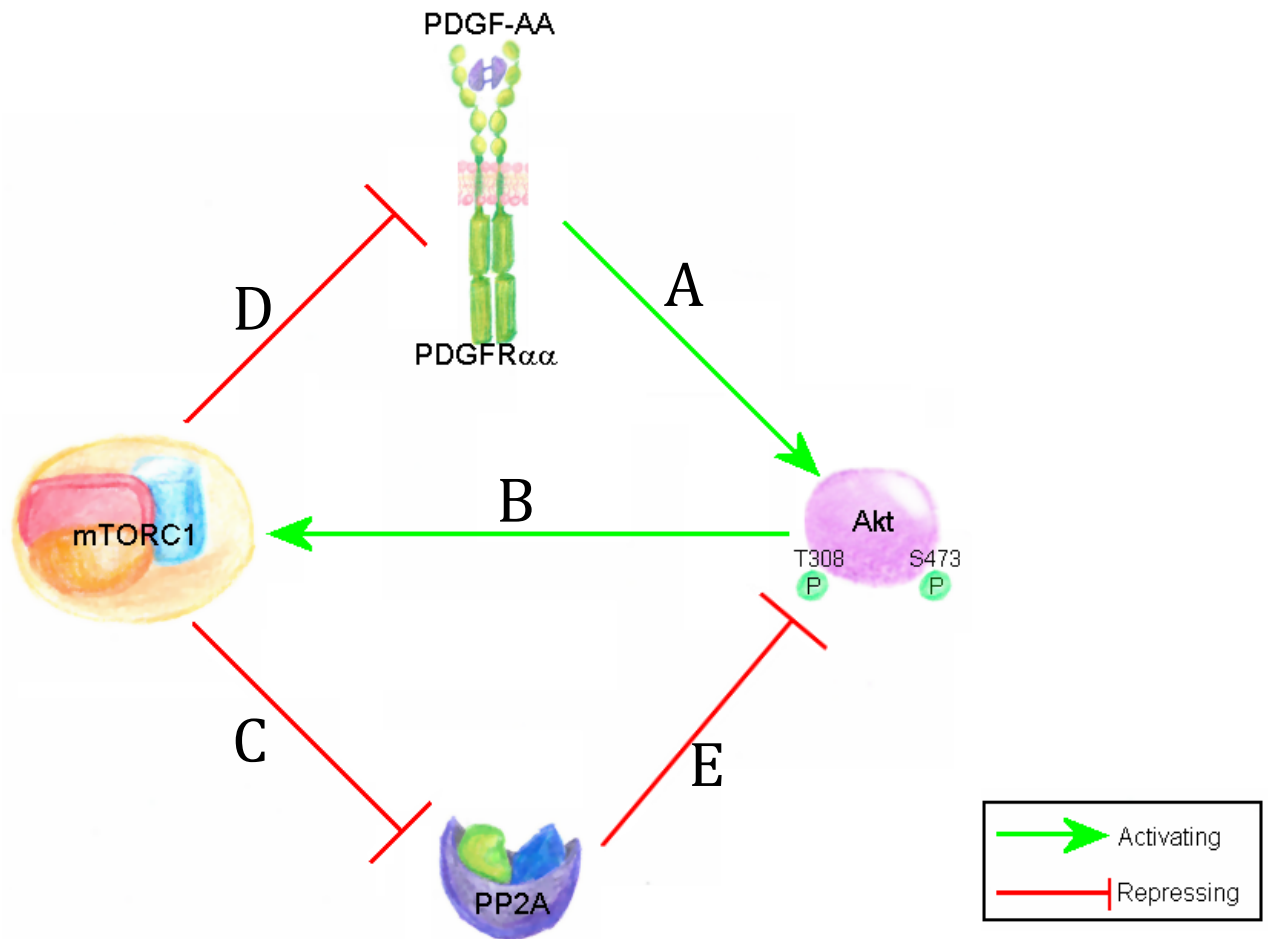


Figure 5.3 PDGF-AA/ $\alpha$ , Akt, mTORC1, and PP2A interact with one another to regulated pathway activity.

A- PDGF-AA/ $\alpha$  activates PI3K, which leads to phosphorylation of Akt on threonine 308 (P-Akt<sup>T308</sup>) and serine 473 (P-Akt<sup>S473</sup>).

B-Activated Akt inhibits TSC1/2, which promotes activation of mTORC1.

C-mTORC1 signaling inhibits PP2A activity as a way to maintain phosphorylation/activation of Akt, and thus activation of mTORC1.

D-mTORC1 signaling leads to down-regulation of PDGFR $\alpha$  as a way to “turn-off” signaling to Akt.

E-Decreased PDGFR $\alpha$  leads to decreased activation of Akt and mTORC1. As mTORC1 inhibition of PP2A is relieved, PP2A is able to dephosphorylate P-Akt<sup>T308</sup>. This reduces the kinase activity of Akt and further “turns-off” Akt signaling.

## References

- Alessi, D.R., Andjelkovic, M., Caudwell, B., Cron, P., Morrice, N., Cohen, P., and Hemmings, B.A. (1996). Mechanism of activation of protein kinase B by insulin and IGF-1. *EMBO J.* 15, 6541–6551.
- Alessi, D.R., Deak, M., Casamayor, A., Barry Caudwell, F., Morrice, N., Norman, D.G., Gaffney, P., Reese, C.B., MacDougall, C.N., Harbison, D., et al. (1997a). 3-Phosphoinositide-dependent protein kinase-1 (PDK1): structural and functional homology with the *Drosophila* DSTPK61 kinase. *Curr. Biol.* 7, 776–789.
- Alessi, D.R., James, S.R., Downes, C.P., Holmes, A.B., Gaffney, P.R., Reese, C.B., and Cohen, P. (1997b). Characterization of a 3-phosphoinositide-dependent protein kinase which phosphorylates and activates protein kinase Balpha. *Curr. Biol.* 7, 261–269.
- Andersen, J.S., Wilkinson, C.J., Mayor, T., Mortensen, P., Nigg, E.A., and Mann, M. (2003). Proteomic characterization of the human centrosome by protein correlation profiling. *Nature* 426, 570–574.
- Anderson, R.G. (1972). The three-dimensional structure of the basal body from the rhesus monkey oviduct. *J. Cell Biol.* 54, 246–265.
- Andjelković, M., Jakubowicz, T., Cron, P., Ming, X.F., Han, J.W., and Hemmings, B.A. (1996). Activation and phosphorylation of a pleckstrin homology domain containing protein kinase (RAC-PK/PKB) promoted by serum and protein phosphatase inhibitors. *Proc. Natl. Acad. Sci. U. S. A.* 93, 5699–5704.
- Arino, J., Woon, C.W., Brautigan, D.L., Miller, T.B., and Johnson, G.L. (1988). Human liver phosphatase 2A: cDNA and amino acid sequence of two catalytic subunit isotypes. *Proc. Natl. Acad. Sci. U. S. A.* 85, 4252–4256.
- De Baere, I., Derua, R., Janssens, V., Van Hoof, C., Waelkens, E., Merlevede, W., and Goris, J. (1999). Purification of porcine brain protein phosphatase 2A leucine carboxyl methyltransferase and cloning of the human homologue. *Biochemistry* 38, 16539–16547.
- Ballou, L.M. (1988). S6 Kinase in Quiescent Swiss Mouse 3T3 Cells is Activated by Phosphorylation in Response to Serum Treatment. *Proc. Natl. Acad. Sci.* 85, 7154–7158.
- Ballou, L.M., Jenö, P., and Thomas, G. (1988). Protein phosphatase 2A inactivates the mitogen-stimulated S6 kinase from Swiss mouse 3T3 cells. *J. Biol. Chem.* 263, 1188–1194.

- Bansal, R., and Pfeiffer, S.E. (1992). Novel stage in the oligodendrocyte lineage defined by reactivity of progenitors with R-mAb prior to O1 anti-galactocerebroside. *J. Neurosci. Res.* *32*, 309–316.
- Bansal, R., Warrington, A.E., Gard, A.L., Ranscht, B., and Pfeiffer, S.E. (1989). Multiple and novel specificities of monoclonal antibodies O1, O4, and R-mAb used in the analysis of oligodendrocyte development. *J. Neurosci. Res.* *24*, 548–557.
- Barres, B.A., Hart, I.K., Coles, H.S., Burne, J.F., Voyvodic, J.T., Richardson, W.D., and Raff, M.C. (1992). Cell death and control of cell survival in the oligodendrocyte lineage. *Cell* *70*, 31–46.
- Basu, S. (2011). PP2A in the regulation of cell motility and invasion. *Curr. Protein Pept. Sci.* *12*, 3–11.
- Baumann, N., and Pham-Dinh, D. (2001). Biology of Oligodendrocyte and Myelin in the Mammalian Central Nervous System. *Physiol Rev* *81*, 871–927.
- Bazenet, C.E., Gelderloos, J.A., and Kazlauskas, A. (1996). Phosphorylation of tyrosine 720 in the platelet-derived growth factor alpha receptor is required for binding of Grb2 and SHP-2 but not for activation of Ras or cell proliferation. *Mol. Cell. Biol.* *16*, 6926–6936.
- Behal, R.H., Miller, M.S., Qin, H., Lucker, B.F., Jones, A., and Cole, D.G. (2012). Subunit interactions and organization of the *Chlamydomonas reinhardtii* intraflagellar transport complex A proteins. *J. Biol. Chem.* *287*, 11689–11703.
- Bellacosa, A., Testa, J.R., Staal, S.P., and Tschlis, P.N. (1991). A retroviral oncogene, akt, encoding a serine-threonine kinase containing an SH2-like region. *Science* *254*, 274–277.
- Bellacosa, A., Franke, T.F., Gonzalez-Portal, M.E., Datta, K., Taguchi, T., Gardner, J., Cheng, J.Q., Testa, J.R., and Tschlis, P.N. (1993). Structure, expression and chromosomal mapping of c-akt: relationship to v-akt and its implications. *Oncogene* *8*, 745–754.
- Bellacosa, A., Chan, T.O., Ahmed, N.N., Datta, K., Malstrom, S., Stokoe, D., McCormick, F., Feng, J., and Tschlis, P. (1998). Akt activation by growth factors is a multiple-step process: the role of the PH domain. *Oncogene* *17*, 313–325.
- Berger, T., and Frotscher, M. (1994). Distribution and morphological characteristics of oligodendrocytes in the rat hippocampus in situ and in vitro: an immunocytochemical study with the monoclonal Rip antibody. *J. Neurocytol.* *23*, 61–74.

- Bhatia, B., Northcott, P.A., Hambarzumyan, D., Govindarajan, B., Brat, D.J., Arbiser, J.L., Holland, E.C., Taylor, M.D., and Kenney, A.M. (2009). Tuberous sclerosis complex suppression in cerebellar development and medulloblastoma: separate regulation of mammalian target of rapamycin activity and p27 Kip1 localization. *Cancer Res.* *69*, 7224–7234.
- Blacque, O.E., Li, C., Inglis, P.N., Esmail, M.A., Ou, G., Mah, A.K., Baillie, D.L., Scholey, J.M., and Leroux, M.R. (2006). The WD repeat-containing protein IFTA-1 is required for retrograde intraflagellar transport. *Mol. Biol. Cell* *17*, 5053–5062.
- Boehlke, C., Kotsis, F., Patel, V., Braeg, S., Voelker, H., Brecht, S., Beyer, T., Janusch, H., Hamann, C., Gödel, M., et al. (2010). Primary cilia regulate mTORC1 activity and cell size through Lkb1. *Nat. Cell Biol.* *12*, 1115–1122.
- Bradl, M., and Lassmann, H. (2010). Oligodendrocytes: biology and pathology. *Acta Neuropathol.* *119*, 37–53.
- Brook-Carter, P.T., Peral, B., Ward, C.J., Thompson, P., Hughes, J., Maheshwar, M.M., Nellist, M., Gamble, V., Harris, P.C., and Sampson, J.R. (1994). Deletion of the TSC2 and PKD1 genes associated with severe infantile polycystic kidney disease--a contiguous gene syndrome. *Nat. Genet.* *8*, 328–332.
- Brown, E.J., Albers, M.W., Shin, T.B., Ichikawa, K., Keith, C.T., Lane, W.S., and Schreiber, S.L. (1994). A mammalian protein targeted by G1-arresting rapamycin-receptor complex. *Nature* *369*, 756–758.
- BUNGE, R.P., and GLASS, P.M. (1965). SOME OBSERVATIONS ON MYELIN-GLIAL RELATIONSHIPS AND ON THE ETIOLOGY OF THE CEREBROSPINAL FLUID EXCHANGE LESION. *Ann. N. Y. Acad. Sci.* *122*, 15–28.
- Buonamici, S., Williams, J., Morrissey, M., Wang, A., Guo, R., Vattay, A., Hsiao, K., Yuan, J., Green, J., Ospina, B., et al. (2010). Interfering with resistance to smoothed antagonists by inhibition of the PI3K pathway in medulloblastoma. *Sci. Transl. Med.* *2*, 51ra70.
- Burgering, B.M., and Coffey, P.J. (1995). Protein kinase B (c-Akt) in phosphatidylinositol-3-OH kinase signal transduction. *Nature* *376*, 599–602.
- Burnett, P.E., Barrow, R.K., Cohen, N.A., Snyder, S.H., and Sabatini, D.M. (1998). RAFT1 phosphorylation of the translational regulators p70 S6 kinase and 4E-BP1. *Proc. Natl. Acad. Sci. U. S. A.* *95*, 1432–1437.

- Cai, S.-L., Tee, A.R., Short, J.D., Bergeron, J.M., Kim, J., Shen, J., Guo, R., Johnson, C.L., Kiguchi, K., and Walker, C.L. (2006). Activity of TSC2 is inhibited by AKT-mediated phosphorylation and membrane partitioning. *J. Cell Biol.* *173*, 279–289.
- Calleja, V., Alcor, D., Laguerre, M., Park, J., Vojnovic, B., Hemmings, B.A., Downward, J., Parker, P.J., and Larijani, B. (2007). Intramolecular and intermolecular interactions of protein kinase B define its activation in vivo. *PLoS Biol.* *5*, e95.
- Calnan, D.R., and Brunet, A. (2008). The FoxO code. *Oncogene* *27*, 2276–2288.
- Calver, a R., Hall, a C., Yu, W.P., Walsh, F.S., Heath, J.K., Betsholtz, C., and Richardson, W.D. (1998). Oligodendrocyte population dynamics and the role of PDGF in vivo. *Neuron* *20*, 869–882.
- Canaud, G., Knebelmann, B., Harris, P.C., Vrtovsnik, F., Correas, J.-M., Pallet, N., Heyer, C.M., Letavernier, E., Bienaimé, F., Thervet, E., et al. (2010). Therapeutic mTOR inhibition in autosomal dominant polycystic kidney disease: What is the appropriate serum level? *Am. J. Transplant* *10*, 1701–1706.
- Cantagrel, V., Silhavy, J.L., Bielas, S.L., Swistun, D., Marsh, S.E., Bertrand, J.Y., Audollent, S., Attié-Bitach, T., Holden, K.R., Dobyns, W.B., et al. (2008). Mutations in the cilia gene ARL13B lead to the classical form of Joubert syndrome. *Am. J. Hum. Genet.* *83*, 170–179.
- Caspary, T., Larkins, C.E., and Anderson, K. V. (2007). The graded response to Sonic Hedgehog depends on cilia architecture. *Dev. Cell* *12*, 767–778.
- Casso, D.J., Liu, S., Iwaki, D.D., Ogden, S.K., and Kornberg, T.B. (2008). A screen for modifiers of hedgehog signaling in *Drosophila melanogaster* identifies *swm* and *mts*. *Genetics* *178*, 1399–1413.
- Cenacchi, G., Giangaspero, F., Cerasoli, S., Manetto, V., and Martinelli, G.N. (1996). Ultrastructural characterization of oligodendroglial-like cells in central nervous system tumors. *Ultrastruct. Pathol.* *20*, 537–547.
- Chen, J., Martin, B.L., and Brautigan, D.L. (1992). Regulation of protein serine-threonine phosphatase type-2A by tyrosine phosphorylation. *Science* *257*, 1261–1264.
- Chen, M.-H., Wilson, C.W., Li, Y.-J., Law, K.K. Lo, Lu, C.-S., Gacayan, R., Zhang, X., Hui, C., and Chuang, P.-T. (2009). Cilium-independent regulation of Gli protein function by Sufu in Hedgehog signaling is evolutionarily conserved. *Genes Dev.* *23*, 1910–1928.

- Chen, Y., Yue, S., Xie, L., Pu, X., Jin, T., and Cheng, S.Y. (2011). Dual Phosphorylation of suppressor of fused (Sufu) by PKA and GSK3 $\beta$  regulates its stability and localization in the primary cilium. *J. Biol. Chem.* *286*, 13502–13511.
- Chiu, M.I., Katz, H., and Berlin, V. (1994). RAPT1, a mammalian homolog of yeast Tor, interacts with the FKBP12/rapamycin complex. *Proc. Natl. Acad. Sci. U. S. A.* *91*, 12574–12578.
- Chizhikov, V. V., Davenport, J., Zhang, Q., Shih, E.K., Cabello, O.A., Fuchs, J.L., Yoder, B.K., and Millen, K.J. (2007). Cilia proteins control cerebellar morphogenesis by promoting expansion of the granule progenitor pool. *J. Neurosci.* *27*, 9780–9789.
- Chung, H., Nairn, A.C., Murata, K., and Brautigan, D.L. (1999). Mutation of Tyr307 and Leu309 in the protein phosphatase 2A catalytic subunit favors association with the  $\alpha$ 4 subunit which promotes dephosphorylation of elongation factor-2. *Biochemistry* *38*, 10371–10376.
- Claesson-Welsh, L., Eriksson, A., Westermark, B., and Heldin, C.H. (1989). cDNA cloning and expression of the human A-type platelet-derived growth factor (PDGF) receptor establishes structural similarity to the B-type PDGF receptor. *Proc. Natl. Acad. Sci. U. S. A.* *86*, 4917–4921.
- Coffer, P.J., and Woodgett, J.R. (1991). Molecular cloning and characterisation of a novel putative protein-serine kinase related to the cAMP-dependent and protein kinase C families. *Eur. J. Biochem.* *201*, 475–481.
- Cohen, P., Klumpp, S., and Schelling, D.L. (1989). An improved procedure for identifying and quantitating protein phosphatases in mammalian tissues. *FEBS Lett.* *250*, 596–600.
- Cole, D.G., Diener, D.R., Himelblau, A.L., Beech, P.L., Fuster, J.C., and Rosenbaum, J.L. (1998). Chlamydomonas kinesin-II-dependent intraflagellar transport (IFT): IFT particles contain proteins required for ciliary assembly in *Caenorhabditis elegans* sensory neurons. *J. Cell Biol.* *141*, 993–1008.
- Corbit, K.C., Aanstad, P., Singla, V., Norman, A.R., Stainier, D.Y.R., and Reiter, J.F. (2005). Vertebrate Smoothed functions at the primary cilium. *Nature* *437*, 1018–1021.
- Cote, G.G., and Crain, R.C. (1993). Biochemistry of Phosphoinositides. *Annu. Rev. Plant Physiol. Plant Mol. Biol.* *44*, 333–356.
- Cuevas, B.D., Lu, Y., Mao, M., Zhang, J., LaPushin, R., Siminovitch, K., and Mills, G.B. (2001). Tyrosine phosphorylation of p85 relieves its inhibitory activity on phosphatidylinositol 3-kinase. *J. Biol. Chem.* *276*, 27455–27461.

- Cui, Q.-L., Zheng, W.-H., Quirion, R., and Almazan, G. (2005). Inhibition of Src-like kinases reveals Akt-dependent and -independent pathways in insulin-like growth factor I-mediated oligodendrocyte progenitor survival. *J. Biol. Chem.* *280*, 8918–8928.
- Danilov, A.I., Gomes-Leal, W., Ahlenius, H., Kokaia, Z., Carlemalm, E., and Lindvall, O. (2009). Ultrastructural and antigenic properties of neural stem cells and their progeny in adult rat subventricular zone. *Glia* *57*, 136–152.
- Deane, J.A., Cole, D.G., Seeley, E.S., Diener, D.R., and Rosenbaum, J.L. (2001). Localization of intraflagellar transport protein IFT52 identifies basal body transitional fibers as the docking site for IFT particles. *Curr. Biol.* *11*, 1586–1590.
- Decker, L., and French-Constant, C. (2004). Lipid rafts and integrin activation regulate oligodendrocyte survival. *J. Neurosci.* *24*, 3816–3825.
- Denef, N., Neubüser, D., Perez, L., and Cohen, S.M. (2000). Hedgehog Induces Opposite Changes in Turnover and Subcellular Localization of Patched and Smoothed. *Cell* *102*, 521–531.
- Dessaud, E., McMahon, A.P., and Briscoe, J. (2008). Pattern formation in the vertebrate neural tube: a sonic hedgehog morphogen-regulated transcriptional network. *Development* *135*, 2489–2503.
- Ding, Q., Motoyama, J., Gasca, S., Mo, R., Sasaki, H., Rossant, J., and Hui, C.C. (1998). Diminished Sonic hedgehog signaling and lack of floor plate differentiation in *Gli2* mutant mice. *Development* *125*, 2533–2543.
- Ding, Q., Fukami, S. i, Meng, X., Nishizaki, Y., Zhang, X., Sasaki, H., Dlugosz, A., Nakafuku, M., and Hui, C. c (1999). Mouse suppressor of *fused* is a negative regulator of sonic hedgehog signaling and alters the subcellular distribution of *Gli1*. *Curr. Biol.* *9*, 1119–1122.
- Distefano, G., Boca, M., Rowe, I., Wodarczyk, C., Ma, L., Piontek, K.B., Germino, G.G., Pandolfi, P.P., and Boletta, A. (2009). Polycystin-1 regulates extracellular signal-regulated kinase-dependent phosphorylation of tuberlin to control cell size through mTOR and its downstream effectors S6K and 4EBP1. *Mol. Cell. Biol.* *29*, 2359–2371.
- Dowling, R.J.O., Topisirovic, I., Fonseca, B.D., and Sonenberg, N. (2010). Dissecting the role of mTOR: lessons from mTOR inhibitors. *Biochim. Biophys. Acta* *1804*, 433–439.

- Du, H., Huang, Y., Zaghlula, M., Walters, E., Cox, T.C., and Massiah, M.A. (2013). The MID1 E3 ligase catalyzes the polyubiquitination of Alpha4 ( $\alpha 4$ ), a regulatory subunit of protein phosphatase 2A (PP2A): novel insights into MID1-mediated regulation of PP2A. *J. Biol. Chem.* 288, 21341–21350.
- Echelard, Y., Epstein, D.J., St-Jacques, B., Shen, L., Mohler, J., McMahon, J.A., and McMahon, A.P. (1993). Sonic hedgehog, a member of a family of putative signaling molecules, is implicated in the regulation of CNS polarity. *Cell* 75, 1417–1430.
- Edelstein, J., and Rockwell, P. (2012). Okadaic acid induces Akt hyperphosphorylation and an oxidative stress-mediated cell death in serum starved SK-N-SH human neuroblastoma cells that are augmented by rapamycin. *Neurosci. Lett.* 531, 74–79.
- Eijkelenboom, A., and Burgering, B.M.T. (2013). FOXOs: signalling integrators for homeostasis maintenance. *Nat. Rev. Mol. Cell Biol.* 14, 83–97.
- Ek, B., and Heldin, C.H. (1984). Use of an antiserum against phosphotyrosine for the identification of phosphorylated components in human fibroblasts stimulated by platelet-derived growth factor. *J. Biol. Chem.* 259, 11145–11152.
- Elam, C.A., Wirschell, M., Yamamoto, R., Fox, L.A., York, K., Kamiya, R., Dutcher, S.K., and Sale, W.S. (2011). An axonemal PP2A B-subunit is required for PP2A localization and flagellar motility. *Cytoskeleton (Hoboken)*. 68, 363–372.
- Ellison, J.A., and de Vellis, J. (1994). Platelet-derived growth factor receptor is expressed by cells in the early oligodendrocyte lineage. *J. Neurosci. Res.* 37, 116–128.
- Eriksson, A., Nånberg, E., Rönnstrand, L., Engström, U., Hellman, U., Rupp, E., Carpenter, G., Heldin, C.H., and Claesson-Welsh, L. (1995). Demonstration of functionally different interactions between phospholipase C-gamma and the two types of platelet-derived growth factor receptors. *J. Biol. Chem.* 270, 7773–7781.
- Evans, D.R., and Hemmings, B.A. (2000). Mutation of the C-terminal leucine residue of PP2Ac inhibits PR55/B subunit binding and confers supersensitivity to microtubule destabilization in *Saccharomyces cerevisiae*. *Mol. Gen. Genet.* 264, 425–432.
- Falasca, M., and Maffucci, T. (2012). Regulation and cellular functions of class II phosphoinositide 3-kinases. *Biochem. J.* 443, 587–601.

- Falkenburger, B.H., Jensen, J.B., Dickson, E.J., Suh, B.-C., and Hille, B. (2010). Phosphoinositides: lipid regulators of membrane proteins. *J. Physiol.* *588*, 3179–3185.
- Favre, B., Zolnierowicz, S., Turowski, P., and Hemmings, B.A. (1994). The catalytic subunit of protein phosphatase 2A is carboxyl-methylated in vivo. *J. Biol. Chem.* *269*, 16311–16317.
- Ferrari, S., Bandi, H.R., Hofsteenge, J., Bussian, B.M., and Thomas, G. (1991). Mitogen-activated 70K S6 kinase. Identification of in vitro 40 S ribosomal S6 phosphorylation sites. *J. Biol. Chem.* *266*, 22770–22775.
- Flegg, C.P., Sharma, M., Medina-Palazon, C., Jamieson, C., Galea, M., Brocardo, M.G., Mills, K., and Henderson, B.R. (2010). Nuclear export and centrosome targeting of the protein phosphatase 2A subunit B56alpha: role of B56alpha in nuclear export of the catalytic subunit. *J. Biol. Chem.* *285*, 18144–18154.
- Flores, A.I., Mallon, B.S., Matsui, T., Ogawa, W., Rosenzweig, A., Okamoto, T., and Macklin, W.B. (2000). Akt-mediated survival of oligodendrocytes induced by neuregulins. *J. Neurosci.* *20*, 7622–7630.
- Flores, A.I., Narayanan, S.P., Morse, E.N., Shick, H.E., Yin, X., Kidd, G., Avila, R.L., Kirschner, D.A., and Macklin, W.B. (2008). Constitutively active Akt induces enhanced myelination in the CNS. *J. Neurosci.* *28*, 7174–7183.
- Fogelgren, B., Lin, S.-Y., Zuo, X., Jaffe, K.M., Park, K.M., Reichert, R.J., Bell, P.D., Burdine, R.D., and Lipschutz, J.H. (2011). The exocyst protein Sec10 interacts with Polycystin-2 and knockdown causes PKD-phenotypes. *PLoS Genet.* *7*, e1001361.
- Foran, D.R., and Peterson, A.C. (1992). Myelin acquisition in the central nervous system of the mouse revealed by an MBP-Lac Z transgene. *J. Neurosci.* *12*, 4890–4897.
- Franke, T.F., Yang, S.I., Chan, T.O., Datta, K., Kazlauskas, A., Morrison, D.K., Kaplan, D.R., and Tschlis, P.N. (1995). The protein kinase encoded by the Akt proto-oncogene is a target of the PDGF-activated phosphatidylinositol 3-kinase. *Cell* *81*, 727–736.
- Fredman, P., Magnani, J.L., Nirenberg, M., and Ginsburg, V. (1984). Monoclonal antibody A2B5 reacts with many gangliosides in neuronal tissue. *Arch. Biochem. Biophys.* *233*, 661–666.
- Fredriksson, L., Li, H., and Eriksson, U. (2004). The PDGF family: four gene products form five dimeric isoforms. *Cytokine Growth Factor Rev.* *15*, 197–204.

- Friedland-Little, J.M., Hoffmann, A.D., Ocbina, P.J.R., Peterson, M.A., Bosman, J.D., Chen, Y., Cheng, S.Y., Anderson, K. V, and Moskowitz, I.P. (2011). A novel murine allele of Intraflagellar Transport Protein 172 causes a syndrome including VACTERL-like features with hydrocephalus. *Hum. Mol. Genet.* *20*, 3725–3737.
- Friedman, B., Hockfield, S., Black, J.A., Woodruff, K.A., and Waxman, S.G. (1989). In situ demonstration of mature oligodendrocytes and their processes: an immunocytochemical study with a new monoclonal antibody, *rip*. *Glia* *2*, 380–390.
- Frost, E.E., Zhou, Z., Krasnesky, K., and Armstrong, R.C. (2009). Initiation of oligodendrocyte progenitor cell migration by a PDGF-A activated extracellular regulated kinase (ERK) signaling pathway. *Neurochem. Res.* *34*, 169–181.
- Fruttiger, M., Karlsson, L., Hall, A.C., Abramsson, A., Calver, A.R., Boström, H., Willetts, K., Bertold, C.H., Heath, J.K., Betsholtz, C., et al. (1999). Defective oligodendrocyte development and severe hypomyelination in PDGF-A knockout mice. *Development* *126*, 457–467.
- Fruttiger, M., Calver, A.R., and Richardson, W.D. (2000). Platelet-derived growth factor is constitutively secreted from neuronal cell bodies but not from axons. *Curr. Biol.* *10*, 1283–1286.
- Gan, X., Wang, J., Su, B., and Wu, D. (2011). Evidence for direct activation of mTORC2 kinase activity by phosphatidylinositol 3,4,5-trisphosphate. *J. Biol. Chem.* *286*, 10998–11002.
- Gangal, A., and Fuchs, J.L. (2009). Oligodendrocyte Precursors in the Developmental Mouse Brain have a Primary Cilium (Denton).
- Gao, W., Lin, W., Chen, Y., Gerig, G., Smith, J.K., Jewells, V., and Gilmore, J.H. (2009). Temporal and spatial development of axonal maturation and myelination of white matter in the developing brain. *AJNR. Am. J. Neuroradiol.* *30*, 290–296.
- Garcia-Gonzalo, F.R., Corbit, K.C., Sirerol-Piquer, M.S., Ramaswami, G., Otto, E.A., Noriega, T.R., Seol, A.D., Robinson, J.F., Bennett, C.L., Josifova, D.J., et al. (2011). A transition zone complex regulates mammalian ciliogenesis and ciliary membrane composition. *Nat. Genet.* *43*, 776–784.
- Gard, A.L., and Pfeiffer, S.E. (1990). Two proliferative stages of the oligodendrocyte lineage (A2B5+O4- and O4+GalC-) under different mitogenic control. *Neuron* *5*, 615–625.

- Gard, A.L., and Pfeiffer, S.E. (1993). Glial cell mitogens bFGF and PDGF differentially regulate development of O4+GalC- oligodendrocyte progenitors. *Dev. Biol.* *159*, 618–630.
- Gilula, N.B., and Satir, P. (1972). The ciliary necklace. A ciliary membrane specialization. *J. Cell Biol.* *53*, 494–509.
- Goetz, S.C., and Anderson, K. V (2010). The primary cilium: a signalling centre during vertebrate development. *Nat. Rev. Genet.* *11*, 331–344.
- Götz, J., Probst, A., Ehler, E., Hemmings, B., and Kues, W. (1998). Delayed embryonic lethality in mice lacking protein phosphatase 2A catalytic subunit Calpha. *Proc. Natl. Acad. Sci. U. S. A.* *95*, 12370–12375.
- Graus-Porta, D., Blaess, S., Senften, M., Littlewood-Evans, A., Damsky, C., Huang, Z., Orban, P., Klein, R., Schittny, J.C., and Müller, U. (2001). Beta1-class integrins regulate the development of laminae and folia in the cerebral and cerebellar cortex. *Neuron* *31*, 367–379.
- Green, D.D., Yang, S.I., and Mumby, M.C. (1987). Molecular cloning and sequence analysis of the catalytic subunit of bovine type 2A protein phosphatase. *Proc. Natl. Acad. Sci. U. S. A.* *84*, 4880–4884.
- Greenberg, M.E., and Ziff, E.B. Stimulation of 3T3 cells induces transcription of the c-fos proto-oncogene. *Nature* *311*, 433–438.
- Guertin, D. a, Stevens, D.M., Thoreen, C.C., Burds, A. a, Kalaany, N.Y., Moffat, J., Brown, M., Fitzgerald, K.J., and Sabatini, D.M. (2006). Ablation in mice of the mTORC components raptor, rictor, or mLST8 reveals that mTORC2 is required for signaling to Akt-FOXO and PKCalpha, but not S6K1. *Dev. Cell* *11*, 859–871.
- Haesen, D., Sents, W., and Ivanova, E. (2012). Cellular inhibitors of Protein Phosphatase PP2A in cancer. *Biomed. Res.* *23*, 197–211.
- Hahn, K., Miranda, M., Francis, V.A., Vendrell, J., Zorzano, A., and Teleman, A.A. (2010). PP2A regulatory subunit PP2A-B' counteracts S6K phosphorylation. *Cell Metab.* *11*, 438–444.
- Halbritter, J., Bizet, A.A., Schmidts, M., Porath, J.D., Braun, D.A., Gee, H.Y., McInerney-Leo, A.M., Krug, P., Filhol, E., Davis, E.E., et al. (2013). Defects in the IFT-B Component IFT172 Cause Jeune and Mainzer-Saldino Syndromes in Humans. *Am. J. Hum. Genet.* *93*, 915–925.

- Hambardzumyan, D., Becher, O.J., Rosenblum, M.K., Pandolfi, P.P., Manova-Todorova, K., and Holland, E.C. (2008). PI3K pathway regulates survival of cancer stem cells residing in the perivascular niche following radiation in medulloblastoma in vivo. *Genes Dev.* 22, 436–448.
- Haniu, M., Hsieh, P., Rohde, M.F., and Kenney, W.C. (1994). Characterization of disulfide linkages in platelet-derived growth factor AA. *Arch. Biochem. Biophys.* 310, 433–437.
- Hara, K., Maruki, Y., Long, X., Yoshino, K., Oshiro, N., Hidayat, S., Tokunaga, C., Avruch, J., and Yonezawa, K. (2002). Raptor, a binding partner of target of rapamycin (TOR), mediates TOR action. *Cell* 110, 177–189.
- Hart, I.K., Richardson, W.D., Bolsover, S.R., and Raff, M.C. (1989). PDGF and intracellular signaling in the timing of oligodendrocyte differentiation. *J. Cell Biol.* 109, 3411–3417.
- Harting, I., Kotzaeridou, U., Poretti, a, Seitz, a, Pietz, J., Bendszus, M., and Boltshauser, E. (2011). Interpeduncular heterotopia in Joubert syndrome: a previously undescribed MR finding. *AJNR. Am. J. Neuroradiol.* 32, 1286–1289.
- Haycraft, C.J., Banizs, B., Aydin-Son, Y., Zhang, Q., Michaud, E.J., and Yoder, B.K. (2005). Gli2 and Gli3 localize to cilia and require the intraflagellar transport protein polaris for processing and function. *PLoS Genet.* 1, e53.
- Heldin, C.H., Westermark, B., and Wasteson, A. (1981). Platelet-derived growth factor. Isolation by a large-scale procedure and analysis of subunit composition. *Biochem. J.* 193, 907–913.
- Heller, R.F., and Gordon, R.E. (1986). Chronic effects of nitrogen dioxide on cilia in hamster bronchioles. *Exp. Lung Res.* 10, 137–152.
- Hemmings, B.A., Adams-Pearson, C., Maurer, F., Müller, P., Goris, J., Merlevede, W., Hofsteenge, J., and Stone, S.R. (1990). alpha- and beta-forms of the 65-kDa subunit of protein phosphatase 2A have a similar 39 amino acid repeating structure. *Biochemistry* 29, 3166–3173.
- Henault, D., Galleguillos, L., Moore, C., Johnson, T., Bar-Or, A., and Antel, J. (2013). Basis for fluctuations in lymphocyte counts in fingolimod-treated patients with multiple sclerosis. *Neurology* 81, 1768–1772.
- Heron-Milhavet, L., Khouya, N., Fernandez, A., and Lamb, N.J. (2011). Akt1 and Akt2: differentiating the aktion. *Histol. Histopathol.* 26, 651–662.

- Hers, I., Vincent, E.E., and Tavaré, J.M. (2011). Akt signalling in health and disease. *Cell. Signal.* 23, 1515–1527.
- Heuser, T., Raytchev, M., Krell, J., Porter, M.E., and Nicastro, D. (2009). The dynein regulatory complex is the nexin link and a major regulatory node in cilia and flagella. *J. Cell Biol.* 187, 921–933.
- Hildebrandt, F., Benzing, T., and Katsanis, N. (2011). Ciliopathies. *N. Engl. J. Med.* 364, 1533–1543.
- Hoch, R. V, and Soriano, P. (2003). Roles of PDGF in animal development. *Development* 130, 4769–4784.
- Hooshmand-Rad, R., Yokote, K., Heldin, C.H., and Claesson-Welsh, L. (1998). PDGF alpha-receptor mediated cellular responses are not dependent on Src family kinases in endothelial cells. *J. Cell Sci.* 111 ( Pt 5, 607–614.
- Hopkins, J.M. (1970). Subsidiary components of the flagella of *Chlamydomonas reinhardtii*. *J. Cell Sci.* 7, 823–839.
- Horn, V., Thelu, J., Garcia, A., Albiges-Rizo, C., Block, M.R., and Viallet, J. (2007). Functional Interaction of Aurora-A and PP2A during Mitosis. *Mol. Biol. Cell* 18, 1233–1241.
- Hou, Y., Pazour, G.J., and Witman, G.B. (2004). A dynein light intermediate chain, D1bLIC, is required for retrograde intraflagellar transport. *Mol. Biol. Cell* 15, 4382–4394.
- Hu, Q., Milenkovic, L., Jin, H., Scott, M.P., Nachury, M. V, Spiliotis, E.T., and Nelson, W.J. (2010). A septin diffusion barrier at the base of the primary cilium maintains ciliary membrane protein distribution. *Science* 329, 436–439.
- Huang, B., Rifkin, M.R., and Luck, D.J. (1977). Temperature-sensitive mutations affecting flagellar assembly and function in *Chlamydomonas reinhardtii*. *J. Cell Biol.* 72, 67–85.
- Huangfu, D., and Anderson, K. V (2005). Cilia and Hedgehog responsiveness in the mouse. *Proc. Natl. Acad. Sci. U. S. A.* 102, 11325–11330.
- Huangfu, D., Liu, A., Rakeman, A.S., and Murcia, N.S. (2003). Hedgehog signalling in the mouse requires intraflagellar transport proteins. *Nature* 426, 83–87.
- Hui, C.C., Slusarski, D., Platt, K.A., Holmgren, R., and Joyner, A.L. (1994). Expression of three mouse homologs of the *Drosophila* segment polarity gene *cubitus interruptus*, *Gli*, *Gli-2*, and *Gli-3*, in ectoderm- and mesoderm-derived tissues suggests multiple roles during postimplantation development. *Dev. Biol.* 162, 402–413.

- Humke, E.W., Dorn, K. V, Milenkovic, L., Scott, M.P., and Rohatgi, R. (2010). The output of Hedgehog signaling is controlled by the dynamic association between Suppressor of Fused and the Gli proteins. *Genes Dev.* *24*, 670–682.
- Ibraghimov-Beskrovnaya, O., and Natoli, T.A. (2011). mTOR signaling in polycystic kidney disease. *Trends Mol. Med.* *17*, 625–633.
- Ikehara, T., Ikehara, S., Imamura, S., Shinjo, F., and Yasumoto, T. (2007). Methylation of the C-terminal leucine residue of the PP2A catalytic subunit is unnecessary for the catalytic activity and the binding of regulatory subunit (PR55/B). *Biochem. Biophys. Res. Commun.* *354*, 1052–1057.
- Ikenaka, K., Kagawa, T., and Mikoshiba, K. (1992). Selective expression of DM-20, an alternatively spliced myelin proteolipid protein gene product, in developing nervous system and in nonglial cells. *J. Neurochem.* *58*, 2248–2253.
- Ikuno, Y., Leong, F.-L., and Kazlauskas, A. (2002). PI3K and PLCgamma play a central role in experimental PVR. *Invest. Ophthalmol. Vis. Sci.* *43*, 483–489.
- Inoki, K., Li, Y., Zhu, T., Wu, J., and Guan, K.-L. (2002). TSC2 is phosphorylated and inhibited by Akt and suppresses mTOR signalling. *Nat. Cell Biol.* *4*, 648–657.
- Inui, S., Sanjo, H., Maeda, K., Yamamoto, H., Miyamoto, E., and Sakaguchi, N. (1998). Ig receptor binding protein 1 (alpha4) is associated with a rapamycin-sensitive signal transduction in lymphocytes through direct binding to the catalytic subunit of protein phosphatase 2A. *Blood* *92*, 539–546.
- Isensee, J., Diskar, M., Waldherr, S., Buschow, R., Hasenauer, J., Prinz, A., Allgöwer, F., Herberg, F.W., and Hucho, T. (2013). Pain modulators regulate the dynamics of PKA-RII phosphorylation in subgroups of sensory neurons. *J. Cell Sci.*
- Isotani, S., Hara, K., Tokunaga, C., Inoue, H., Avruch, J., and Yonezawa, K. (1999). Immunopurified mammalian target of rapamycin phosphorylates and activates p70 S6 kinase alpha in vitro. *J. Biol. Chem.* *274*, 34493–34498.
- Jacinto, E., Facchinetti, V., Liu, D., Soto, N., Wei, S., Jung, S.Y., Huang, Q., Qin, J., and Su, B. (2006). SIN1/MIP1 maintains rictor-mTOR complex integrity and regulates Akt phosphorylation and substrate specificity. *Cell* *127*, 125–137.

- Jackson, J.B., and Pallas, D.C. (2012). Circumventing cellular control of PP2A by methylation promotes transformation in an Akt-dependent manner. *Neoplasia* 14, 585–599.
- Janssens, V., and Goris, J. (2001). Protein phosphatase 2A: a highly regulated family of serine/threonine phosphatases implicated in cell growth and signalling. *Biochem. J.* 353, 417–439.
- Jeno, P. (1988). Identification and Characterization of a Mitogen-Activated S6 Kinase. *Proc. Natl. Acad. Sci.* 85, 406–410.
- Jia, H., Liu, Y., Yan, W., and Jia, J. (2009). PP4 and PP2A regulate Hedgehog signaling by controlling Smo and Ci phosphorylation. *Development* 136, 307–316.
- Jones, P.F., Jakubowicz, T., Pitossi, F.J., Maurer, F., and Hemmings, B.A. (1991). Molecular cloning and identification of a serine/threonine protein kinase of the second-messenger subfamily. *Proc. Natl. Acad. Sci. U. S. A.* 88, 4171–4175.
- Jordan, C., Jr, V.F., and Dubois-Dalcq, M. (1989). In situ hybridization analysis of myelin gene transcripts in developing mouse spinal cord. *J. Neurosci.* 9, 248–257.
- Jóźwiak, J., Sontowska, I., Bikowska, B., Grajkowska, W., Galus, R., and Roszkowski, M. (2011). Favourable prognosis in medulloblastoma with extensive nodularity is associated with mitogen-activated protein kinase upregulation. *Folia Neuropathol.* 49, 257–261.
- Kappos, L., Antel, J., Comi, G., Montalban, X., O'Connor, P., Polman, C.H., Haas, T., Korn, A.A., Karlsson, G., and Radue, E.W. (2006). Oral fingolimod (FTY720) for relapsing multiple sclerosis. *N. Engl. J. Med.* 355, 1124–1140.
- Kelly, J.D., Haldeman, B.A., Grant, F.J., Murray, M.J., Seifert, R.A., Bowen-Pope, D.F., Cooper, J.A., and Kazlauskas, A. (1991). Platelet-derived growth factor (PDGF) stimulates PDGF receptor subunit dimerization and intersubunit trans-phosphorylation. *J. Biol. Chem.* 266, 8987–8992.
- Kessaris, N., Fogarty, M., Iannarelli, P., Grist, M., Wegner, M., and Richardson, W.D. (2006). Competing waves of oligodendrocytes in the forebrain and postnatal elimination of an embryonic lineage. *Nat. Neurosci.* 9, 173–179.
- Kessaris, N., Pringle, N., and Richardson, W.D. (2008). Specification of CNS glia from neural stem cells in the embryonic neuroepithelium. *Philos. Trans. R. Soc. Lond. B. Biol. Sci.* 363, 71–85.

- Khew-Goodall, Y., Mayer, R.E., Maurer, F., Stone, S.R., and Hemmings, B.A. (1991). Structure and transcriptional regulation of protein phosphatase 2A catalytic subunit genes. *Biochemistry* 30, 89–97.
- Kikusui, T., and Mori, Y. (2009). Behavioural and neurochemical consequences of early weaning in rodents. *J. Neuroendocrinol.* 21, 427–431.
- Kim, S.K., Shindo, A., Park, T.J., Oh, E.C., Ghosh, S., Gray, R.S., Lewis, R.A., Johnson, C.A., Attie-Bittach, T., Katsanis, N., et al. (2010). Planar cell polarity acts through septins to control collective cell movement and ciliogenesis. *Science* 329, 1337–1340.
- Klinghoffer, R.A., Hamilton, T.G., Hoch, R., and Soriano, P. (2002a). An Allelic Series at the PDGF $\alpha$ R Locus Indicates Unequal Contributions of Distinct Signaling Pathways During Development. *Dev. Cell* 2, 103–113.
- Klinghoffer, R.A., Hamilton, T.G., Hoch, R., and Soriano, P. (2002b). An Allelic Series at the PDGF $\alpha$ R Locus Indicates Unequal Contributions of Distinct Signaling Pathways During Development. *Dev. Cell* 2, 103–113.
- Kogerman, P., Grimm, T., Kogerman, L., Krause, D., Undén, A.B., Sandstedt, B., Toftgård, R., and Zaphiropoulos, P.G. (1999). Mammalian suppressor-of-fused modulates nuclear-cytoplasmic shuttling of Gli-1. *Nat. Cell Biol.* 1, 312–319.
- Kohn, A.D., Kovacina, K.S., and Roth, R.A. (1995). Insulin stimulates the kinase activity of RAC-PK, a pleckstrin homology domain containing ser/thr kinase. *EMBO J.* 14, 4288–4295.
- Kotsis, F., Boehlke, C., and Kuehn, E.W. (2013). The ciliary flow sensor and polycystic kidney disease. *Nephrol. Dial. Transplant* 28, 518–526.
- Kozminski, K.G., Johnson, K.A., Forscher, P., and Rosenbaum, J.L. (1993). A motility in the eukaryotic flagellum unrelated to flagellar beating. *Proc. Natl. Acad. Sci. U. S. A.* 90, 5519–5523.
- Krauss, S., Foerster, J., Schneider, R., and Schweiger, S. (2008). Protein phosphatase 2A and rapamycin regulate the nuclear localization and activity of the transcription factor GLI3. *Cancer Res.* 68, 4658–4665.
- Krauss, S., So, J., Hambrock, M., Köhler, A., Kunath, M., Scharff, C., Wessling, M., Grzeschik, K.-H., Schneider, R., and Schweiger, S. (2009). Point mutations in GLI3 lead to misregulation of its subcellular localization. *PLoS One* 4, e7471.

- Kuhlbrodt, K., Herbarth, B., Sock, E., Hermans-Borgmeyer, I., and Wegner, M. (1998). Sox10, a novel transcriptional modulator in glial cells. *J. Neurosci.* 18, 237–250.
- Kuo, Y.-C., Huang, K.-Y., Yang, C.-H., Yang, Y.-S., Lee, W.-Y., and Chiang, C.-W. (2008). Regulation of phosphorylation of Thr-308 of Akt, cell proliferation, and survival by the B55alpha regulatory subunit targeting of the protein phosphatase 2A holoenzyme to Akt. *J. Biol. Chem.* 283, 1882–1892.
- Lange, K.I., Heinrichs, J., Cheung, K., and Srayko, M. (2013). Suppressor mutations identify amino acids in PAA-1/PR65 that facilitate regulatory RSA-1/B" subunit targeting of PP2A to centrosomes in *C. elegans*. *Biol. Open* 2, 88–94.
- Larkins, C.E., Aviles, G.D.G., East, M.P., Kahn, R.A., and Caspary, T. (2011). Arl13b regulates ciliogenesis and the dynamic localization of Shh signaling proteins. *Mol. Biol. Cell* 22, 4694–4703.
- Lee, J., and Stock, J. (1993). Protein phosphatase 2A catalytic subunit is methyl-esterified at its carboxyl terminus by a novel methyltransferase. *J. Biol. Chem.* 268, 19192–19195.
- Lee, J., Chen, Y., Tolstykh, T., and Stock, J. (1996). A specific protein carboxyl methyltransferase that demethylates phosphoprotein phosphatase 2A in bovine brain. *Proc. Natl. Acad. Sci. U. S. A.* 93, 6043–6047.
- Lee, R.S., House, C.M., Cristiano, B.E., Hannan, R.D., Pearson, R.B., and Hannan, K.M. (2011). Relative Expression Levels Rather Than Specific Activity Plays the Major Role in Determining In Vivo AKT Isoform Substrate Specificity. *Enzyme Res.* 2011, 720985.
- Lendahl, U., Zimmerman, L.B., and McKay, R.D. (1990). CNS stem cells express a new class of intermediate filament protein. *Cell* 60, 585–595.
- Leulliot, N., Quevillon-Cheruel, S., Sorel, I., Li de La Sierra-Gallay, I., Collinet, B., Graille, M., Blondeau, K., Bettache, N., Poupon, A., Janin, J., et al. (2004). Structure of protein phosphatase methyltransferase 1 (PPM1), a leucine carboxyl methyltransferase involved in the regulation of protein phosphatase 2A activity. *J. Biol. Chem.* 279, 8351–8358.
- Li, M., Makkinje, A., and Damuni, Z. (1996). The myeloid leukemia-associated protein SET is a potent inhibitor of protein phosphatase 2A. *J. Biol. Chem.* 271, 11059–11062.

- Li, Y., Wang, X., Yue, P., Tao, H., Ramalingam, S.S., Owonikoko, T.K., Deng, X., Wang, Y., Fu, H., Khuri, F.R., et al. (2013). Protein phosphatase 2A and DNA-dependent protein kinase are involved in mediating rapamycin-induced Akt phosphorylation. *J. Biol. Chem.* *288*, 13215–13224.
- Liem, K.F., Ashe, A., He, M., Satir, P., Moran, J., Beier, D., Wicking, C., and Anderson, K. V (2012). The IFT-A complex regulates Shh signaling through cilia structure and membrane protein trafficking. *J. Cell Biol.* *197*, 789–800.
- Lin, F., Hiesberger, T., Cordes, K., Sinclair, A.M., Goldstein, L.S.B., Somlo, S., and Igarashi, P. (2003). Kidney-specific inactivation of the KIF3A subunit of kinesin-II inhibits renal ciliogenesis and produces polycystic kidney disease. *Proc. Natl. Acad. Sci. U. S. A.* *100*, 5286–5291.
- Liu, A., Wang, B., and Niswander, L.A. (2005). Mouse intraflagellar transport proteins regulate both the activator and repressor functions of Gli transcription factors. *Development* *132*, 3103–3111.
- Liu, J., Heydeck, W., Zeng, H., and Liu, A. (2012). Dual function of suppressor of fused in Hh pathway activation and mouse spinal cord patterning. *Dev. Biol.* *362*, 141–153.
- Longin, S., Zwaenepoel, K., Martens, E., Louis, J. V, Rondelez, E., Goris, J., and Janssens, V. (2008). Spatial control of protein phosphatase 2A (de)methylation. *Exp. Cell Res.* *314*, 68–81.
- Lu, Q.R., Sun, T., Zhu, Z., Ma, N., Garcia, M., Stiles, C.D., and Rowitch, D.H. (2002). Common Developmental Requirement for Olig Function Indicates a Motor Neuron/Oligodendrocyte Connection. *Cell* *109*, 75–86.
- Lucker, B.F., Behal, R.H., Qin, H., Siron, L.C., Taggart, W.D., Rosenbaum, J.L., and Cole, D.G. (2005). Characterization of the intraflagellar transport complex B core: direct interaction of the IFT81 and IFT74/72 subunits. *J. Biol. Chem.* *280*, 27688–27696.
- Mainwaring, L.A., and Kenney, A.M. (2011). Divergent functions for eIF4E and S6 kinase by sonic hedgehog mitogenic signaling in the developing cerebellum. *Oncogene* *30*, 1784–1797.
- Marigo, V., and Tabin, C.J. (1996). Regulation of patched by sonic hedgehog in the developing neural tube. *Proc. Natl. Acad. Sci. U. S. A.* *93*, 9346–9351.
- Marigo, V., Davey, R.A., Zuo, Y., Cunningham, J.M., and Tabin, C.J. (1996). Biochemical evidence that patched is the Hedgehog receptor. *Nature* *384*, 176–179.

Matise, M.P., Epstein, D.J., Park, H.L., Platt, K.A., and Joyner, A.L. (1998). Gli2 is required for induction of floor plate and adjacent cells, but not most ventral neurons in the mouse central nervous system.

*Development* 125, 2759–2770.

May, S.R., Ashique, A.M., Karlen, M., Wang, B., Shen, Y., Zarbalis, K., Reiter, J., Ericson, J., and Peterson, A.S. (2005). Loss of the retrograde motor for IFT disrupts localization of Smo to cilia and prevents the expression of both activator and repressor functions of Gli. *Dev. Biol.* 287, 378–389.

Mayo, L.D., and Donner, D.B. (2001). A phosphatidylinositol 3-kinase/Akt pathway promotes translocation of Mdm2 from the cytoplasm to the nucleus. *Proc. Natl. Acad. Sci. U. S. A.* 98, 11598–11603.

McBride, S.M., Perez, D.A., Polley, M.-Y., Vandenberg, S.R., Smith, J.S., Zheng, S., Lamborn, K.R., Wiencke, J.K., Chang, S.M., Prados, M.D., et al. (2010). Activation of PI3K/mTOR pathway occurs in most adult low-grade gliomas and predicts patient survival. *J. Neurooncol.* 97, 33–40.

McKean-Cowdin, R., Razavi, P., Barrington-Trimis, J., Baldwin, R.T., Asgharzadeh, S., Cockburn, M., Tihan, T., and Preston-Martin, S. (2013). Trends in childhood brain tumor incidence, 1973-2009. *J. Neurooncol.* 115, 153–160.

McKinnon, R.D., Waldron, S., and Kiel, M.E. (2005). PDGF alpha-receptor signal strength controls an RTK rheostat that integrates phosphoinositol 3'-kinase and phospholipase Cgamma pathways during oligodendrocyte maturation. *J. Neurosci.* 25, 3499–3508.

McLean, A., and Bennett, S. (2013). A protocol for densitometric quantification of Western blots using Image J.

Merrill, A.E., Merriman, B., Farrington-Rock, C., Camacho, N., Sebald, E.T., Funari, V.A., Schibler, M.J., Firestein, M.H., Cohn, Z.A., Priore, M.A., et al. (2009). Ciliary abnormalities due to defects in the retrograde transport protein DYNC2H1 in short-rib polydactyly syndrome. *Am. J. Hum. Genet.* 84, 542–549.

Méthot, N., and Basler, K. (2000). Suppressor of fused opposes hedgehog signal transduction by impeding nuclear accumulation of the activator form of Cubitus interruptus. *Development* 127, 4001–4010.

Meyer, N.P., and Roelink, H. (2003). The amino-terminal region of Gli3 antagonizes the Shh response and acts in dorsoventral fate specification in the developing spinal cord. *Dev. Biol.* 257, 343–355.

- Miller, S., Oleksy, A., Perisic, O., and Williams, R.L. (2010). Finding a fitting shoe for Cinderella: searching for an autophagy inhibitor. *Autophagy* 6, 805–807.
- Milner, R., Anderson, H.J., Rippon, R.F., McKay, J.S., Franklin, R.J., Marchionni, M. a, Reynolds, R., and Ffrench-Constant, C. (1997). Contrasting effects of mitogenic growth factors on oligodendrocyte precursor cell migration. *Glia* 19, 85–90.
- Moore, P.A., Rosen, C.A., and Carter, K.C. (1996). Assignment of the human FKBP12-rapamycin-associated protein (FRAP) gene to chromosome 1p36 by fluorescence in situ hybridization. *Genomics* 33, 331–332.
- Moore, S.F., Hunter, R.W., and Hers, I. (2011). mTORC2 protein complex-mediated Akt (Protein Kinase B) Serine 473 Phosphorylation is not required for Akt1 activity in human platelets [corrected]. *J. Biol. Chem.* 286, 24553–24560.
- Moyer, J.H., Lee-Tischler, M.J., Kwon, H.Y., Schrick, J.J., Avner, E.D., Sweeney, W.E., Godfrey, V.L., Cacheiro, N.L., Wilkinson, J.E., and Woychik, R.P. (1994). Candidate gene associated with a mutation causing recessive polycystic kidney disease in mice. *Science* 264, 1329–1333.
- Mudhar, H.S., Pollock, R.A., Wang, C., Stiles, C.D., and Richardson, W.D. (1993a). PDGF and its receptors in the developing rodent retina and optic nerve. *Development* 118, 539–552.
- Mudhar, H.S., Pollock, R.A., Wang, C., Stiles, C.D., and Richardson, W.D. (1993b). PDGF and its receptors in the developing rodent retina and optic nerve. *Development* 118, 539–552.
- Mueller, S., and Chang, S. (2009). Pediatric brain tumors: current treatment strategies and future therapeutic approaches. *Neurotherapeutics* 6, 570–586.
- Nagahashi, M., Hait, N.C., Maceyka, M., Avni, D., Takabe, K., Milstien, S., and Spiegel, S. (2013). Sphingosine-1-phosphate in chronic intestinal inflammation and cancer. *Adv. Biol. Regul.*
- Narayanan, S.P., Flores, A.I., Wang, F., and Macklin, W.B. (2009). Akt signals through the mammalian target of rapamycin pathway to regulate CNS myelination. *J. Neurosci.* 29, 6860–6870.
- Neviani, P., Harb, J.G., Oaks, J.J., Santhanam, R., Walker, C.J., Ellis, J.J., Ferenchak, G., Dorrance, A.M., Paisie, C.A., Eiring, A.M., et al. (2013). PP2A-activating drugs selectively eradicate TKI-resistant chronic myeloid leukemic stem cells. *J. Clin. Invest.* 123, 4144–4157.

- Nishiyama, A., Lin, X.H., Giese, N., Heldin, C.H., and Stallcup, W.B. (1996). Co-localization of NG2 proteoglycan and PDGF alpha-receptor on O2A progenitor cells in the developing rat brain. *J. Neurosci. Res.* *43*, 299–314.
- Noll, E., and Miller, R.H. (1993). Oligodendrocyte precursors originate at the ventral ventricular zone dorsal to the ventral midline region in the embryonic rat spinal cord. *Development* *118*, 563–573.
- Nybakken, K., Vokes, S.A., Lin, T.-Y., McMahon, A.P., and Perrimon, N. (2005). A genome-wide RNA interference screen in *Drosophila melanogaster* cells for new components of the Hh signaling pathway. *Nat. Genet.* *37*, 1323–1332.
- Oaks, J.J., Santhanam, R., Walker, C.J., Roof, S., Harb, J.G., Ferenchak, G., Eisfeld, A.-K., Van Brocklyn, J.R., Briesewitz, R., Saddoughi, S.A., et al. (2013). Antagonistic activities of the immunomodulator and PP2A-activating drug FTY720 (Fingolimod, Gilenya) in Jak2-driven hematologic malignancies. *Blood* *122*, 1923–1934.
- Ocbina, P.J.R., and Anderson, K. V (2008). Intraflagellar transport, cilia, and mammalian Hedgehog signaling: analysis in mouse embryonic fibroblasts. *Dev. Dyn.* *237*, 2030–2038.
- Ocbina, P.J.R., Eggenschwiler, J.T., Moskowitz, I., and Anderson, K. V (2011). Complex interactions between genes controlling trafficking in primary cilia. *Nat. Genet.* *43*, 547–553.
- Ogris, E., Du, X., Nelson, K.C., Mak, E.K., Yu, X.X., Lane, W.S., and Pallas, D.C. (1999). A protein phosphatase methylesterase (PME-1) is one of several novel proteins stably associating with two inactive mutants of protein phosphatase 2A. *J. Biol. Chem.* *274*, 14382–14391.
- Okumura, E., Fukuhara, T., Yoshida, H., Hanada Si, S., Kozutsumi, R., Mori, M., Tachibana, K., and Kishimoto, T. (2002). Akt inhibits Myt1 in the signalling pathway that leads to meiotic G2/M-phase transition. *Nat. Cell Biol.* *4*, 111–116.
- Ou, G., Blacque, O.E., Snow, J.J., Leroux, M.R., and Scholey, J.M. (2005). Functional coordination of intraflagellar transport motors. *Nature* *436*, 583–587.
- Pan, Y., Bai, C.B., Joyner, A.L., and Wang, B. (2006). Sonic hedgehog signaling regulates Gli2 transcriptional activity by suppressing its processing and degradation. *Mol. Cell. Biol.* *26*, 3365–3377.

- Di Pardo, A., Amico, E., Favellato, M., Castrataro, R., Fucile, S., Squitieri, F., and Maglione, V. (2013). FTY720 (fingolimod) is a neuroprotective and disease-modifying agent in cellular and mouse models of Huntington disease. *Hum. Mol. Genet.*
- Patel, S., Bhatnagar, A., Wear, C., Osiro, S., Gabriel, A., Kimball, D., John, A., Fields, P.J., Tubbs, R.S., and Loukas, M. (2013). Are pediatric brain tumors on the rise in the USA? Significant incidence and survival findings from the SEER database analysis. *Childs. Nerv. Syst.*
- Pazour, G.J., Wilkerson, C.G., and Witman, G.B. (1998). A dynein light chain is essential for the retrograde particle movement of intraflagellar transport (IFT). *J. Cell Biol.* *141*, 979–992.
- Pazour, G.J., Dickert, B.L., and Witman, G.B. (1999). The DHC1b (DHC2) isoform of cytoplasmic dynein is required for flagellar assembly. *J. Cell Biol.* *144*, 473–481.
- Pazour, G.J., Dickert, B.L., Vucica, Y., Seeley, E.S., Rosenbaum, J.L., Witman, G.B., and Cole, D.G. (2000). *Chlamydomonas* IFT88 and its mouse homologue, polycystic kidney disease gene *tg737*, are required for assembly of cilia and flagella. *J. Cell Biol.* *151*, 709–718.
- Pazour, G.J., San Agustin, J.T., Follit, J.A., Rosenbaum, J.L., and Witman, G.B. (2002). Polycystin-2 localizes to kidney cilia and the ciliary level is elevated in *orpk* mice with polycystic kidney disease. *Curr. Biol.* *12*, R378–80.
- Pearse, R. V., Collier, L.S., Scott, M.P., and Tabin, C.J. (1999). Vertebrate homologs of *Drosophila* suppressor of fused interact with the *gli* family of transcriptional regulators. *Dev. Biol.* *212*, 323–336.
- Pedersen, L.B., Miller, M.S., Geimer, S., Leitch, J.M., Rosenbaum, J.L., and Cole, D.G. (2005). *Chlamydomonas* IFT172 is encoded by *FLA11*, interacts with CrEB1, and regulates IFT at the flagellar tip. *Curr. Biol.* *15*, 262–266.
- Persson, M., Stamatakis, D., te Welscher, P., Andersson, E., Böse, J., Rütger, U., Ericson, J., and Briscoe, J. (2002). Dorsal-ventral patterning of the spinal cord requires Gli3 transcriptional repressor activity. *Genes Dev.* *16*, 2865–2878.
- Peterson, R.T., Desai, B.N., Hardwick, J.S., and Schreiber, S.L. (1999). Protein phosphatase 2A interacts with the 70-kDa S6 kinase and is activated by inhibition of FKBP12-rapamycin-associated protein. *Proc. Natl. Acad. Sci. U. S. A.* *96*, 4438–4442.

- Peyron, F., Timsit, S., Thomas, J.L., Kagawa, T., Ikenaka, K., and Zalc, B. (1997). In situ expression of PLP/DM-20, MBP, and CNP during embryonic and postnatal development of the jimpy mutant and of transgenic mice overexpressing PLP. *J. Neurosci. Res.* *50*, 190–201.
- Piperno, G., and Mead, K. (1997). Transport of a novel complex in the cytoplasmic matrix of *Chlamydomonas* flagella. *Proc. Natl. Acad. Sci. U. S. A.* *94*, 4457–4462.
- Pledger, W.J., Hart, C.A., Locatell, K.L., and Scher, C.D. (1981). Platelet-derived growth factor-modulated proteins: constitutive synthesis by a transformed cell line. *Proc. Natl. Acad. Sci. U. S. A.* *78*, 4358–4362.
- Porter, M.E., Bower, R., Knott, J.A., Byrd, P., and Dentler, W. (1999). Cytoplasmic dynein heavy chain 1b is required for flagellar assembly in *Chlamydomonas*. *Mol. Biol. Cell* *10*, 693–712.
- Potter, C.J., Pedraza, L.G., and Xu, T. (2002). Akt regulates growth by directly phosphorylating Tsc2. *Nat. Cell Biol.* *4*, 658–665.
- Pringle, N.P., and Richardson, W.D. (1993). A singularity of PDGF alpha-receptor expression in the dorsoventral axis of the neural tube may define the origin of the oligodendrocyte lineage. *Development* *117*, 525–533.
- Qi, Yingchuan, Tan, Min, Hui, Chi-Chung, Qui, M. (2003). Gli2 is required for normal Shh signaling and oligodendrocyte development in the spinal cord. *Mol. Cell. Neurosci.* *23*, 10.
- Qin, H., Rosenbaum, J.L., and Barr, M.M. (2001). An autosomal recessive polycystic kidney disease gene homolog is involved in intraflagellar transport in *C. elegans* ciliated sensory neurons. *Curr. Biol.* *11*, 457–461.
- Qin, J., Lin, Y., Norman, R.X., Ko, H.W., and Eggenschwiler, J.T. (2011). Intraflagellar transport protein 122 antagonizes Sonic Hedgehog signaling and controls ciliary localization of pathway components. *Proc. Natl. Acad. Sci. U. S. A.* *108*, 1456–1461.
- Quisling, R.G., Barkovich, a. J., and Maria, B.L. (1999). Magnetic Resonance Imaging Features and Classification of Central Nervous System Malformations in Joubert Syndrome. *J. Child Neurol.* *14*, 628–635.
- Raff, M.C., Fields, K.L., Hakomori, S.I., Mirsky, R., Pruss, R.M., and Winter, J. (1979). Cell-type-specific markers for distinguishing and studying neurons and the major classes of glial cells in culture. *Brain Res.* *174*, 283–308.

- Raines, E.W., and Ross, R. (1982). Platelet-derived growth factor. I. High yield purification and evidence for multiple forms. *J. Biol. Chem.* *257*, 5154–5160.
- Reiter, J.F., Blacque, O.E., and Leroux, M.R. (2012). The base of the cilium: roles for transition fibres and the transition zone in ciliary formation, maintenance and compartmentalization. *EMBO Rep.* *13*, 608–618.
- Richardson, W.D., Pringle, N., Mosley, M.J., Westermark, B., and Dubois-Dalcq, M. (1988). A role for platelet-derived growth factor in normal gliogenesis in the central nervous system. *Cell* *53*, 309–319.
- Riobó, N.A., Lu, K., Ai, X., Haines, G.M., and Emerson, C.P. (2006). Phosphoinositide 3-kinase and Akt are essential for Sonic Hedgehog signaling. *Proc. Natl. Acad. Sci. U. S. A.* *103*, 4505–4510.
- Robinson, S., Tani, M., Strieter, R.M., Ransohoff, R.M., and Miller, R.H. (1998). The chemokine growth-regulated oncogene- $\alpha$  promotes spinal cord oligodendrocyte precursor proliferation. *J. Neurosci.* *18*, 10457–10463.
- Rodrik-Outmezguine, V.S., Chandarlapaty, S., Pagano, N.C., Poulikakos, P.I., Scaltriti, M., Moskatel, E., Baselga, J., Guichard, S., and Rosen, N. (2011). mTOR kinase inhibition causes feedback-dependent biphasic regulation of AKT signaling. *Cancer Discov.* *1*, 248–259.
- Rogister, B., Ben-Hur, T., and Dubois-Dalcq, M. (1999). From neural stem cells to myelinating oligodendrocytes. *Mol. Cell. Neurosci.* *14*, 287–300.
- Rohatgi, R., Milenkovic, L., and Scott, M.P. (2007). Patched1 regulates hedgehog signaling at the primary cilium. *Science* *317*, 372–376.
- Rosa, R., Marciano, R., Malapelle, U., Formisano, L., Nappi, L., D'Amato, C., D'Amato, V., Damiano, V., Marfè, G., Del Vecchio, S., et al. (2013). Sphingosine kinase 1 overexpression contributes to cetuximab resistance in human colorectal cancer models. *Clin. Cancer Res.* *19*, 138–147.
- Ross, R., Glomset, J., Kariya, B., and Harker, L. (1974). A platelet-dependent serum factor that stimulates the proliferation of arterial smooth muscle cells in vitro. *Proc. Natl. Acad. Sci. U. S. A.* *71*, 1207–1210.
- Rowitch, D.H. (2004). Glial specification in the vertebrate neural tube. *Nat. Rev. Neurosci.* *5*, 409–419.
- Ruiz i Altaba, A. (1998). Combinatorial Gli gene function in floor plate and neuronal inductions by Sonic hedgehog. *Development* *125*, 2203–2212.

- Rupp, E., Siegbahn, A., Rönstrand, L., Wernstedt, C., Claesson-Welsh, L., and Heldin, C.H. (1994). A unique autophosphorylation site in the platelet-derived growth factor alpha receptor from a heterodimeric receptor complex. *Eur. J. Biochem.* 225, 29–41.
- Rydholm, S., Zwart, G., Kowalewski, J.M., Kamali-Zare, P., Frisk, T., and Brismar, H. (2010). Mechanical properties of primary cilia regulate the response to fluid flow. *Am. J. Physiol. Renal Physiol.* 298, F1096–102.
- Sabers, C.J., Martin, M.M., Brunn, G.J., Williams, J.M., Dumont, F.J., Wiederrecht, G., and Abraham, R.T. (1995). Isolation of a protein target of the FKBP12-rapamycin complex in mammalian cells. *J. Biol. Chem.* 270, 815–822.
- Saddoughi, S.A., Gencer, S., Peterson, Y.K., Ward, K.E., Mukhopadhyay, A., Oaks, J., Bielawski, J., Szulc, Z.M., Thomas, R.J., Selvam, S.P., et al. (2013). Sphingosine analogue drug FTY720 targets I2PP2A/SET and mediates lung tumour suppression via activation of PP2A-RIPK1-dependent necroptosis. *EMBO Mol. Med.* 5, 105–121.
- Sancak, Y., Thoreen, C.C., Peterson, T.R., Lindquist, R.A., Kang, S.A., Spooner, E., Carr, S.A., and Sabatini, D.M. (2007). PRAS40 is an insulin-regulated inhibitor of the mTORC1 protein kinase. *Mol. Cell* 25, 903–915.
- Sarbassov, D.D., Ali, S.M., Kim, D.-H., Guertin, D.A., Latek, R.R., Erdjument-Bromage, H., Tempst, P., and Sabatini, D.M. (2004). Rictor, a novel binding partner of mTOR, defines a rapamycin-insensitive and raptor-independent pathway that regulates the cytoskeleton. *Curr. Biol.* 14, 1296–1302.
- Sarbassov, D.D., Guertin, D. a, Ali, S.M., and Sabatini, D.M. (2005). Phosphorylation and regulation of Akt/PKB by the rictor-mTOR complex. *Science* 307, 1098–1101.
- Sarbassov, D.D., Ali, S.M., Sengupta, S., Sheen, J.-H., Hsu, P.P., Bagley, A.F., Markhard, A.L., and Sabatini, D.M. (2006). Prolonged rapamycin treatment inhibits mTORC2 assembly and Akt/PKB. *Mol. Cell* 22, 159–168.
- Sasaki, H., Nishizaki, Y., Hui, C., Nakafuku, M., and Kondoh, H. (1999). Regulation of Gli2 and Gli3 activities by an amino-terminal repression domain: implication of Gli2 and Gli3 as primary mediators of Shh signaling. *Development* 126, 3915–3924.

- Schindelin, J., Arganda-Carreras, I., Frise, E., Kaynig, V., Longair, M., Pietzsch, T., Preibisch, S., Rueden, C., Saalfeld, S., Schmid, B., et al. (2012). Fiji: an open-source platform for biological-image analysis. *Nat. Methods* *9*, 676–682.
- Schmidts, M., Arts, H.H., Bongers, E.M.H.F., Yap, Z., Oud, M.M., Antony, D., Duijkers, L., Emes, R.D., Stalker, J., Yntema, J.-B.L., et al. (2013). Exome sequencing identifies DYNC2H1 mutations as a common cause of asphyxiating thoracic dystrophy (Jeune syndrome) without major polydactyly, renal or retinal involvement. *J. Med. Genet.* *50*, 309–323.
- Schmitz, M.H.A., Held, M., Janssens, V., Hutchins, J.R.A., Hudecz, O., Ivanova, E., Goris, J., Trinkle-Mulcahy, L., Lamond, A.I., Poser, I., et al. (2010). Live-cell imaging RNAi screen identifies PP2A-B55alpha and importin-beta1 as key mitotic exit regulators in human cells. *Nat. Cell Biol.* *12*, 886–893.
- Schneider, L., Clement, C.A., Teilmann, S.C., Pazour, G.J., Hoffmann, E.K., Satir, P., and Christensen, S.T. (2005). PDGFR $\alpha$  signaling is regulated through the primary cilium in fibroblasts. *Curr. Biol.* *15*, 1861–1866.
- Schneider, L., Cammer, M., Lehman, J., Nielsen, S.K., Guerra, C.F., Veland, I.R., Stock, C., Hoffmann, E.K., Yoder, B.K., Schwab, A., et al. (2010). Directional cell migration and chemotaxis in wound healing response to PDGF-AA are coordinated by the primary cilium in fibroblasts. *Cell. Physiol. Biochem.* *25*, 279–292.
- Senocak, E.U., Oğuz, K.K., Haliloğlu, G., Topçu, M., and Cila, A. (2010). Structural abnormalities of the brain other than molar tooth sign in Joubert syndrome-related disorders. *Diagn. Interv. Radiol.* *16*, 3–6.
- Sents, W., Ivanova, E., Lambrecht, C., Haesen, D., and Janssens, V. (2013). The biogenesis of active protein phosphatase 2A holoenzymes: a tightly regulated process creating phosphatase specificity. *FEBS J.* *280*, 644–661.
- Shiba, D., Takamatsu, T., and Yokoyama, T. (2005). Primary cilia of *inv/inv* mouse renal epithelial cells sense physiological fluid flow: bending of primary cilia and Ca<sup>2+</sup> influx. *Cell Struct. Funct.* *30*, 93–100.
- Shillingford, J.M., Murcia, N.S., Larson, C.H., Low, S.H., Hedgepeth, R., Brown, N., Flask, C.A., Novick, A.C., Goldfarb, D.A., Kramer-Zucker, A., et al. (2006). The mTOR pathway is regulated by polycystin-1, and its inhibition reverses renal cystogenesis in polycystic kidney disease. *Proc. Natl. Acad. Sci. U. S. A.* *103*, 5466–5471.

- Smetana, J.H.C., Oliveira, C.L.P., Jablonka, W., Aguiar Pertinhez, T., Carneiro, F.R.G., Montero-Lomeli, M., Torriani, I., and Zanchin, N.I.T. (2006). Low resolution structure of the human alpha4 protein (IgBP1) and studies on the stability of alpha4 and of its yeast ortholog Tap42. *Biochim. Biophys. Acta* 1764, 724–734.
- Solly, S.K., Thomas, J.L., Monge, M., Demerens, C., Lubetzki, C., Gardinier, M. V, Matthieu, J.M., and Zalc, B. (1996). Myelin/oligodendrocyte glycoprotein (MOG) expression is associated with myelin deposition. *Glia* 18, 39–48.
- Sommer, I., and Schachner, M. (1981). Monoclonal antibodies (O1 to O4) to oligodendrocyte cell surfaces: an immunocytological study in the central nervous system. *Dev. Biol.* 83, 311–327.
- Soriano, P. (1997). The PDGF $\alpha$  receptor is required for neural crest cell development and for normal patterning of the somites. *Cancer Res.* 2700, 2691–2700.
- SOROKIN, S. (1962). Centrioles and the formation of rudimentary cilia by fibroblasts and smooth muscle cells. *J. Cell Biol.* 15, 363–377.
- Spassky, N., Han, Y.-G., Aguilar, A., Strehl, L., Besse, L., Laclef, C., Ros, M.R., Garcia-Verdugo, J.M., and Alvarez-Buylla, A. (2008). Primary cilia are required for cerebellar development and Shh-dependent expansion of progenitor pool. *Dev. Biol.* 317, 246–259.
- Sprinkle, T.J. (1989). 2',3'-cyclic nucleotide 3'-phosphodiesterase, an oligodendrocyte-Schwann cell and myelin-associated enzyme of the nervous system. *Crit. Rev. Neurobiol.* 4, 235–301.
- Stamatakis, D., Ulloa, F., Tsoni, S. V, Mynett, A., and Briscoe, J. (2005). A gradient of Gli activity mediates graded Sonic Hedgehog signaling in the neural tube. *Genes Dev.* 19, 626–641.
- Stambolic, V., and Woodgett, J.R. (2006). Functional distinctions of protein kinase B/Akt isoforms defined by their influence on cell migration. *Trends Cell Biol.* 16, 461–466.
- Stephens, L.R., Hughes, K.T., and Irvine, R.F. (1991). Pathway of phosphatidylinositol(3,4,5)-trisphosphate synthesis in activated neutrophils. *Nature* 351, 33–39.
- Stiles, C.D., Capone, G.T., Scher, C.D., Antoniades, H.N., Van Wyk, J.J., and Pledger, W.J. (1979). Dual control of cell growth by somatomedins and platelet-derived growth factor. *Proc. Natl. Acad. Sci. U. S. A.* 76, 1279–1283.

- Stone, D.M., Murone, M., Luoh, S., Ye, W., Armanini, M.P., Gurney, A., Phillips, H., Brush, J., Goddard, A., de Sauvage, F.J., et al. (1999). Characterization of the human suppressor of fused, a negative regulator of the zinc-finger transcription factor Gli. *J. Cell Sci.* *112* ( Pt 2, 4437–4448).
- Stottmann, R.W., Tran, P. V, Turbe-Doan, a, and Beier, D.R. (2009). Ttc21b is required to restrict sonic hedgehog activity in the developing mouse forebrain. *Dev. Biol.* *335*, 166–178.
- Su, C.-Y. (2011). The role of Arl13b in the maintenance of neural tube patterning and oligodendrocyte development. Emory University.
- Su, C.-Y., Bay, S.N., Mariani, L.E., Hillman, M.J., and Casparly, T. (2012). Temporal deletion of Arl13b reveals that a mispatterned neural tube corrects cell fate over time. *Development* *139*, 4062–4071.
- Su, Y., Ospina, J.K., Zhang, J., Michelson, A.P., Schoen, A.M., and Zhu, A.J. (2011). Sequential phosphorylation of smoothed transduces graded hedgehog signaling. *Sci. Signal.* *4*, ra43.
- Sun, T., Echelard, Y., Lu, R., Yuk, D.I., Kaing, S., Stiles, C.D., and Rowitch, D.H. (2001). Olig bHLH proteins interact with homeodomain proteins to regulate cell fate acquisition in progenitors of the ventral neural tube. *Curr. Biol.* *11*, 1413–1420.
- Taipale, J., Cooper, M.K., Maiti, T., and Beachy, P.A. (2002). Patched acts catalytically to suppress the activity of Smoothened. *Nature* *418*, 892–897.
- Taveggia, C., Feltri, M.L., and Wrabetz, L. (2010). Signals to promote myelin formation and repair. *Nat. Rev. Neurol.* *6*, 276–287.
- Tempé, D., Casas, M., Karaz, S., Blanchet-Tournier, M.-F., and Concordet, J.-P. (2006). Multisite protein kinase A and glycogen synthase kinase 3beta phosphorylation leads to Gli3 ubiquitination by SCFbetaTrCP. *Mol. Cell. Biol.* *26*, 4316–4326.
- Thomas, K., and Ziemssen, T. (2013). Management of fingolimod in clinical practice. *Clin. Neurol. Neurosurg.* *115*, S60–S64.
- Thomas, C.C., Deak, M., Alessi, D.R., and van Aalten, D.M.F. (2002). High-resolution structure of the pleckstrin homology domain of protein kinase b/akt bound to phosphatidylinositol (3,4,5)-trisphosphate. *Curr. Biol.* *12*, 1256–1262.

- Timsit, S., Martinez, S., Allinquant, B., Peyron, F., Puelles, L., and Zalc, B. (1995). Oligodendrocytes originate in a restricted zone of the embryonic ventral neural tube defined by DM-20 mRNA expression. *J. Neurosci.* *15*, 1012–1024.
- Tobin, J.L., and Beales, P.L. (2009). The nonmotile ciliopathies. *Genet. Med.* *11*, 386–402.
- Tolstykh, T., Lee, J., Vafai, S., and Stock, J.B. (2000). Carboxyl methylation regulates phosphoprotein phosphatase 2A by controlling the association of regulatory B subunits. *EMBO J.* *19*, 5682–5691.
- Tran, P. V., Haycraft, C.J., Besschetnova, T.Y., Turbe-Doan, A., Stottmann, R.W., Herron, B.J., Chesebro, A.L., Qiu, H., Scherz, P.J., Shah, J. V, et al. (2008). THM1 negatively modulates mouse sonic hedgehog signal transduction and affects retrograde intraflagellar transport in cilia. *Nat. Genet.* *40*, 403–410.
- Trapp, B.D., Nishiyama, A., Cheng, D., and Macklin, W. (1997). Differentiation and death of premyelinating oligodendrocytes in developing rodent brain. *J. Cell Biol.* *137*, 459–468.
- Trapp, M.L., Galtseva, A., Manning, D.K., Beier, D.R., Rosenblum, N.D., and Quarman, L.M. (2008). Defects in ciliary localization of Nek8 is associated with cystogenesis. *Pediatr. Nephrol.* *23*, 377–387.
- Tronche, F., Kellendonk, C., Kretz, O., Gass, P., Anlag, K., Orban, P.C., Bock, R., Klein, R., and Schütz, G. (1999). Disruption of the glucocorticoid receptor gene in the nervous system results in reduced anxiety. *Nat. Genet.* *23*, 99–103.
- Tsao, C.-C., and Gorovsky, M.A. (2008). Tetrahymena IFT122A is not essential for cilia assembly but plays a role in returning IFT proteins from the ciliary tip to the cell body. *J. Cell Sci.* *121*, 428–436.
- Tucker, R.W., Pardee, A.B., and Fujiwara, K. (1979). Centriole ciliation is related to quiescence and DNA synthesis in 3T3 cells. *Cell* *17*, 527–535.
- Tukachinsky, H., Lopez, L. V, and Salic, A. (2010). A mechanism for vertebrate Hedgehog signaling: recruitment to cilia and dissociation of SuFu-Gli protein complexes. *J. Cell Biol.* *191*, 415–428.
- Turowski, P., Fernandez, a, Favre, B., Lamb, N.J., and Hemmings, B. a (1995). Differential methylation and altered conformation of cytoplasmic and nuclear forms of protein phosphatase 2A during cell cycle progression. *J. Cell Biol.* *129*, 397–410.
- Tuson, M., He, M., and Anderson, K. V (2011). Protein kinase A acts at the basal body of the primary cilium to prevent Gli2 activation and ventralization of the mouse neural tube. *Development* *138*, 4921–4930.

- Tyler, W.A., Gangoli, N., Gokina, P., Kim, H.A., Covey, M., Levison, S.W., and Wood, T.L. (2009a). Activation of the mammalian target of rapamycin (mTOR) is essential for oligodendrocyte differentiation. *J. Neurosci.* *29*, 6367–6378.
- Tyler, W.A., Gangoli, N., Gokina, P., Kim, H.A., Covey, M., Levison, S.W., and Wood, T.L. (2009b). Activation of the mammalian target of rapamycin (mTOR) is essential for oligodendrocyte differentiation. *J. Neurosci.* *29*, 6367–6378.
- Uemura, T., Shiomi, K., Togashi, S., and Takeichi, M. (1993). Mutation of twins encoding a regulator of protein phosphatase 2A leads to pattern duplication in *Drosophila* imaginal discs. *Genes Dev.* *7*, 429–440.
- Vallstedt, Anna, Klos, Joanna M., Ericson, J. (2005). Multiple Dorsoventral Origins of Oligodendrocyte Generation in the Spinal Cord and Hindbrain.
- Vereshchagina, N., Ramel, M.-C., Bitoun, E., and Wilson, C. (2008). The protein phosphatase PP2A-B' subunit Widerborst is a negative regulator of cytoplasmic activated Akt and lipid metabolism in *Drosophila*. *J. Cell Sci.* *121*, 3383–3392.
- Verity, A.N., and Campagnoni, A.T. (1988). Regional expression of myelin protein genes in the developing mouse brain: in situ hybridization studies. *J. Neurosci. Res.* *21*, 238–248.
- Vincent, E.E., Elder, D.J.E., Thomas, E.C., Phillips, L., Morgan, C., Pawade, J., Sohail, M., May, M.T., Hetzel, M.R., and Tavaré, J.M. (2011). Akt phosphorylation on Thr308 but not on Ser473 correlates with Akt protein kinase activity in human non-small cell lung cancer. *Br. J. Cancer* *104*, 1755–1761.
- Virshup, D.M., and Shenolikar, S. (2009). From promiscuity to precision: protein phosphatases get a makeover. *Mol. Cell* *33*, 537–545.
- Vogel, U.S., and Thompson, R.J. (1988). Molecular structure, localization, and possible functions of the myelin-associated enzyme 2',3'-cyclic nucleotide 3'-phosphodiesterase. *J. Neurochem.* *50*, 1667–1677.
- Vora, P., Pillai, P.P., Zhu, W., Mustapha, J., Namaka, M.P., and Frost, E.E. (2011). Differential effects of growth factors on oligodendrocyte progenitor migration. *Eur. J. Cell Biol.* *90*, 649–656.
- Vorobjev, I.A., and Chentsov YuS (1982). Centrioles in the cell cycle. I. Epithelial cells. *J. Cell Biol.* *93*, 938–949.

- Walczak-Sztulpa, J., Eggenschwiler, J., Osborn, D., Brown, D.A., Emma, F., Klingenberg, C., Hennekam, R.C., Torre, G., Garshasbi, M., Tzschach, A., et al. (2010). Cranioectodermal Dysplasia, Sensenbrenner syndrome, is a ciliopathy caused by mutations in the IFT122 gene. *Am. J. Hum. Genet.* *86*, 949–956.
- Walker, K.S., Deak, M., Paterson, A., Hudson, K., Cohen, P., and Alessi, D.R. (1998). Activation of protein kinase B beta and gamma isoforms by insulin in vivo and by 3-phosphoinositide-dependent protein kinase-1 in vitro: comparison with protein kinase B alpha. *Biochem. J.* *331* ( Pt 1, 299–308.
- Wang, B., and Li, Y. (2006). Evidence for the direct involvement of  $\beta$ TrCP in Gli3 protein processing. *Proc. Natl. Acad. Sci. U. S. A.* *103*, 33–38.
- Wang, W., and Brautigan, D.L. (2008). Phosphatase inhibitor 2 promotes acetylation of tubulin in the primary cilium of human retinal epithelial cells. *BMC Cell Biol.* *9*, 62.
- Wang, B., Fallon, J.F., and Beachy, P.A. (2000a). Hedgehog-regulated processing of Gli3 produces an anterior/posterior repressor gradient in the developing vertebrate limb. *Cell* *100*, 423–434.
- Wang, C., Pan, Y., and Wang, B. (2010). Suppressor of fused and Spop regulate the stability, processing and function of Gli2 and Gli3 full-length activators but not their repressors. *Development* *137*, 2001–2009.
- Wang, G., Amanai, K., Wang, B., and Jiang, J. (2000b). Interactions with Costal2 and suppressor of fused regulate nuclear translocation and activity of cubitus interruptus. *Genes Dev.* *14*, 2893–2905.
- Warner, F.D. (1976). Ciliary inter-microtubule bridges. *J. Cell Sci.* *20*, 101–114.
- Wechsler-Reya, R.J., and Scott, M.P. (1999). Control of neuronal precursor proliferation in the cerebellum by Sonic Hedgehog. *Neuron* *22*, 103–114.
- Welburn, J.P.I., Tucker, J.A., Johnson, T., Lindert, L., Morgan, M., Willis, A., Noble, M.E.M., and Endicott, J.A. (2007). How tyrosine 15 phosphorylation inhibits the activity of cyclin-dependent kinase 2-cyclin A. *J. Biol. Chem.* *282*, 3173–3181.
- Wen, X., Lai, C.K., Evangelista, M., Hongo, J.-A., de Sauvage, F.J., and Scales, S.J. (2010). Kinetics of hedgehog-dependent full-length Gli3 accumulation in primary cilia and subsequent degradation. *Mol. Cell. Biol.* *30*, 1910–1922.
- Wijgerde, M., McMahon, J.A., Rule, M., and McMahon, A.P. (2002). A direct requirement for Hedgehog signaling for normal specification of all ventral progenitor domains in the presumptive mammalian spinal cord. *Genes Dev.* *16*, 2849–2864.

- Williamson, S.M., Silva, D.A., Richey, E., and Qin, H. (2012). Probing the role of IFT particle complex A and B in flagellar entry and exit of IFT-dynein in *Chlamydomonas*. *Protoplasma* 249, 851–856.
- Włodarski, P., Grajkowska, W., Łojek, M., Rainko, K., and Józwiak, J. (2006). Activation of Akt and Erk pathways in medulloblastoma. *Folia Neuropathol.* 44, 214–220.
- Wolswijk, Guus, Noble, M. (1995). In vitro studies of the development, maintenance and regeneration of the oligodendrocyte-type-2 astrocyte (O-2A) lineage in the adult central nervous system. *Neuroglia* 149–161.
- Wood, P.M., and Bunge, R.P. (1991). The origin of remyelinating cells in the adult central nervous system: the role of the mature oligodendrocyte. *Glia* 4, 225–232.
- Wu, S., Wu, Y., and Capecchi, M.R. (2006). Motoneurons and oligodendrocytes are sequentially generated from neural stem cells but do not appear to share common lineage-restricted progenitors in vivo. *Development* 133, 581–590.
- Wymann, M.P., and Pirola, L. (1998). Structure and function of phosphoinositide 3-kinases. *Biochim. Biophys. Acta* 1436, 127–150.
- Xie, H., and Clarke, S. (1993). Methyl esterification of C-terminal leucine residues in cytosolic 36-kDa polypeptides of bovine brain. A novel eucaryotic protein carboxyl methylation reaction. *J. Biol. Chem.* 268, 13364–13371.
- Yamada, T., Pfaff, S.L., Edlund, T., and Jessell, T.M. (1993). Control of cell pattern in the neural tube: motor neuron induction by diffusible factors from notochord and floor plate. *Cell* 73, 673–686.
- Yang, P., Fox, L., Colbran, R.J., and Sale, W.S. (2000). Protein phosphatases PP1 and PP2A are located in distinct positions in the *Chlamydomonas* flagellar axoneme. *J. Cell Sci.* 113 ( Pt 1), 91–102.
- Yang, Q., Inoki, K., Ikenoue, T., and Guan, K.-L. (2006). Identification of Sin1 as an essential TORC2 component required for complex formation and kinase activity. *Genes Dev.* 20, 2820–2832.
- Yeh, H.J., Ruit, K.G., Wang, Y.X., Parks, W.C., Snider, W.D., and Deuel, T.F. (1991). PDGF A-chain gene is expressed by mammalian neurons during development and in maturity. *Cell* 64, 209–216.
- Yokote, K., Hellman, U., Ekman, S., Saito, Y., Rönstrand, L., Heldin, C.H., and Mori, S. (1998). Identification of Tyr-762 in the platelet-derived growth factor alpha-receptor as the binding site for Crk proteins. *Oncogene* 16, 1229–1239.

- Yu, J.C., Heidarani, M.A., Pierce, J.H., Gutkind, J.S., Lombardi, D., Ruggiero, M., and Aaronson, S.A. (1991). Tyrosine mutations within the alpha platelet-derived growth factor receptor kinase insert domain abrogate receptor-associated phosphatidylinositol-3 kinase activity without affecting mitogenic or chemotactic signal transduction. *Mol. Cell. Biol.* *11*, 3780–3785.
- Yu, J.C., Gutkind, J.S., Mahadevan, D., Li, W., Meyers, K.A., Pierce, J.H., and Heidarani, M.A. (1994). Biological function of PDGF-induced PI-3 kinase activity: its role in alpha PDGF receptor-mediated mitogenic signaling. *J. Cell Biol.* *127*, 479–487.
- Yu, X.X., Du, X., Moreno, C.S., Green, R.E., Ogris, E., Feng, Q., Chou, L., McQuoid, M.J., and Pallas, D.C. (2001). Methylation of the protein phosphatase 2A catalytic subunit is essential for association of Balph regulatory subunit but not SG2NA, striatin, or polyomavirus middle tumor antigen. *Mol. Biol. Cell* *12*, 185–199.
- Yusuf, H.K., Haque, Z., and Mozaffar, Z. (1981). Effect of malnutrition and subsequent rehabilitation on the development of mouse brain myelin. *J. Neurochem.* *36*, 924–930.
- Zalc, B., Monge, M., Dupouey, P., Hauw, J.J., and Baumann, N.A. (1981). Immunohistochemical localization of galactosyl and sulfogalactosyl ceramide in the brain of the 30-day-old mouse. *Brain Res.* *211*, 341–354.
- Zhang, H., Cicchetti, G., Onda, H., Koon, H.B., Asrican, K., Bajraszewski, N., Vazquez, F., Carpenter, C.L., and Kwiatkowski, D.J. (2003). Loss of Tsc1/Tsc2 activates mTOR and disrupts PI3K-Akt signaling through downregulation of PDGFR. *J. Clin. Invest.* *112*, 1223–1233.
- Zhang, H., Bajraszewski, N., Wu, E., Wang, H., Moseman, A.P., Dabora, S.L., Griffin, J.D., and Kwiatkowski, D.J. (2007). PDGFRs are critical for PI3K/Akt activation and negatively regulated by mTOR. *J. Clin. Invest.* *117*, 730–738.
- Zhang, X., Vadas, O., Perisic, O., Anderson, K.E., Clark, J., Hawkins, P.T., Stephens, L.R., and Williams, R.L. (2011). Structure of lipid kinase p110 $\beta$ /p85 $\beta$  elucidates an unusual SH2-domain-mediated inhibitory mechanism. *Mol. Cell* *41*, 567–578.
- Zhang, Y., Fu, L., Qi, X., Zhang, Z., Xia, Y., Jia, J., Jiang, J., Zhao, Y., and Wu, G. (2013). Structural insight into the mutual recognition and regulation between Suppressor of Fused and Gli/Ci. *Nat. Commun.* *4*, 2608.

- Zhao, J.J., Gjoerup, O. V, Subramanian, R.R., Cheng, Y., Chen, W., Roberts, T.M., and Hahn, W.C. (2003). Human mammary epithelial cell transformation through the activation of phosphatidylinositol 3-kinase. *Cancer Cell* 3, 483–495.
- Zhou, Q., and Anderson, D.J. (2002). The bHLH transcription factors OLIG2 and OLIG1 couple neuronal and glial subtype specification. *Cell* 109, 61–73.
- Zhou, J., Pham, H.T., Ruediger, R., and Walter, G. (2003). Characterization of the Aalpha and Abeta subunit isoforms of protein phosphatase 2A: differences in expression, subunit interaction, and evolution. *Biochem. J.* 369, 387–398.
- Zhou, Q., Wang, S., and Anderson, D.J. (2000). Identification of a novel family of oligodendrocyte lineage-specific basic helix-loop-helix transcription factors. *Neuron* 25, 331–343.
- Zhou, Q., Choi, G., and Anderson, D.J. (2001). The bHLH transcription factor Olig2 promotes oligodendrocyte differentiation in collaboration with Nkx2.2. *Neuron* 31, 791–807.
- Zhu, D., Shi, S., Wang, H., and Liao, K. (2009). Growth arrest induces primary-cilium formation and sensitizes IGF-1-receptor signaling during differentiation induction of 3T3-L1 preadipocytes. *J. Cell Sci.* 122, 2760–2768.
- Zou, J., Zhou, L., Du, X.-X., Ji, Y., Xu, J., Tian, J., Jiang, W., Zou, Y., Yu, S., Gan, L., et al. (2011). Rheb1 is required for mTORC1 and myelination in postnatal brain development. *Dev. Cell* 20, 97–108.